MOLECULAR SPECTROSCOPY

Dr. V. Chinnathambi,

Associate Professor of Physics

Sri K.G.S. Arts College,

Srivaikuntam-628 619

Unit - I

MOLECULAR SPECTROSCOPY

Unit 1 : Microwave Spectroscopy

Classification of molecules – Rotational spectra of rigid diatomic molecules – Isotope effect – Non rigid rotator – linear polyatomic molecules – symmetric top molecules – asymmetric top molecules – Microwave spectrometer – information derived from rotational spectra.

Unit II : Infrared Spectroscopy

Vibrational energy of diatomic molecule – Selection rules – vibrating diatomic molecule – diatomic vibrating rotator – asymmetry of rotation – vibration band – vibrations of polyatomic molecules – Rotation – vibration spectra of poly atomic molecules – interpretation of vibrational spectra – IR spectrophotometer – sample handling techniques – Fourier transform IR spectroscope – applications.

Unit III : Raman Spectroscopy

Theory of Raman scattering – rotational Raman spectra – vibrational Raman Spectra – Raman spectrometer – Structure determination using IR and Raman spectroscopy.

Hyper Raman effect – classical treatment of Raman effect – Experimental techniques for Hyper – Raman effect – stimulated Raman scattering – Inverse Raman scattering – CARS – PARS – SERS (basic ideas only).

Unit IV : Electronic spectroscopy

Vibrational coarse structure – Vibrational analysis of band systems – Deslanders table – Progressions and sequences – Franck condon principle – Rotational fine Structure of electronic vibration spectra – the Fortrat parabola – Dissociation – Pre dissociation – photoelectron spectroscopy – Instrumentation – information from photoelectron spectra.

Unit V: NMR, ESR, NQR, Mossbauer spectroscopy

NMR : Magnetic properties of nuclei – resonance condition – NMR instrumentation – relaxation systems – Bloch equations – chemical shift.

ESR :Principle – ESR spectrometer – Hyper fine structure – ESR spectra of Hydrogen atom.

NQR:The quadruple molecules – principle – transitions for axially and nonaxially symmetric systems – NQR instrumentation.

Mossbauer :Recoilless emission and absorption – Mossbauer spectrometer – Isomer shift – application.

Book for study and reference. :

1. G.Aruldhas, " Molecular structure and spectroscopy", second edition, practice – Hall of India, Pvt Ltd., New Delhi – 110001, 2007.
2. Fundamentals of Molecular spectroscopy – Colin N Banwell and Elaine M Mccash
3. Spectroscopy – GR Cghatwal and S.K Anand

Unit – I

Microwave Spectroscopy

1.1 Classification of Molecules

The molecules are usually classified into four groups based on the relative values of principal moments of Inertia I_a, I_b and I_c, where *a,b,c* are axes and are selected in such a way that $I_a > I_b > I_c$

(i) Linear Molecules :

In this type, all the atoms of the molecules are arranged in a straight line. For example, HCl, CO_2, OCS, HCN, C_2H_2 etc are some of the molecules of this category.

The three mutually perpendicular principal axes *a,b,c* of rotation may be taken as :

a → the molecular axis

b → the direction in the plane of the paper passing through the centre of gravity of the molecule and perpendicular to it a – axis.

c → the axis perpendicular to both a and b axes, and passing through the centre of gravity of the molecule.

For a linear molecule, the principal moments of Inertia are $I_a = 0$ and $I_b = I_c$. The moments of Inertia I_b and I_c correspond to the end over end rotation of the molecule and therefore they are equal, and $I_a = 0$. Since the nuclei of the atoms which give the main contribution of mass are situated in the axis *a*.

ii) Symmetric Tops :-

In a symmetric top, two of the principal moments of inertia are equal and all the three are non zero.

The molecule in this class are further subdivided into the groups probate symmetric top and oblate symmetric top. In probate, $I_a > I_b = I_c$ (Ex. CH_3Cl, CH_3F, CH_3CN, NH_3, etc.,) and in oblate , $I_a = I_b < I_c$ (Ex. BH_3, BCl_3, etc.,)

iii) Spherical Tops :

When all the three principal moments of inertia of a molecule are equal, it is called a spherical top. (Ex. CH_4, O_S O_4, SF_6, CCl_4, etc.,)

iv. Asymmetric Tops :-

In an asymmetric top molecule, all the three moments of Inertia are distinct $I_a \neq I_b \neq I_c$. Some of the examples are H_2O, CH_3OH, CH_2CHCl, etc., The majority of the molecules belong to this group.

1.2 Rotational Spectra of Rigid diatomic molecules

A diatomic molecule may be considered as a rigid rotator consisting of atomic masses m_1 and m_2 connected by a rigid bond of length r, (Fig.1.1)

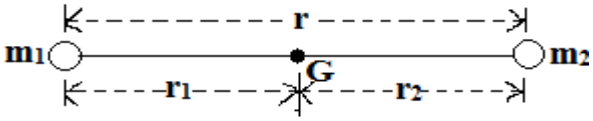

Fig.1.1 A rigid diatomic molecule

Consider the rotation of this rigid rotator about an axis perpendicular to its molecular axis and passing through the centre of gravity. The solution of the Schrodinger equation for the rigid rotator gives the energy eigen values,

$$E_J = \frac{\hbar^2}{2I} J(J+1) \quad \text{Joules,} \qquad J = 0,1,2... \qquad (1.1)$$

Where J is the rotational quantum number, I is the moment of Inertia of the molecule about an axis passing through its centre of gravity G and perpendicular to the molecular axis.

$$I = m_1 r_1^2 + m_2 r_2^2 \; ; \qquad m_1 r_1 = m_2 r_2 \quad ; \quad r = r_1 + r_2 \qquad (1.2)$$

Expressing r_1 and r_2 interms of r and substituting in Eq. (1.2), We get,

$$r_1 = \frac{m_2 r}{m_1 + m_2};\ r_1 = \frac{m_1 r}{m_1 + m_2} \tag{1.3}$$

$$\therefore I = \frac{m_1 m_2}{m_1 + m_2} r^2 = \mu r^2 \tag{1.4}$$

Where $$\mu = \frac{m_1 m_2}{m_1 + m_2} \tag{1.5}$$

In wave number units,

$$\varepsilon_J = \frac{E_J}{hc} = \frac{h}{8\pi^2 IC} J(J+1)\, cm^{-1} \tag{1.6}$$

$$= B\, J(J+1)\, cm^{-1},\ J = 0,1,2..... \tag{1.7}$$

Where B is the rotational constant and is given by

$$B = \frac{h}{8\pi^2 IC}\ cm^{-1},\quad B = \frac{h^2}{8\pi^2 I} \quad \text{Joules} \tag{1.8}$$

Let us denote J" be the lower state and J' be the upper state. Therefore,

$$\Delta\varepsilon_J = \varepsilon_{J'} - \varepsilon_{J''} = B\left[(J'(J'+1) - J''(J''+1)\right].$$

Use of the selction rule , $\Delta J = +1$, ie., J' – J'' = 1, gives the frequency of the absorption line as,

$$\bar{\gamma}_J = \Delta\varepsilon_J = B[(J''+1)(J''+2) - J''(J''+1)]$$

$$\bar{\gamma}_J = 2B(J+1)\, cm^{-1},\ J = 0,1,2,..... \tag{1.9}$$

The rotational constant B is assumed to be the same in both lower and upper rotational states and double prime is dropped from Eq. (1.9). J in Eq. (1.9) in the J value of the lower state. From Eq.(1.9), we get a series of spectral lines with wave number values $2B, 4B, 6B.....cm^{-1}$. The separation between any two adjacent line is 2B. The energy levels and the allowed transitions are shown in Fig (1.2). The value of B can be deduced from the spacing between the observed spectral lines. Use of Eqs. (1.8) and (1.4) immediately gives the internuclear distance of the diatomic molecule.

1.3 Selection rule of rotational spectrum :-

1. The molecule must have a permanent dipole moment.

2. Transitions are allowed only between adjacent rotational levels, ie., $\Delta J = \pm 1$ (plus sign for absorption and minus sign for emission).

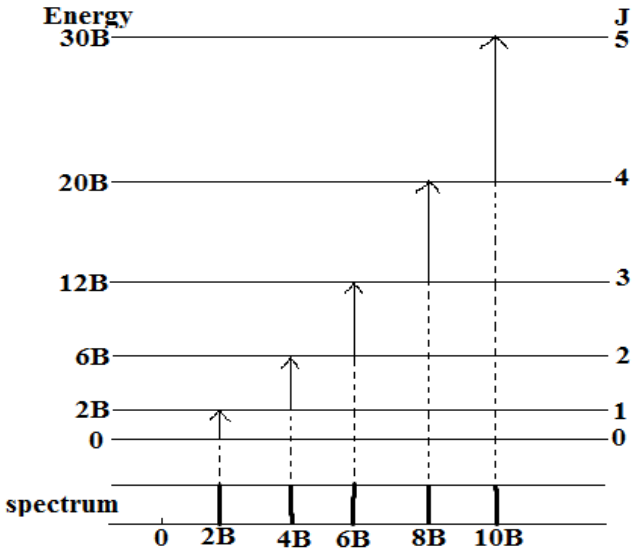

Fig. 1.2 Rotational energy levels and transitions for a rigid diatomic molecule

1.4 Isotope effect in rotational spectra :-

An atom when replaced by one of its isotopes, the interbond distance remains the same but the mass of the nucleus changes leading to a change in the moment of inertia.

Denoting the frequency of the isotopically substituted molecule by single prime

$$\bar{\gamma}' = 2B'(J+1)$$

$$\Delta\bar{\gamma} = \bar{\gamma} - \bar{\gamma}' = 2(J+1)(B - B')$$

$$= 2(J+1)\frac{h}{8\pi^2 IC}\left(1 - \frac{I}{I'}\right) cm^{-1} \qquad (1.10)$$

Where

$$\frac{I}{I'} = \frac{\mu}{\mu'} = \rho^2$$

$$\Delta\bar{\gamma} = 2B\ (J+1)(1-\rho^2) \qquad (1.11)$$

As $\rho = 1$ in most of the cases, the shift will be extremely small. When there is a mass increase, $\rho^2 < 1$ giving a +ve value for $\Delta\bar{\gamma}$. It is evident from Eq.(1.11) that isotope shift increases with

the value of J. The effect of C^{13} isotope substitution on the rotational spectrum of diatomic molecule C^{12}, O^{16} is illustrated in Fig.1.3.

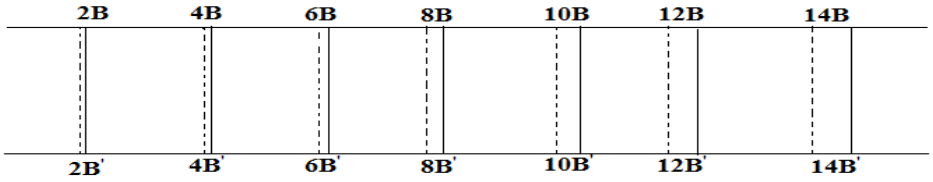

Fig.1.3 Rotational spectrum of (a) diatomic molecule (continuous line) and (b) isotopically substituted diatomic molecule having a mass increase.

1.4 Non- Rigid Rotator

All bonds are elastic to a certain extent and the bond is not rigid as we assumed. The solution of the corresponding Schrodinger equation gives the following energy expression for the energy levels of the non-rigid rotator.

$$\varepsilon_J = BJ\ (J+1) - DJ^2 (J+1)^2\, cm^{-1}, \quad J = 0,1,2,..... \tag{1.12}$$

Where D is the centrifugal distortion constant and D is a small +ve quantity.

For a diatomic molecule, D is related to B and the fundamental vibration frequency $\bar{\gamma}(cm^{-1})$ of the molecule by the relation

$$D = \frac{4B^3}{\bar{\gamma}^2}\, cm^{-1} \tag{1.13}$$

The fundamental frequency of vibration

$$\bar{\gamma} = \frac{\gamma}{c} \quad \frac{1}{2\pi c}\sqrt{\frac{K}{\mu}} \tag{1.14}$$

Where K is the force constant and μ is the reduced mass of the molecule. Substitution of the values of B and $\bar{\gamma}$ gives

$$D = 4\left(\frac{h}{8\pi^2 IC}\right)^3 \frac{4\pi^2 C^2 \mu}{K} = \frac{h^3}{32\pi^4 \mu^2 r^6 CK} \tag{1.15}$$

From the above equation, it is evident that the centrifugal distortion effects are greatest for molecules with small moments of inertia and small force constants, In a given molecule, the

effect of the centrifugal distortion is the decrease the rotational energy (Eq.1.12) which increases rapidly for higher rotational states.

The selection rule for the non-rigid rotator is again $\Delta J = \pm 1$. The frequency of the transition $J \rightarrow J+1$

$$\bar{\gamma}_J = \varepsilon_{J+1} - \varepsilon_J = 2B(J+1) - 4D(J+1)^3 \, cm^{-1} \qquad (1.16)$$

The first term is the same as the one due to a rigid molecule and the additional term gives the shift of the lines from that of the rigid molecules which increases with J as $(J+1)^3$. Fig.1.4 gives a schematic representation of the energy levels and the spectrum of non-rigid rotator. For comparison of the rigid case is also included.

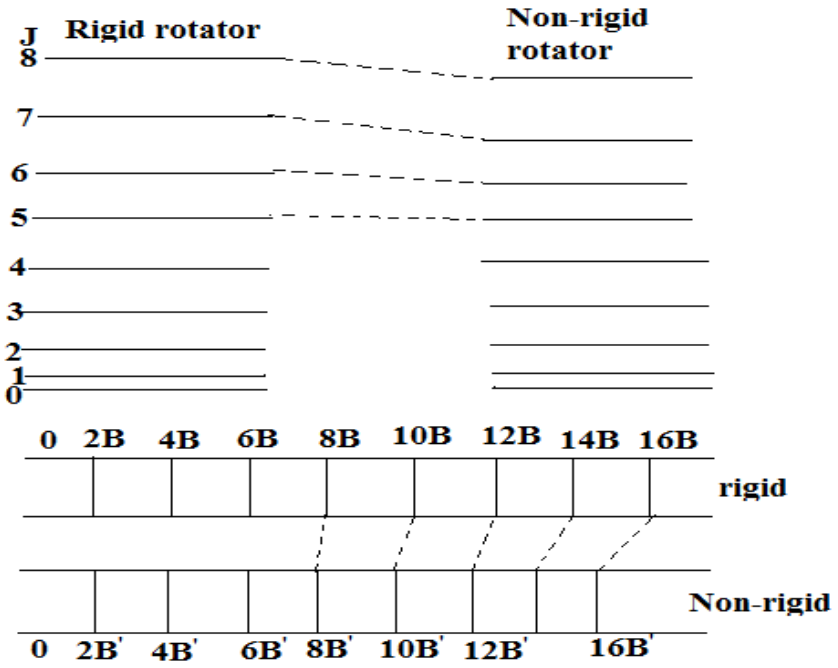

Fig.1.4 Schematic representation of the energy levels and spectrum of rigid and non-rigid rotors

1.5 Linear Polyatomic Molecules :-

A linear molecule containing *n* atoms altogether *(n-1)* individual bond lengths to be determined. Thus in the diatomic *XYZ* molecule, we have the distances r_{xy} and r_{yz}. The experiment will give only one moment of inertia for the end over end rotation. From this one

observation, it is not possible to find two unknowns *ie* r_{xy} and r_{yz}. However, if we study an isotropically substituted molecule we will have a different moment of inertia with the same bond lengths. Hence the determination of bond lengths requires the study of a number of isotopic molecules equal to the number of r_e parameters.

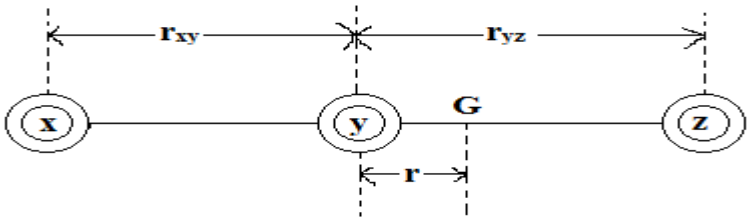

Fig.1.5 The linear XYZ molecule showing the various distances

The calculation of r_e parameters are illustrated for a molecule of the type *XYZ* (Fig.1.5). The atomic masses be m_x, m_y, m_z and the distance of the atom y from the centre of gravity G be r.

The selection rule is $\Delta J = \pm 1$ and the frequency of $J \rightarrow J+1$ transition is again.

$$\bar{\gamma}_j = 2B\,(J+1) - 4D(J+1)^3\, cm^{-1}, \quad J = 0,1,2,.....$$

The moment of inertia for the end to end rotation of the linear triatomic molecule will considerably be greaer than that of the diatomic molecule where as B will be much smaller. For diatomics, $B = 10 cm^{-1}$ while for a linear triatonic molecule $B \cong 1 cm^{-1}$ or even less.

$$m_x(r_{xy}+r) + m_y r = m_z\,(r_{yz} - r)$$

$$r = \frac{m_z\, r_{yz} - m_x r_{xy}}{m}, \qquad M = m_x + m_y + m_z$$

The moment of inertia

$$I = m_x(r_{xy}+r)^2 + m_y r^2 + m_z\,(r_{yz}-r)^2 \qquad (1.17)$$

$$= m_x r^2 xy + m_z r^2 xz - Mr^2$$

Substitution of the value of r and rearrangement gives,

$$I = \frac{m_x m_y r^2_{xy} + m_y m_z r^2_{yz} + m_x m_z (r_{xy} + r_{yz})^2}{m_x + m_y + m_z} \qquad (1.18)$$

Replacement of the atom Z by its isotope of mass m_z' gives

$$I = \frac{m_x m_y r^2_{xy} + m_y m'_z r^2_{yz} + m_x m'_z (r_{xy} + r_{yz})^2}{m_x + m_y + m'_z} \qquad (1.19)$$

1.6 Symmetric Top Molecules :-

For symmetric tops, there are two independent moments of inertia and therefore, there are two directions of rotation in which the molecule might absorb or emit energy. They are the rotation about the top axis or the molecular symmetry axis and the other in a direction perpendicular to this axis.

This type of molecules are further subdivided into the groups prolate symmetric top and the oblate symmetric top. In prolate $I_a > I_b = I_c$ (Ex. CH_3Cl, CH_3F, NH_3, etc.,) and in oblate , $I_a = I_b < I_c$ (Ex. BF_3, BCl_3, etc.,)

For the rigid probate symmetric top, the solution of Schrodinger equation gives the energy levels.

$$E_{J,K} = \frac{h^2}{8\pi^2 I_b} J(J+1) + \left(\frac{h^2}{8\pi^2 I_a} - \frac{h^2}{8\pi^2 I_b} \right) K^2 \quad \text{Joules}$$

$$\varepsilon_J = \frac{E_{J,K}}{hc} = BJ(J+1) + (A-B)K^2 \ cm^{-1} \qquad (1.20)$$

For oblate,

$$\varepsilon_J = BJ(J+1) + (C-B)K^2 \ cm^{-1} \qquad (1.21)$$

The rotational constants A, B, and C in cm^{-1} are

$$A = \frac{h}{8\pi^2 I_a c} \ ; B = \frac{h}{8\pi^2 I_b c} ; C = \frac{h}{8\pi^2 I_c c}$$

$$J = 0,1,2,3,\ldots\ldots\ldots, \ K = 0, \pm 1, \pm 2, \pm 3, \ldots\ldots\ldots\ldots \pm J$$

The quantum number J represents the total angular momentum of the molecule and K represents the projection of the total angular momentum upon the molecular symmetry axis. The +ve and – ve values of K correspond to clockwise and anti clock wise rotations about the top axis. Fig.1.6 gives the energy levels for both oblate and probate top molecular.

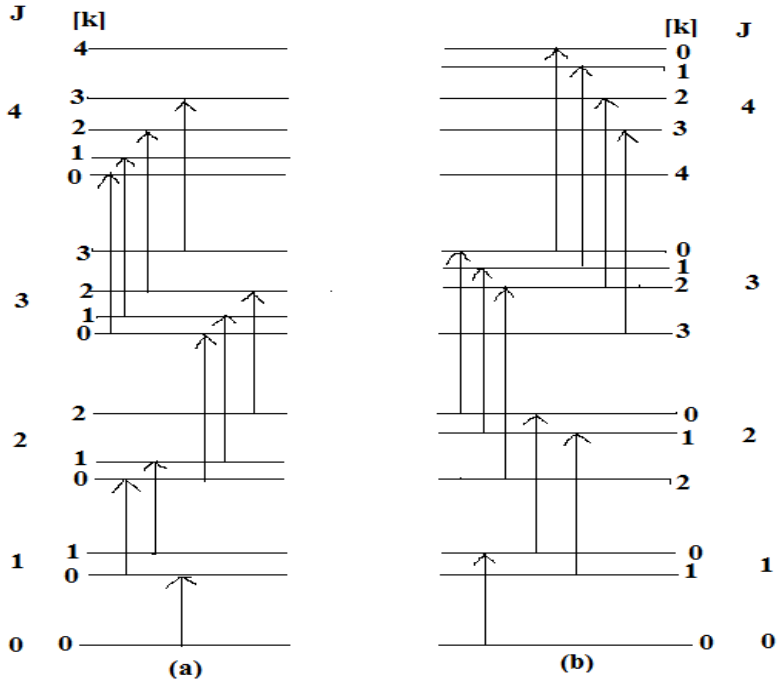

Fig.1.6 Schematic representation of energy levels and transition for (a) the rigid prolate and (b) the rigid oblate symmetric rotors

The selection rule for transitions are

$$\Delta J = \pm 1,\ \Delta K = 0 \qquad (1.22)$$

Here $\Delta K = 0$ means, a rotation of the molecule along the symmetry axis causes no change in the dipole moment. Hence the energy of this type of rotation can not be changed.

The frequencies of the transitions are then given by

$$\bar{\gamma}_{J,K} = \varepsilon_{J+1} - \varepsilon_J = 2B(J+1)\ cm^{-1}\ J = 0,1,2 \qquad (1.23)$$

The spectrum is thus independent of K, indicating that rotational changes about the symmetry axis do not give rise to a rotational spectrum.

For non – rigid type molecule, the rotational energy is

$$\varepsilon_{J,K} = BJ\ (J+1) + (A-B)K^2 - D_J J^2 (J+1)^2 - D_{J,K}\ J(J+1)K^2 - D_K K^4\ Cm^{-1} \quad (1.24)$$

Where, D_J, D_K and D_{JK} are small constants, the selection rules are the same and the frequencies of the spectral transitions are

$$\bar{\gamma}_{J,K} = 2B\ (J+1) - 4D_J (J+1)^3 - 2D_{JK}\ (J+1)K^2 \quad (1.25)$$

The spectrum depends on K, which means that the rotation about the symmetry axis causes change is the dipole moment. Each value of J gives rise to (2J+1) possible values of K.

1.7 Asymmetric Top Molecules

Most of the molecules belong to this category. It is not possible to derive an analytic expression for the rotational energy of an a symmetric rotor. Consequently, the spectra of symmetric rotor becomes very complex. The prolate and the oblate symmetric rotors represent the two extreme limits of an asymmetric rotor. The moment of inertia relations for the different cases are

$I_a \neq I_b \neq I_c$ asymmetric rotor

$I_a < I_b \simeq I_c$ near prolate asymmetric rotor

$I_a = I_b < I_c$ near oblate asymmetric rotor

Consider a molecule some what intermediate to the extreme cases. Its energy levels can be evaluated by the use of perturbation theory by writing the rotational Hamiltonian as,

$$H_r = H_p + H^1$$

Here H_p represents the Hamiltonian for a prolate symmetric rotor while H^1 contains the parts which exists because $I_b \neq I_c$. This second part represents the departure from prolate symmetric top. The energy is obtained by the usual perturbation technique using prolate rotor wave function as basic functions. One can also do the calculation by assuming the Hamiltonian of the given molecule as the sum of H_o, the Hamiltonian for a oblate symmetric rotor plus a term

which represents the deviation from oblate symmetric top. The two correlations must correlate with the two limiting cases. The energy level correlation diagram is shown in Fig. 1.7. the abscissa is some parameter which measures the departure from a prolate or an oblate symmetric top.

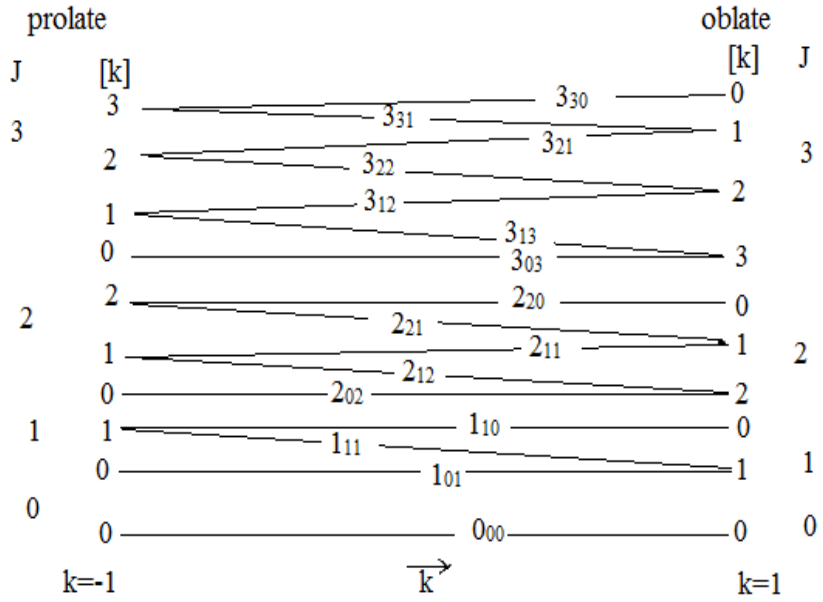

Fig.1.7 Energy level correlation diagram for asymmetric case

The asymmetry factor k is one such parameter defined by

$$k = \frac{2B - A - C}{A - C} \tag{1.26}$$

The limiting values of k are -1 for a proLate top (B=C) and +1 for an oblate top (A=B). The levels have been labelled as J_{mn} where m in the proLate k value and n is the oblate k value. The selection rules for these molecules are $\Delta J = 0, \pm 1$.

1.8 Microwave Spectrometer :-

A schematic representation of a microwave spectrometer is shown in Fig.1.8. Based on the functions of a spectrometer the following parts are needed.

(i) source (ii) Measurement of frequency (iii) guidance of the radiation to the absorbing substance (iv) sample cell (v) detector.

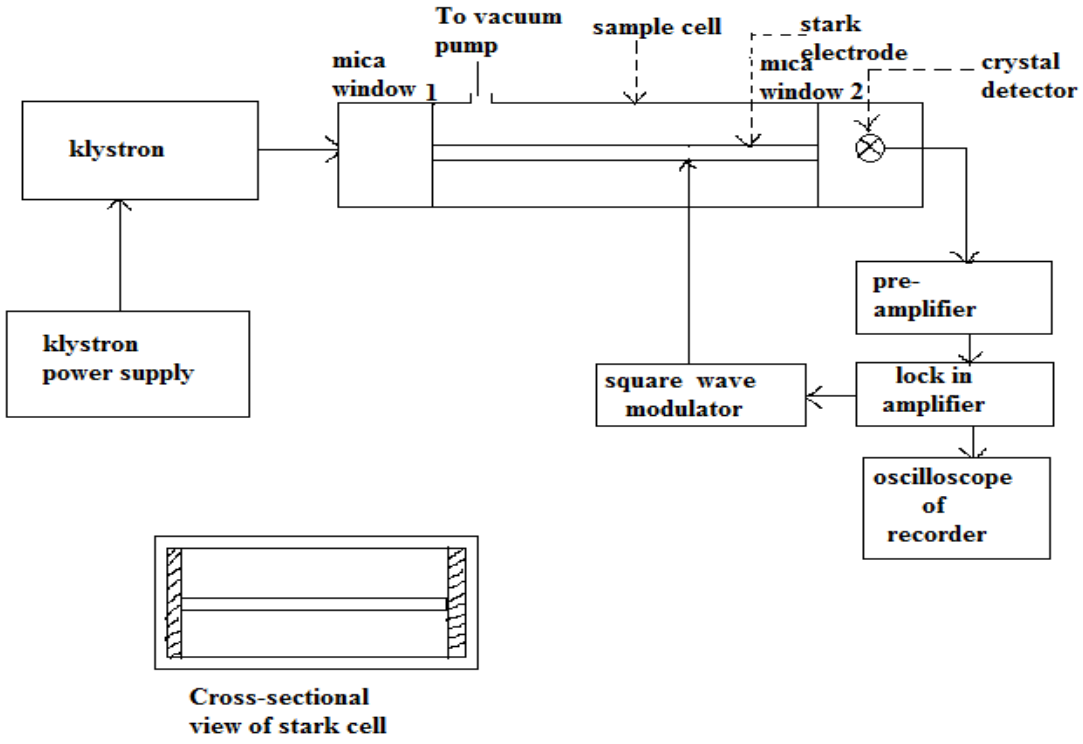

Fig.1.8 Schematic representation of a microwave spectrometer.

(i) Source :-

Most of the spectrometers have in the past used klystrons which emit monochromatic microwave radiation of very high stability. The frequency of the klystron can be varied mechanically over a wide range or electrically over a small range.

In recent times, Gunn diodes are used extensively as they need only 20v imput powere compared to the 300-4000v required for klystron. In place of klystron and Gunn diodes, backward wave oscillators can also be used as a source.

(ii) Frequency measuring device:

Cavity wave meters are used to measure the frequency with accuracy between $\pm 1$to 5 MH_Z. Accurate frequency measurements can be done directly by frequency counters or by the use of a beat techniques.

(iii) Guidance of radiation to cell :-

Microwave radiation from the source can be transmitted to the sample cell through hollow metallic tube (usually copper) of rectangular crosssection called waveguides. Waveguides of different dimensions are needed to depending on the type of spectrometer used X-band (8-12.4 GH_Z). K – band (12.4-18 GHZ) etc.,

It is necessary to couple out a small fraction of power from the main transmission line for frequency measurement, monitoring power, etc., A simple and efficient arrangement for this purpose is the Bethe hole directional computer. Another useful device is the magic tee which is used a power divider, as a bridge for balancing microwave power, etc., In addition to these, one requires waveguide bands, connectors, tapers, impedance matching devices, alternator's etc.,

(iv) Sample cell :

The most commonly used sample cell is Stark cell emplying stark modulation techniques. The sample cell consists of a long (3 to 4m) rectangular wave guide, the ends of which are sealed off by means of thin mica windows. It has provision to evacuate and to admit the sample to be studied. The radiation is allowed to enter the cell through mica window I and that passes through window 2 is detected.

In stark cell, a flat metal strip is mounted half – way between the broad faces of the waveguide cell with a dielectric (Teflon) insulating the plate from the metallic wave guide (Fig.8). By injecting a 0-2000v zero – based square wave potential between the metallic plat and the waveguide, the resonance frequencies of the molecules can be modulated via the Stark effect. The modulation is followed by a phase lock detector which will respond only to molecular resonances. Hence, cell background characteristics are eliminated in *stark modulation spectrographs.*

iv) Detector

A silicon crystal is the most commonly used detector. The incoming radiation gives rise to a DC current. In stark spectrographs, the transmitted radiation is modulated only when a molecular resonance occurs. On resonance, a small square wave is imprinted on the top of the DC signal. The AC components is amplified and detected by a phase sensitive detector which is connected to an oscilloscope or chart recorder. Improved signal to noise ratio is possible only when the modulation frequency is optimum (30-100 KHZ.)

1.9 Information derived from rotational spectra

(i) Molecular structure :

The most important information that one can get from rotational spectra is details about molecular structure.

a) Rotational constants can be obtained with very high accuracy.

b) Information about the position of atoms in a molecule is obtained from three rotational constant from which the three moments of inertia $I_a, I_b,$ and I_c.

c) In a diatomic molecule, interatomic distance can be obtained from rotational spectra. For linear polyatomic molecules, n-1 bond distances to be determined. Additional n-2 bond distances have to be obtained by isotopic substitution.

d) The force constant of a bond can also be estimated from the values of rotational constant B and rotation distortion constant D. We have

$$\bar{\gamma}^2 = \frac{4B^3}{D}, \quad \bar{\gamma} = \frac{1}{2\pi c}\sqrt{\frac{k}{\mu}}$$

The force constant K is then given by

$$K = \frac{16\pi^2 C^2 \mu B^3}{D}$$

(ii) Dipole moment :

Precise determination of electric dipole moment is possible from microwave spectroscopy, by measurement of the *Stark effect*. Dipole moment can also throw light on the nature of molecular bonds.

(iii) Atomic mass :

The rotational spectra of molecules and isotopes give B and B',

$$B = \frac{h}{8\pi^2 IC} \qquad B' = \frac{h}{8\pi^2 I'C}$$

$$\frac{B}{B'} = \frac{I'}{I} = \frac{\mu'}{\mu}$$

From the known value of μ, one can evaluate μ' from which the mass of the isotope may be estimated.

iv) Nuclear Quadruple moment :-

Measurement of the quadrupole hyperfine structure in molecules gives the quantity $e^2qQ,$ the quadrupole coupling constant. For the evaluation of $eQ,$ a knowledge of the quantity q is necessary which can be estimated by others studies.

1.10 Solved Problems :-

1. What is the change in he rotational constant B when hydrogen is replaced by deutrium in the hydrogen molecule ?

Hints : $$\frac{B}{B'} = \frac{I'}{I} = \frac{\mu'}{\mu}$$

$$\mu = \frac{m_H}{2}, \quad \mu' = \frac{m_D}{2} = m_H$$

$$\frac{B}{B'} == \frac{2m_H}{m_H} = 2, \quad B^1 = \frac{B}{2}$$

Change in rotational constant, $B - B^1 = \frac{B}{2}$

2. The first line in rotational spectrum of carbon monoxide has a frequency of 3.8424 cm^{-1} . Calculate the rotational constant and hence the C-O band length in carbon monoxide. Avogadro number is 6.022x 10^{23} mole.

Hints :- $2B = 3.8424 cm^{-1}$, $B = 1.9212 cm^{-1}, = 192.12 m^{-1}$

$$I = \mu r^2 = \frac{h}{8\pi^2 BC} \quad ; \quad r^2 = \frac{h}{8\pi^2 \mu BC}$$

$$\mu = \frac{12\text{x}15.9949}{27.9949\,\text{x}\,6.022\,\text{x}10^3} \quad = 1.1385\,\text{x}\,10^{-23}\ \text{gram}$$

$$r^2 = 1.131\text{x}10^{-16} m = 1.131 A^0$$

3. The first rotational line of $^{12}C\ ^{16}O$ is observed at $3.84235 cm^{-1}$ and that of $^{13}C\ ^{16}O$ at $3.67337 cm^{-1}$. Calculate at atomic weight of $^{13}C\ ^{16}O$, assuming the mass of ^{16}O to be 15.9949.

Solution:

$$\frac{B}{B'} = \frac{I'}{I} = \frac{\mu'}{\mu}$$

Let as atomic weight of 13_C be ‘m’

$$\frac{\mu'}{\mu} = \frac{27.9949}{12 \text{ x } 15.4949} \text{ x } \frac{m \text{ x } 15.9949}{(m + 15.9949)}$$

$$\frac{B}{B'} = \frac{3.84235}{3.67337} = 1.046$$

$$1.046 = \frac{27.9949}{12 \text{ x } 15.9949} = \frac{m \text{ x } 15.9949}{(m + 15.9949)}$$

Simplifying

$$m = 13.001$$

$$\therefore \text{Atomic Weight of } 13_C \text{ is } 13.001$$

4. The observed rotational spectrum of HF shows the $J = 0 \rightarrow J = 1$ absorption at $41.11 cm^{-1}$, the spacing between adjacent absorptions is $40.08 cm^{-1}$ around $J = 5 \rightarrow J = 6$ transition and only $37.81 cm^{-1}$ around $J = 10 \rightarrow J = 11$ transition. Calculate B values and I values from these three given data. What explanation can you give for this variation?

   Soln :

   Around $J = 0 \rightarrow J + 1$, $2B = 41.11 cm^{-1}$, $B = 20.56 cm^{-1}$

   Around $J = 5 \rightarrow J + 6$, $2B = 40.08 cm^{-1}$, $B = 20.04 cm^{-1}$

   Around $J = 10 \rightarrow J + 11$, $2B = 37.81 cm^{-1}$, $B = 18.91 cm^{-1}$

$$B = \frac{h}{8\pi^2 IC}$$

$B = 2056 m^{-1}$ gives,

$$I = \frac{6.626 x 10^{-34} J..S}{8\pi 2 \text{ x } 2056 m^{-1} (3 \text{x} 10^8 m/s)}$$

$$= 1.362 x 10^{-47} kg.m^2$$

$B = 2004 m^{-1}$ *gives,*

$$I = 1.3971 \text{x} 10^{-47}\ kg.m^2$$

$$B = 1891 m^{-1}\ gives,$$

$$I = 1.481 \text{x} 10^{-47}\ kg.m^2$$

Including centrifugal distortion, the expression for the frequency of a transition is

$$\bar{\gamma} = 2B(J+1) - 4D(J+1)^2$$

As the term $4D(J+1)^3$ is always +ve, the separation between energy levels decreases as J increases. In other words, in the excited states the amplitude of the vibration of the atoms are expected to be larger which increases the moment of intertie $I = \mu r^2$.

Unit – II

Infrared Spectroscopy

2.1 I R Spectroscopy:-

Vibrational spectra are due to transitions between vibrational levels within the same electronic level which fall in the infrared region.

2.2 Vibratonal energy of a diatomic molecule :-

Consider a mass m connected to a stretched spring of force constant k whose other end is fixed. The mass excutes simple harmonic motion with a characteristic or fundamental frequency

$$\gamma_0 = \frac{1}{2\pi}\sqrt{\frac{k}{m}} \tag{2.1}$$

Consider a diatomic molecule with masses m_1 and m_2 then the characteristic frequency.

$$\gamma_0 = \frac{1}{2\pi}\sqrt{\frac{k}{\mu}} \tag{2.2}$$

Here m is replaced by reduced mass $\left(\mu = \frac{m_1 m_2}{m_1 + m_2}\right)$ of the system,

Quantum mechanically, the vibrational energy of such a harmonic system is given by

$$E_V = \left(V + \frac{1}{2}\right) h\gamma_0 \qquad V = 0,1,2,\ldots\ldots\ldots\ldots \tag{2.3}$$

Where V is the virbational quantum number. Expressing the energy in cm^{-1}

$$\varepsilon_V = \frac{E_V}{hc} = \left(V + \frac{1}{2}\right)\frac{\gamma_0}{C} \quad = \quad \left(V + \frac{1}{2}\right)\overline{\gamma_0} \quad cm^{-1} \tag{2.4}$$

Where γ_0 is the wave number in cm^{-1} units. These energy levels are equally spaced and the energy of lowest state (ie. $V = 0$)

$$\varepsilon_0 = \frac{1}{2}\bar{\gamma}0 \tag{2.5}$$

is called the *Zero – point energy*.

In a diatomic molecules, the actual potential curve is not of the simple harmonic type but given by

$$U(r) = D_e\left[1 - \exp\left[-a(r - r_e)\right]\right]^2 \tag{2.6}$$

Where D_e is the dissociation energy, a is a constant for the given molecule and r_e is the internuclear distance corresponding to $U(r)=0$. This potential function is due to P.M.Morse and is called the Morse function. Fig. 2.1 shows the shape of this function.

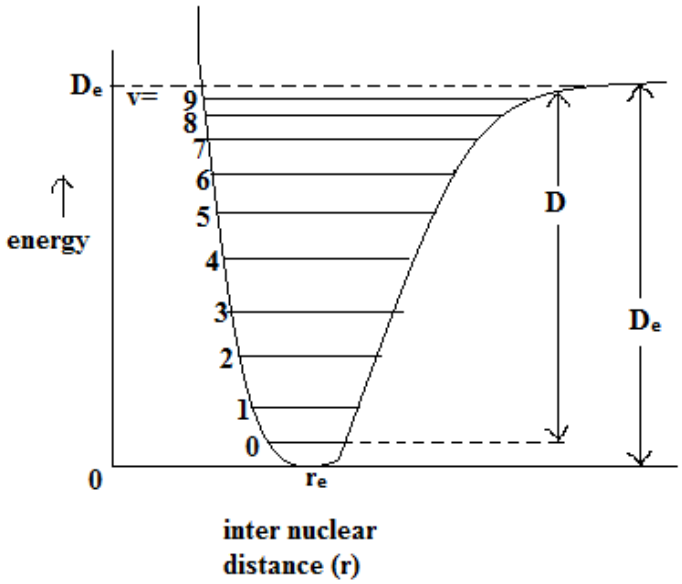

Fig.2.1 The Morse curve and the energy levels of a diatomic molecule

With the potential in Eq.(2.6), the Schroedinger equation of such an anharmonic oscillator gives the allowed vibrational energy eigenvalues.

$$\varepsilon_V = \left(V+\frac{1}{2}\right)\bar{\gamma}_e - \left(V+\frac{1}{2}\right)^2 x_e\,\bar{\gamma}_e + \left(V+\frac{1}{2}\right)^3 y_e\,\bar{\gamma}_e + \ldots. \tag{2.7}$$

Where x_e and y_e are anharmonicity constants which are very small and positive. Retaining the first anharmonic term

$$\varepsilon_V = \left(V+\frac{1}{2}\right)\bar{\gamma}_e - \left(V+\frac{1}{2}\right)^2 x_e\,\bar{\gamma}_e\ cm^{-1} \tag{2.8}$$

As x_e is +ve, the effect of anharmonicity is to crowd and more closely the virbational levels. From Eq. (2.8).

$$\varepsilon_{V+1} - \varepsilon_V = \bar{\gamma}_e - 2x_e\,\bar{\gamma}_e\,(V+1)\,cm^{-1} \tag{2.9}$$

The exact Zero point energy is

$$\varepsilon_0 = \frac{1}{2}\left(1-\frac{1}{2}x_e\right)\bar{\gamma}_e \tag{2.10}$$

The transition between the vibrational levels gives the vibrational spectrum of a molecule. It is observed in the region $50-4000 cm^{-1}$

2.3 Infrared selection rules:-

The vibrational quantum number change $\Delta V = \pm 1$ under harmonic approximation. For anharmonic oscillator, $\Delta V = \pm 1, \pm 2, \pm 3.....$

In addition, the symmetry of the molecule also restricts the activity of vibrations. Homonuclear diatomic molecules have no dipole moment and they have no change in dipole moment vibration. Hence vibrational spectra are observation only in the case of heteronuclear diatomic molecules. Vibrational spectra are usually studies in absorption and hence $\Delta V = \pm 1,$ is the part that is important in the above selection rule.

2.4 Vibrating Diatomic molecule:-

For the harmonic vibration, the energy of a vibrational level is given by

$$\varepsilon_V = (V + \frac{1}{2})\ \bar{\gamma}_0\ cm^{-1} \tag{2.11}$$

The selection rule $\Delta V = \pm 1$ allows transition between any two adjacent levels. The frequency of the transition from $V \to V+1$ is given by

$$\bar{\gamma} = (V + \frac{3}{2})\ \bar{\gamma}_0 - (V + \frac{1}{2})\ \bar{\gamma}_0 = \bar{\gamma}_0 \tag{2.12}$$

ie all transitions lead to the same frequency.

For anharmonic vibration, the energy of a vibraional spectrum is given by

$$\varepsilon_V = \left(V + \frac{1}{2}\right)\ \bar{\gamma}_e - \left(V + \frac{1}{2}\right)^2 x_e\ \bar{\gamma}_e\ cm^{-1} \tag{2.13}$$

and the selection rule is $\Delta V = \pm 1, \pm 2, \pm 3.....$ from Eq. (2.13) the frequencies of the first few transitions are $V = 0 \to V = 1$ (fundamental absorption).

$$\bar{\gamma}_{0\to 1} = \left(1+\frac{1}{2}\right)\ \bar{\gamma}_e - \left(1+\frac{1}{2}\right)^2 x_e\ \bar{\gamma}_e - (\frac{1}{2}\bar{\gamma}_e - \frac{1}{4}x_e\ \bar{\gamma}_e)$$

$$= \bar{\gamma}_e - (1 - 2x_e) cm^{-1} \tag{2.14}$$

$V = 0 \to V = 2$ (first overtone)

$$\bar{\gamma}_{0\to 2} = \left(2+\frac{1}{2}\right)\ \bar{\gamma}_e - \left(2+\frac{1}{2}\right)^2 x_e\ \bar{\gamma}_e - (\frac{1}{2}\bar{\gamma}_e - \frac{1}{4}x_e\ \bar{\gamma}_e)$$

$$= 2\bar{\gamma}_e - (1-3x_e)cm^{-1} \qquad (2.15)$$

$V = 0 \rightarrow V = 3$ (second overtone) :

$$\bar{\gamma}_{0\rightarrow 3} = \left(3+\frac{1}{2}\right)\bar{\gamma}_e - \left(3+\frac{1}{2}\right)^2 x_e\ \bar{\gamma}_e - \left(\frac{1}{2}\bar{\gamma}_e - \frac{1}{4}x_e\ \bar{\gamma}_e\right)$$

$$= 3\bar{\gamma}_e - (1-4x_e)cm^{-1} \qquad (2.16)$$

So far we gave ignored transitions from $V = 1$ to higher states. If the temperature of the sample is high, or if the $V = 1$ level is not far separated for the $V = 0$ level, the population of the $V = 1$ state may be appreciable. The wavenumber of the transition $V = 1 \rightarrow V = 2$ is given by

$$\bar{\gamma}_{1\rightarrow 2} = \left(2+\frac{1}{2}\right)\bar{\gamma}_e - \left(2+\frac{1}{2}\right)^2 x_e\ \bar{\gamma}_e - \left[\left(1+\frac{1}{2}\right)\bar{\gamma}_e - \left(1+\frac{1}{2}\right)^2 x_e\ \bar{\gamma}_e\right]$$

$$= \bar{\gamma}_e - (1-4x_e)cm^{-1} \qquad (2.17)$$

If this absorption is excited, it will be observed very close to and on the low frequency side of the fundamental as $\bar{\gamma}_{0\rightarrow 1}$ appears at $\bar{\gamma}_e(1-2x_e)$. Such weak absorptions are usually referred to as *hot bands* since high temperature is one of the conditions for their appearance. A hot band will increase in intensity as the temperature of the sample is increased. Fig. 2.2 illustrates the fundamental, overtones and hot bands transitions.

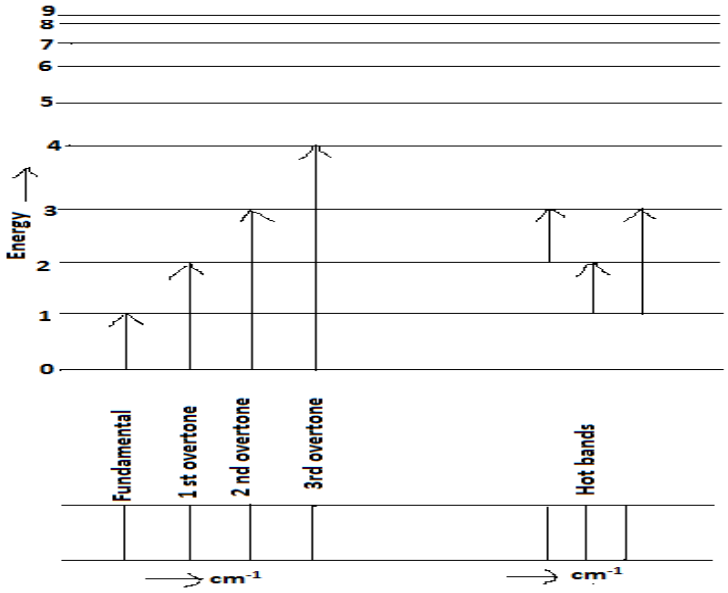

Fig.2.2 Energy levels showing the fundamental, overtones and hot bands

2.5 Diatomic vibration rotator:

A molecule rotates while executing vibration and therefore rotational energy changes occur also accompany vibrational energy change. Consequently each vibrational band is found to contain rotational fine structure. As the energies of vibraional and rotational motions differ considerably, a diatomic molecule can execute both rotations and vibrations considerably. Excluding electronic energy

$$\varepsilon_{total} = \varepsilon_{rot} + \varepsilon_{vib}$$

ie.,

$$\varepsilon_{j,V} = \varepsilon_j + \varepsilon_V$$

But we know

$$\varepsilon_j = BJ(J+1) - DJ^2(J+1)^2$$

and

$$\varepsilon_V = \left(V+\frac{1}{2}\right)\ \bar{\gamma}_e - \ \left(V+\frac{1}{2}\right)^2 x_e\ \ \bar{\gamma}_e\ cm^{-1}$$

$$\therefore \varepsilon_{j,V} = BJ(J+1) - DJ^2(J+1)^2 + (V+\frac{1}{2})\bar{\gamma}_e - \left(V+\frac{1}{2}\right)^2\ x_e\ \ \bar{\gamma}_e\ cm^{-1} \qquad (2.18)$$

Where $J = 0,1,2.....$ and $V = 0,1,2.....$

The selection rules for the combined motions are the same as those for separate motion, that is

$$\Delta V = \pm 1, \pm 2, \pm 3....., and \quad \Delta J = \pm 1, \qquad (2.19)$$

Consider the vibration transition $V = 0 \to V = 1$. Assuming B and D the same for both $V = 0$ and $V = 1$ states and denoting upper state by single prime and lower state by double prime.

$$\bar{\gamma} = B\left[J'(J'+1) - J''(J''+1) - D\left[J'^2(J'+1)^2 \_ - J''^2(J''+1)^2\right]\right]$$

$$+\left(\frac{3}{2}\bar{\gamma}_e - \frac{9}{4}x_e\bar{\gamma}_e\right) - \left(\frac{1}{2}\bar{\gamma}_e - \frac{1}{4}x_e\bar{\gamma}_e\right) cm^{-1}$$

$$\bar{\gamma} = \bar{\gamma_e}(1-2x_e) + B(J'-J'')\ (J'+J''+1) - D\left[J'^2(J'+1)^2 \_ - J''^2(J''+1)^2\right] cm^{-1}$$

Use of the selection rule $\Delta J = \pm 1, ie\ \ j'-J'' = +1,$ gives

$$\bar{\gamma}_R = \bar{\gamma_0}\ + 2B(J''+1) - 4D\ (J''+1)^3\ cm^{-1} \qquad (2.20)$$

$$\Delta J = -1, ie\ \ j'-J'' = -1, \text{gives}$$

$$\bar{\gamma}_P = \bar{\gamma_0}\ - 2B(J'+1) + 4D(J'+1)^3\ cm^{-1} \qquad (2.21)$$

Where $\bar{\gamma}_0 = \bar{\gamma}_e\ ((1-2x_e)$ which is the frequency of the $V = 0 \to V = 1$ transition.

Lines corresponding to $\Delta J = -1$ are called the *P branch* and those corresponding to $\Delta J = +1$ are referred to as *R branch*. The frequency $\bar{\gamma}_0$ is called the *band centre* or *band origin*. Eqs. (2.20) and (2.21) may be combined into a single equation as

$$\bar{\gamma}_{P,R} = \bar{\gamma}_0 + 2Bm - 4Dm^3 \ cm^{-1}, m = \pm 1, \pm 2, \pm 3 \ldots\ldots \tag{2.22}$$

Where m replace $J''+1$ in Eq. (2.20) and $J'+1$ in Eq. (2.21). It takes +ve values for R branch and –ve values for P branch. Usually D is extremely small and in such cases

$$\bar{\gamma}_{P,R} = \bar{\gamma}_0 + 2Bm \ cm^{-1} \tag{2.23}$$

The vibration–rotaion spectrum Eq. (2.23) will have both P and R branches each consisting of equally spaced lines with separation 2B, the P branch appearing on the low frequency side. Fig.2.3 represents the rotational levels of the vibrational levels $V = 0$ and $V = 1$ along with the P and R branch transitions.

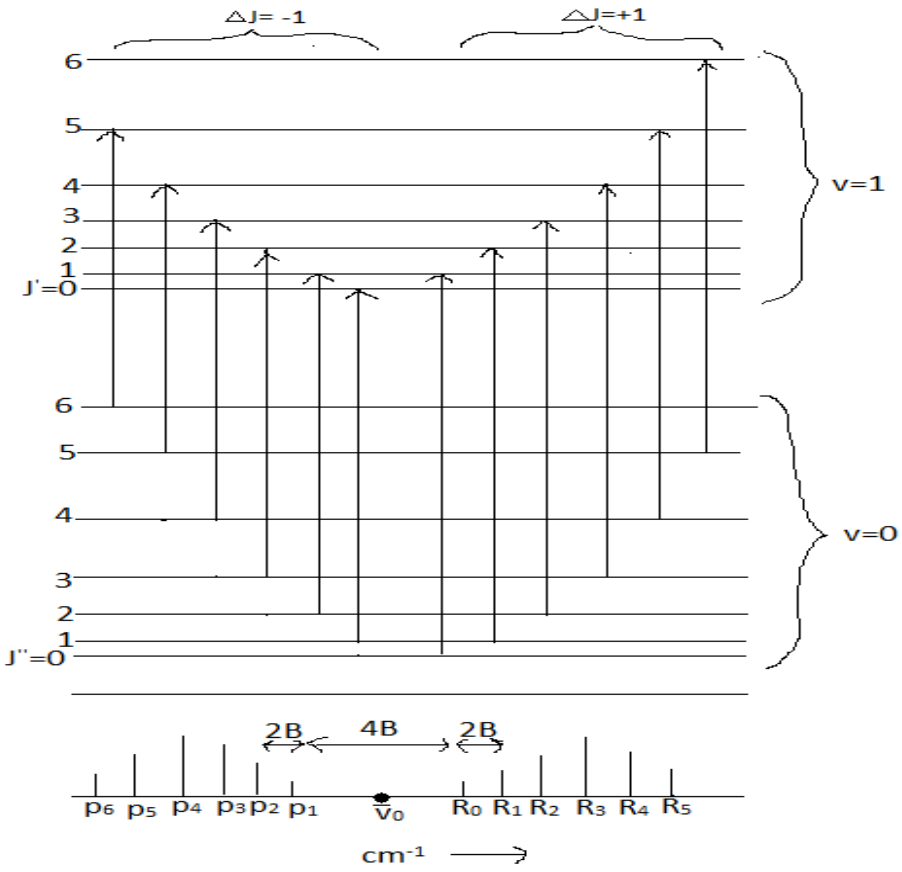

Fig. 2.3: Rotational energy levels of the vibrational states $V = 0$ and $V = 1$ and the rotation -vibration transition of a diatomic molecule.

For maximum population and hence the maximum intensity of transition occurs at the value of *m* is

$$m = \sqrt{\frac{KT}{2hcB}} + \frac{1}{2} \quad (\therefore m = J + 1) \tag{2.24}$$

$$\therefore \bar{\gamma}_{\max.\text{int}} = \overline{\gamma_0} \pm 2B \left(\sqrt{\frac{KT}{2hcB}} + \frac{1}{2} \right) \tag{2.25}$$

Where the + sign is for R branch and –ve sign is for P branch. The separation between the maxima in the P and R branches is

$$\Delta\bar{\gamma} = 4B \left(\sqrt{\frac{KT}{2hcB}} + \frac{1}{2} \right) = \sqrt{\frac{8KTB}{hc}} + 2B$$

This procedure offers a method to estimate the rotational constant B.

2.6 Symmetry of rotation–vibration band:-

The asymmetry shape of the potential energy curve increases the average internuclear distance as the vibrational quantum number V increases. This in turn increases the moment of inertia and decreases the rotational constant B. However, we assumed the same value of B for both $V = 0$ *and* $V = 1$ vibrational states.

Neglecting centrifugal distortion effects and assuming different rotational constants for the different state, the frequency of the $V = 0$ and $V = 1$ transition.

$$\bar{\gamma} = \overline{\gamma_0} + BJ'(J'+1) - B_0 J''(J''+1)$$

For R branch, $\Delta J + 1$ *or* $J' - J'' = +1$

$$\begin{aligned}
\bar{\gamma}_R &= \overline{\gamma_0} + B_1 (J''+1)(J''+2) - B_0 J''(J''+1) \\
&= \overline{\gamma_0} + (J''+1)\,(B_1 J'' + B_1 + B_1 - B_0 J'' - B_0 + B_0) \\
\bar{\gamma}_R &= \overline{\gamma_0} + (J''+1)\,[\,(B_1 - B_0) J'' + (B_1 - B_0) + (B_1 + B_0)\,] \\
&= \overline{\gamma_0} + (J''+1)(B_1 - B_0) + (B_1 - B_0)\,(J''+1)^2\, cm^{-1}
\end{aligned} \tag{2.26}$$

$$J'' = 0,1,2,\ldots\ldots\ldots\ldots$$

Similarly for P branch

$$\bar{\gamma}_P = \overline{\gamma_0} - (J'+1)(B_1 - B_0) + (B_1 - B_0)\,(J'+1)^2\, cm^{-1} \tag{2.27}$$

$$J' = 0,1,2,\ldots\ldots\ldots\ldots$$

Eqs. (2.26) and (2.27) can be combined into the single expression,

$$\bar{\gamma}_{P,R} = \overline{\gamma_0} + (B_1 + B_0)m + (B_1 - B_0)\ m^2\, cm^{-1} \tag{2.28}$$

Where $m = \pm 1, \pm 2, \pm 3, \ldots$ and m is +ve for R branch and negative for P branch. If $B_1 = B_0$, Eq.(2.28) reduces to the symmetric case (Eq.(2.23)).

For the case $B_1 < B_0$, $(B_1 - B_0)\ m^2$ is always –ve irrespective of the sign of m and the magnitude increases as m increases. As the first two terms are +ve, the effect of this term is to *crowd the rotational lines* of the R branch with increasing m. For the P branch lines, the second and third terms are –ve and the lines become *more widely spaced*.

2.7 Vibration of polyatomic molecules :

A molecule of n atoms has $3n$ degrees freedom. A nonlinear molecule of n atoms has $3n-6$ degrees of freedom. If the molecule is linear, there is no rotation about the bond axis and it will have $3n-5$ degrees of freedom. The $(3n-6)/(3n-5)$ vibrations are called the *internal vibrations* or *normal vibrations* or *fundamental vibration* of the molecule.

A normal vibration is defined as a molecular motion in which all the atoms move in phase and with the same frequency. During a normal vibration, the centre of gravity of the molecule remains unchanged. Since a molecule having n atoms has $n-1$ bonds, out of the $(3n-6)/(3n-5)$ vibrations, $(n-1)$ would be bond stretching and $(2n-5)/(2n-4)$ would be deformation vibrations.

(i) Normal vibrations of CO_2 and H_2O molecules:

The CO_2 molecule is linear and will have 4 normal vibrations. They are depicted in Fig.2.4. The first and second vibrations are completely symmetric. Hence, they are called respectively the symmetric stretching and symmetric bending modes. These two vibrations are unchanged in character when the molecule is rotated by 180° about an axis perpendicular to the bond axis and passing through the carbon atoms

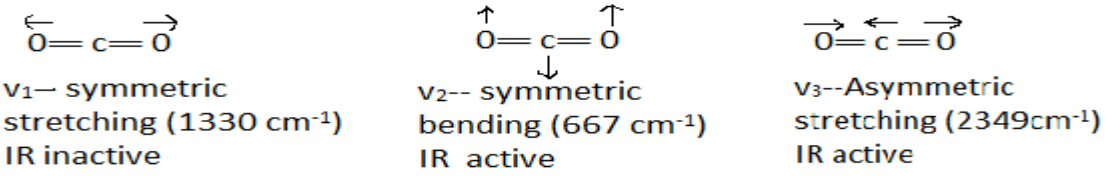

Fig.2.4. The normal vibrations of CO_2 molecule.

The normal vibrations are labelled as γ_1, γ_2 and γ_3 (Fig.2.4). The γ_2 vibration actually consists of 2 vibrations – one in the plane of the paper and the other in a plane perpendicular to it. Hence it is doubly degenerate. The observed vibraional frequencies are given in brackets. The three normal modes of the nonlinear triatomic water molecule are as shown in Fig.2.5.

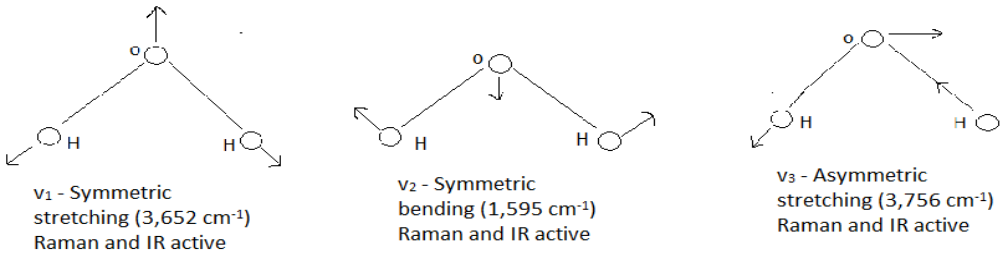

Fig.2.5 The normal modes of water molecules

2.8 Rotation–vibration spectra of polyatomic molecules

The rotaion – vibration spectra of diatomic molecules give rise to equally spaced lines for P and R branches in the first approximation. For the vibrations to be active, there must be a change of dipole moment during the vibration. For complex molecules, vibrations can be divided into the categories – vibrations causing a dipole change (i) parallel to the major axis of rotational symmetry and (ii) perpendicular to the major axis of rotational symmetry. There are called *parallel* and *perpendicular* vibrations. Often the selection rules are different for parallel and perpendicular vibrations. The selection rules also depend on the shape of the molecules.

(i) Linear molecules :- The selection rules of the parallel vibrations $\Delta V = \pm 1$ and $\Delta V = \pm 1$ are identical with those for diatomic molecules. The spectra will have the P and R branches with almost equally spaced lines. The spacing between lines is likely to be less and moment of inertia is expected to be large. When moment of inertia is extremely large, the individual lines of the branches coalesce resulting in two lines.

For perpendicular vibrations, the spectrum will have P, Q and R branches. If the B values of upper and lower vibrational states are equal, all $\Delta J = 0$ transitions give line at the band centre resulting in an intense Q branches lines. This line is likely to be broadened a little as the B values of the involved stats are likely to differ slightly. Polyatomic molecules not having a permanent dipole moment do not show pure rotational spectrum. However such molecules show vibraional spectrum in the IR region and sometimes with the rotational fine structure. In such cases, one can estimate the rotational constant B which gives the bond length value. The rotational energy levels and the transions are represented in Fig.2.6.

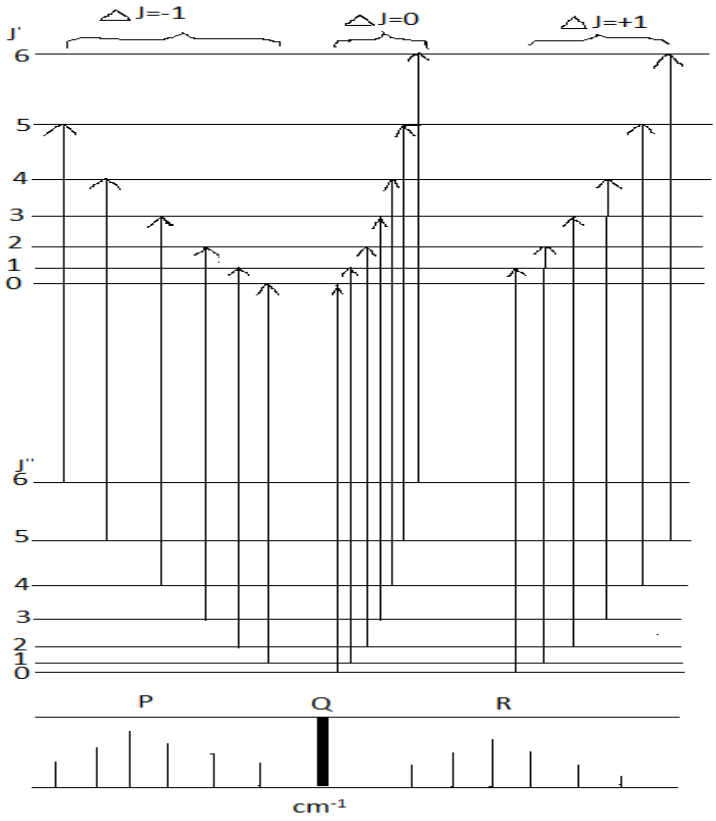

Fig.2.6 The rotational levels for two-vibrational states and the transition showing the perpendicular vibrations of a linear polyatomic molecule.

(i) Symmetric top molecules :-

The selection rules for parallel and perpendicular vibrations are different in symmetric top also. The vibration – rotation energy levels of a symmetric top is given by

$$\varepsilon_{j,V} = \left(V+\frac{1}{2}\right)\bar{\gamma}_e - \left(V+\frac{1}{2}\right)^2 x_e\,\bar{\gamma}_e + BJ(J+1)+(A-B)k^2\,cm^{-1} \tag{2.29}$$

Where A $=\frac{h}{8\pi^2 I_a C}$ and $B=\frac{h}{8\pi^2 I_b C}$, I_a and I_b are the principal moments of inertia of the symmetric top. For parallel vibrations, the selection rules are

$$\Delta V=\pm 1 \quad \Delta J=0,\pm 1, \ \Delta k=0 \tag{2.30}$$

As $\Delta k=0$, the spectrum will have features similar to those observed for the perpendicular vibrations of linear molecules. For perpendicular vibrations, the selection rules.

$$\Delta V=\pm 1 \quad \Delta J=0,\pm 1, \ \Delta k=\pm 1 \tag{2.31}$$

lead to the following frequencies for the three branches.

R branch :-

$$\Delta J = \pm 1,\ \Delta k = \pm 1$$
$$\bar{\gamma}_R = \overline{\gamma_0} + 2B(J+1) - (A-B)(1 \pm 2k)\, cm^{-1}. \tag{2.32}$$

P branch :

$$\Delta J = -1, \qquad \Delta k = \pm 1$$
$$\bar{\gamma}_P = \overline{\gamma_0} + 2B(J+1) - (A-B)(1 \pm 2k)\, cm^{-1}. \tag{2.33}$$

Q branch :-

$$\Delta J = 0, \quad \Delta k = \pm 1$$
$$\bar{\gamma}_Q = \overline{\gamma_0} + (A-B)(1 \pm 2k)\, cm^{-1}. \tag{2.34}$$

Since for each J value, k has the allowed values $-J, -J+1, \ldots\ldots J-1, J$, we expect many sets of P and R branches. The Q branch also consists of a series of lines on both sides of $\overline{\gamma_0}$ with 2(A-B) separation between lines.

2.9 Interpretation of vibrational spectra – Group frequencies :-

The vibrational spectrum of a molecule consists of two major regions, the group frequency region and finger print region. Group frequencies are vibrations that are associated in the certain structural units such as - $-CH_3, -NH_2, -C \equiv N$, etc and appear in fairly constant regions in the spectrum. The approximate constancy of the position of group frequencies form the basic for the structural analysis of compounds. The region $900 - 1450\, cm^{-1}$ is very rich in absorption bands and contains mainly bendings and certain stretching vibrations. Though molecules having similar groups show very similar spectra out side this region, they show bands typical of the molecule in this region. Hence the name finger print region. The factor affecting group vibrations are

(i) Internal factors involving changes in atomic mass, vibrational coupling, resonance filed effects, hydrogen bonding, etc.,

(ii) External factors involving physical state (gas, liquid, solid, solution, solvent and concentration) and temperature. Often, one factor is isolated from the rest, so that its influence upon are particulars frequency can be studied along with intensities.

2.10 IR Spectrophotometer – Instrumentation

The essential components of IR spectrophotometer are : (1) source of radiation (ii) fore optics, (iii) monochromator (iv) detector with an amplifier and (v) recorder. The block diagram of a double beam IR spectrophotometer is shown in Fig. 2.7.

In a double beam instruments, the beam is split into two parts, one is directed through the sample cell and the other through the references cell. The two beams are then compared either continuously or alternatively many times a second. Thus in a double beam instrument, the fluctuations in the source intensity, the detector response an amplifier gain are compensated by the observing the ratio signal between sample and reference.

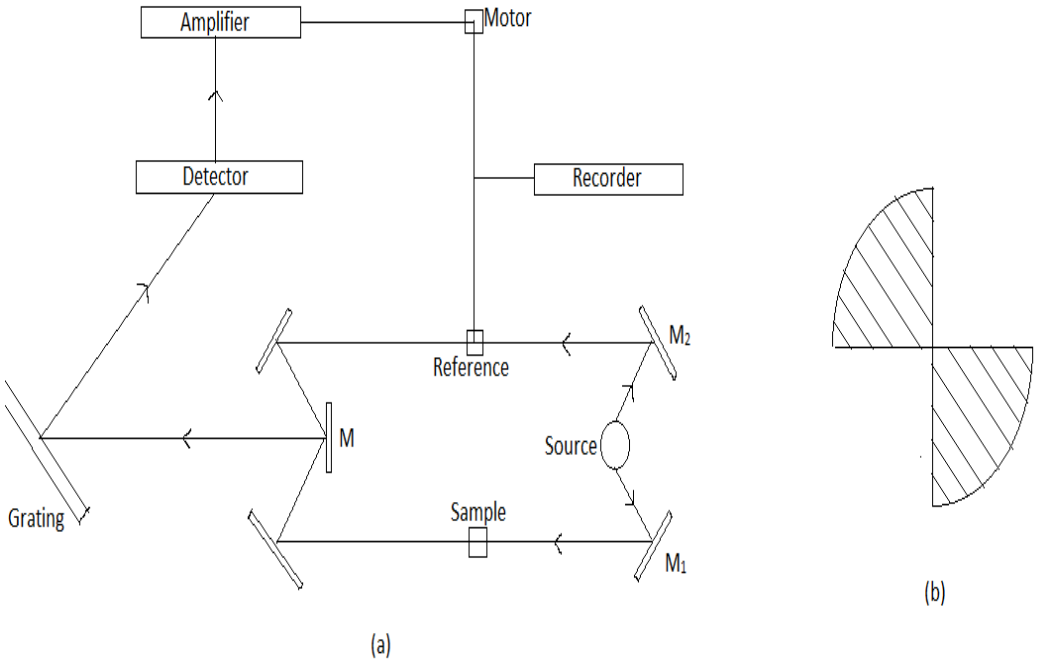

Fig.2.7 (a) Schematic diagram of IR spectrometer (b) View of the sector mirror

(i) Sources of radiation :-

Ideal source is black body radiator. The most commonly used sources are the Globar filament and the Nernst glower

(ii) The fore optics:

The fore optics consists of the source, mirror M_1 and M_2 and a rotating mirror/ chopper M. M_1 and M_2 divide the source radiation into two equivalent beams, of which one passes through the sample and the other passes through an equivalent path and is called the reference beam. The two beams meet at the rotating sector mirror /chopper. The rotating mirror alternately allows the sample beam through the spaces or reflects the reference beam with a predetermined period to the monochromator slit. Consequently, the detector receives the sample beam and reference beam alternately.

(iii) Monochromator :

It is the most important part of the spectrometer as its splits the polychromatic radiation into its components. This is achieved by using prisms or gratings or both.

(iii) Detector :-

Infrared detectors measure the radiant energy by its heating effect. Thermopiles, bolometers and Golay cells are used as detectors.

(v) The recorder :-

The amplified signal in used to move an alternator (comb) which cuts down the radiation coming out of the referencen beam until energy balance is restored. This is achieved by a motor which driver the comb into the reference beam when an absorbing band is encountered and out of the beam when the band is passed over.

2.11 Sample Handling techniques :-

Three different techniques are employed commonly in recording the spectra.

(i) Mull technique :-

In this method, a slurry or mull of the substance is prepared by grinding it into a fine powder and dispersing it in the mulling agent such as paraffin oil (nujol), hexachlorobutadiene and perfluorokerosene (fluorotube). It is smeared between two cell windows which are then held together. The mull spreads out as a very thin film and window setup is placed in the path of the IR beam. The main disadvantages of this technique is the interference due to the absorption bands of the mulling agent. For best results the size of the sample particles must be less than that of the wave length of radiation used.

(ii) Pellet technique :-

The first step in this method is to grind the sample very finely with potassium bromide. The mixture is then pressed into transparent pellets with the help of suitable dies. This is then placed in the IR beam in a suitable holder.

Advantages :-

1. Absence of interfering bands
2. Lower scattering losses
3. Higher resolution spectra
4. Possibility of storage for future studies.
5. Ease in examination.

The main disadvantages is that anomalous spectra may result from physical and chemical changes induced during grinding.

(iii) Solid films :-

Spectra of solids may also be recorded by depositing a thin film of a solid on a suitable window material. A concentrated layer of the solution of the substance is allowed to evaporate slowly in the window material forming a thin uniform film. Thickness can be adjusted by changing the concentration of the solution. Interference caused by multiple reflections between parallel surfaces affect the accuracy of measurements.

2.12 Fourier Transform Infrared Spectroscopy :-

(i) Principle :-

The conventional spectroscopy called the frequency domain spectroscopy, records the radiant power G(ω) as a function of frequency ω. In the time domain spectroscopy, the changes in radiant power f(t) is recorded as a function of time t. In a Fourier transform spectrometer, a time domain plot is converted into a frequency domain spectrum.

In mathematics, the Fourier transform of the function f(t) is defined by

$$G(\omega)=\frac{1}{\sqrt{2\pi}}\int_{-\omega}^{\alpha} f(t)\,e^{i\omega t}\,dt \qquad (2.35)$$

Then the inverse relation is

$$f(x)=\frac{1}{\sqrt{2\pi}}\int_{-\omega}^{\alpha} G(\omega)\,e^{-i\omega x}\,d\omega \qquad (2.36)$$

Equation (2.35) and (2.36) are said to form a Fourier transform pair.

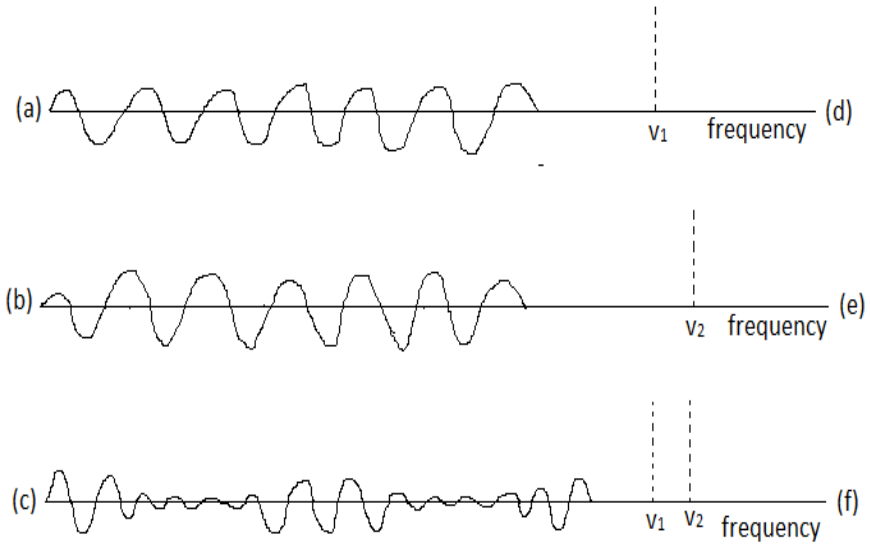

Fig.2.8 (a)n Sine wave (b) sine wave slightly differing frequency. (c) sum of the sine wave in (a) and (b); (d)-(f); the frequency domain spectra of the waves

To illustrate the use of Fourier transform, consider the superposition of two sine waves , Fig.2.8(a) and (b) of the same amplitude but of slightly different frequencies . Fig.2.8(c) represents the superposed wave. The Fourier transform of the individual sine waves and the superposed wave train gives the frequencies in the frequency domain and are represented in Fig.2.8(d), (e) and (f).

(ii) Interferometer arrangement :

The basic components of a Fourier Transform spectrometer are given in Fig.2.9.

The basic components of a Fourier transform spectrometer are given in Fig.2.9. The source is the usual glower operated at very high temperature. The Michelson interferometer consists of a source S, a beam splitter B and two plane mirrors, M_1 and M_2 (Fig.2.9) Mirror M_1 is fixed and M_2 is capable of to and fro movements. The beam splitter allows 50% of the radiation to mirror M_1 and the other 50% to mirror M_2 . The two beams are reflected back to B where they recombine with 50% going to the source and the other 50% going to the sample. For monochromatic source, if the path lengths BM_1B and BM_2B differ by an integral number including zero of wavelengths, one gets constructive interference of the two beams at B (bright beam). Destructive interference results when the difference in path lengths is half odd integral number of wavelengths.

.

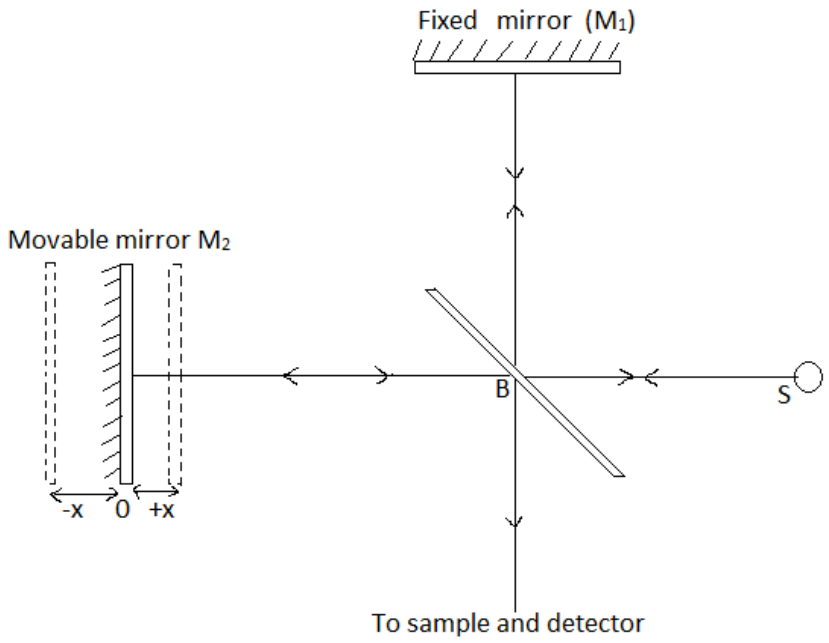

Fig.2.9 Interferometer arrangement of Fourier Transform spectrometer.

Thus, if mirror M_2 is moved towards or away from B, the sample and detector will see in alternation in intensity. If two different monochromatic frequencies γ_1 and γ_2 are used instead of one, a more complicated interference pattern would follow when M_2 is moved. A Fourier transform of the resultant signal would give the two originals with the appropriate intensities. Extending this, a whight light produces an extremely complicated interference pattern which can be transformed back to the original frequency distribution. The recombined beam if directed through a sample absorption will show up as gaps in the frequency distribution which on transformation gives a normal absorption spectrum, In the experiment, the detector signal is collected into a multichannel computer while mirror M_2 is moved. The computer then carriers out the Fourier transform of the stored data and plots it on a paper

UNIT – III

Raman Spectroscopy

3.1 Raman effect :-

The scattering of light has a slightly different frequency from that of incident light and there is a change in the atomic oscillations within molecule is called *Raman effect*.

If γ_1 *and* γ_2 are the frequencies of incident and that of scattered light, then the difference $\Delta\gamma = \gamma_i - \gamma_S$ is known as *Raman frequency*. The series of lines in the scattering of light is known as *Raman spectra*.

In the spectra of scattered radiation, the Raman lines appear in the spectrum on either side of the line of incident radiation with higher, as well as lower frequencies. The Raman lines on the lower frequency side are called *stokes lines*, ie, when $\gamma_i > \gamma_S$ and those on the higher frequency side are called *anti-stokes lines* ie, $\gamma_S > \gamma_i$. (Fig.3.1)

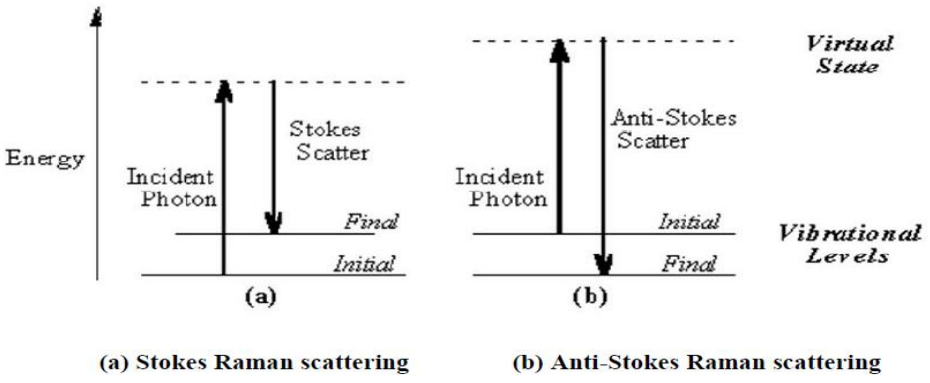

Fig.3.1 Energy level diagram for Raman scattering

3.2 Classical theory of Raman effect :-

If an atom or molecule is placed in an electric field, the electrons and nuclei are displaced. An induced dipole moment is produced in the molecule due to displacement of nuclei and electrons and the molecule is said to be polarized. The intensity of the scattered radiation can be deduced from the classical theory as shown in Fig.3.2.

If E is the strength of the electric field and μ is the magnitude of induced dipole moment, then,

$$\mu = \alpha E \qquad (3.1)$$

Where α is the polarizability of the molecule. The strength E of the electric field of an e.m. wave of frequency γ, can be expressed as

$$E = E_0 \sin 2\pi\gamma_0 t \tag{3.2}$$

From Eq. (3.1), $$\mu = \alpha E_0 \sin 2\pi\gamma_0 t \tag{3.3}$$

While arriving at an equation (3.3), no internal motion e.g. vibration and rotation of the molecule has been consider.

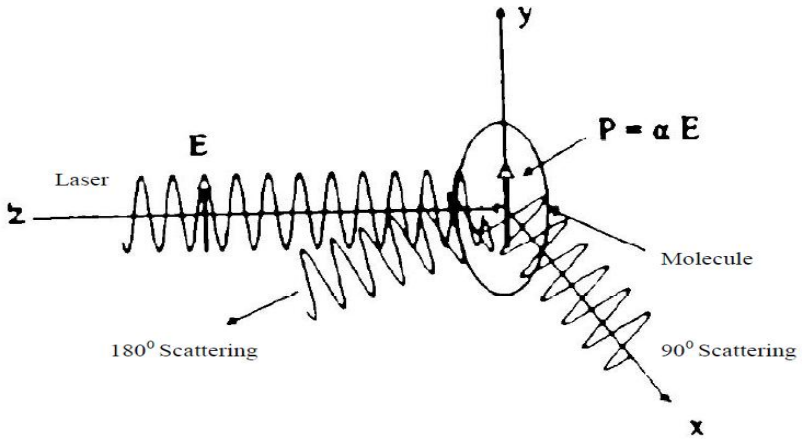

Fig.3.2 Polarization (p) induced in a molecule's slectron cloud by an incident optical electric filed (E).

Let us consider first the effect of vibration. Suppose thec molecule is diatomic, then as the two nuclei vibration along the line joining them, the polarizabiltiy (α) of the molecule will vary. The variation in polarizability α with small displacement x from equilibrium position is given by

$$\alpha = \alpha_0 + \beta \frac{x}{A} \tag{3.4}$$

Where α_0 is the equilibrium polarizability, β is the rate of variation of the polarizability with displacement and A is the vibrational amplitude. If the molecule executes simple harmonic motion, the displacement x can be express as

$$x = A\sin 2\pi\gamma_o t \tag{3.5}$$

Where γ_0 is the frequency of vibration of the molecule.

Therefore,

$$\alpha = \alpha_o + \beta \sin 2\pi\gamma_o t \tag{3.6}$$

Which when substituted in Eq.(3.3), gives,

$$\mu = \alpha_0 E_0 \sin 2\pi\gamma t + \beta E_0 \sin 2\pi\gamma t \sin 2\pi\gamma_0 t$$

$$= \alpha_0 E_0 \sin 2\pi\gamma t + \frac{1}{2}\beta E_0 \left[\cos 2\pi(\gamma - \gamma_0 t - \cos 2\pi(\gamma + \gamma_0)t\right] \tag{3.7}$$

Thus, induced dipole moment oscillates with frequencies γ (equal to the frequencies of the incident radiation, ie., Rayleigh scattering), $(\gamma + \gamma_0)$ and $(\gamma - \gamma_0)$. The last two frequencies are more and less then the frequency of incident radiation and predict the existence of Raman scattering.

(i) Rayleigh line $(\gamma = \gamma_0)$

(ii) Raman stokes lines $(\gamma - \gamma_0)$

(iii) Raman antistokes $(\gamma + \gamma_0)$

Now we consider the effect of rotation of molecule on polarizability. Expressing variation of α by an equation identical to equation (3.6), we get

$$\mu = \alpha_0 + \beta^1 \sin 2\pi\ (2\gamma_r)t \tag{3.8}$$

Where γ_r is the frequency of the rotation. Substituting Eq. (38) in Eq.(3.3) we get

$$\mu = \alpha_0 E_0 \sin 2\pi\gamma t + \beta^1 E_0 \sin 2\pi\gamma t \sin 4\pi\gamma_r t$$

$$= \alpha E_0 \sin 2\pi\gamma t + \frac{1}{2}\beta^1 E_0 \left[\cos 2\pi(\gamma - 2\gamma_r)t - \cos 2\pi(\gamma + 2\gamma_r)t\right]$$

For above expression, we find that the frequencies of Raman lines will be $(\gamma + 2\gamma_r), (\gamma - 2\gamma_r), \gamma$.

3.3 Quantum theory of Raman effect :-

In explaining Raman scattering, the incident radiation of frequency γ_0 is considered as a stream of particles (Photons) undergoing collision with molecules. If the collision is perfectly elastic there will be not be any exchange of energy between the photons and the molecule. However, there will be exchange of energy between the two if the collision is inelastic. The

molecule can gain or lose energy equal to the energy difference ΔE between any two of its allowed states. If the molecules gains energy, the scattered photons will have frequency $\gamma_0 - \gamma_m$ where $\gamma_m = \frac{\Delta E}{h}$ (stokes line). On the other hand if it loses energy the scattered photon will have the frequency $\gamma_0 + \gamma_m$ (anti – stokes lines). The different processes giving rise to Rayleigh, stokes and antistokes lines are illustrated in Fig.3.3.

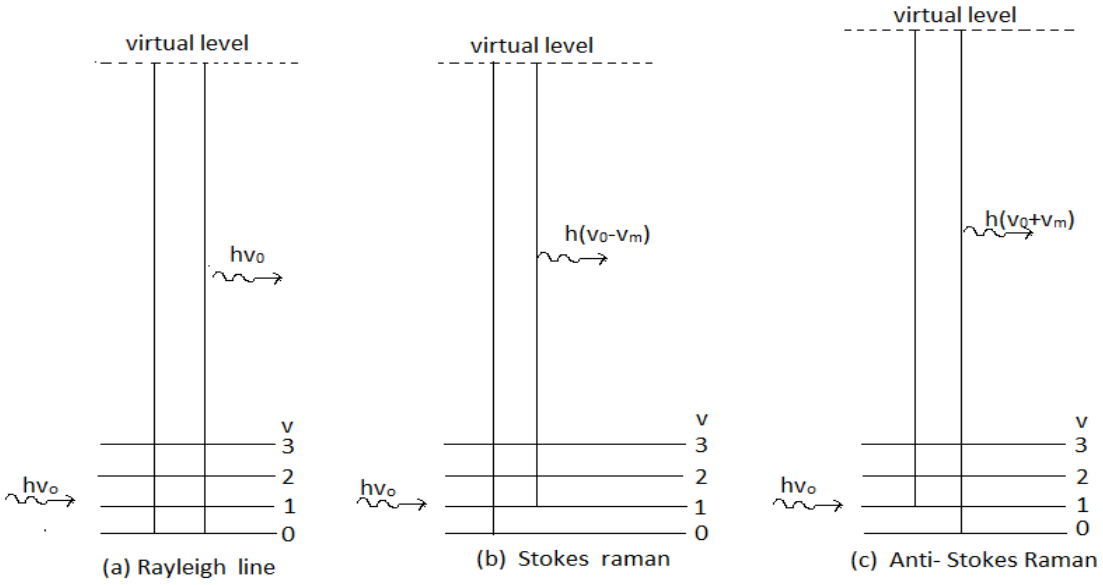

Fig.3.3 Energy level diagram showing Rayleigh and Raman lines. Γ = 0,1,2,3,... are the vibrational levels of the ground electronic state.

When a system interacts with a radiation of frequency γ_0 it may make an upward transition to virtual state system. Most of the molecules of the system return to the original state from the virtual state giving the Rayleigh scattering. However, a very small fraction returns to state of higher and lower energies giving rises to stokes and Anti stokes line respectively. If the virtual state of the system coincides with the real state of the system, it wll lead to *resonance Raman effect.*

The intensity of a spectral line depends on number of factors, the most important being the initial population of the state from which the transition originates. The stokes lines

originating from $V=0$ and the anti-stokes from $V=1$ give the same Raman shift γ_m . Based on Baltzmann distribution for the population in states, the intensity ratio of stokes to anti-stokes is given by

$$\frac{I_S}{I_{AS}} = \exp \frac{h\gamma_m}{KT} \tag{3.9}$$

Where K is the Boltzmann constant and T is the temperature in Kelvin. By taking other factors in to account, Eq. (3.9) gives,

$$\frac{I_S}{I_{AS}} = \frac{(\gamma_0 - \gamma_m)^4}{(\gamma_0 + \gamma_m)^4} \exp \frac{h\gamma_m}{KT} \tag{3.10}$$

Anti – stokes lines have much less intensity than stokes lines.

3.4 Rotational Raman Spectra

(i) For Linear Molecule : The rotational energy levels of a linear molecule can be written as

$$\varepsilon_J = BJ(J+1)cm^{-1} \quad J = 0,1,2,3..... \tag{3.11}$$

Selection rule for rotational Raman spectra is

$$\Delta J = 0, \pm 2.$$

$\Delta J = 0$ corresponds to Rayleigh scattering. $\Delta J = -2$ may be ignored and $\Delta J = +2$ only allowed one, ie $\Delta J = J^1 - J^{11} = +2$ (S-branch). The frequency of rotational Raman lines,

$$\bar{\gamma} = \varepsilon_{J'=J+2} - \varepsilon_{J''=J} = B\,J^1(J^1+1) - B\,J^{11}(J^{11}+1) = B(4J+6) \tag{3.12}$$

During collision, if the molecule gains rotational energy from the photon, it gives rise to a series of lines on the low frequency side of the exciting line. Such spectral lines are the stokes lines. Raman spectra deals with the displacement each Raman line form the exciting line $\bar{\gamma}_0$. Hence we may write for stokes lines

$$\bar{\gamma} = \bar{\gamma}_0 - B(4J+6)cm^{-1} \tag{3.13a}$$

During collision, if the molecule gives energy to the photon, the S-branch lines appear on the high frequency side of the exciting line. These are the anti-stokes and their frequencies are given by

$$\bar{\gamma} = \bar{\gamma}_0 + B(4J+6)cm^{-1} \tag{3.13b}$$

Combining Eqs. (3.13a) and (3.13b), gives

$$\bar{\gamma} = \bar{\gamma}_0 \pm B(4J+6)cm^{-1} \tag{3.14}$$

Here +ve sign refers to anti-stokes and –ve sign to stokes line (Figure 3.4).

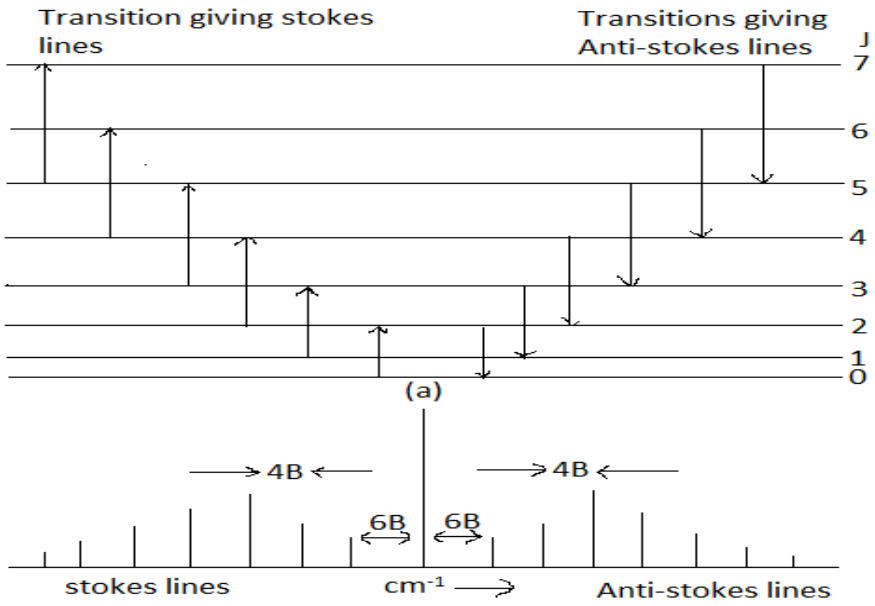

(b)

Fig.3.4: (a) The allowed transitions between rotational energy levels of a linear molecule (b). The predicated rotational Raman spectrum. The spectral lines are numbered according to their lower J values.

The Raman shift of the first stokes or anti-stokes from the exciting line is $6Bcm^{-1}$. The separation between successive lines on either side of the exciting line is 4B. The stokes and Anti-stokes lines appear with considerable intensity as all the rotational levels belong to $V=0$ vibration state which makes all the levels reasonably populated.

Already we know that, homonuclear diatomic molecule do not give an IR or microwave spectrum. However such molecule give pure rotational Raman spectra since the polarizabiltiy change during the rotational motion. Another interesting feature observed is the effect of nuclear spin on the spectra of molecules having centre of symmetry as in IR spectra. In which, levels with even J values are empty in molecules like O_2 and CO_2 (nuclear spin of oxygen is zero), and

therefore, transitions labelled 0,2,4,..... in Fig.3.4a) will be absent, consequently, a spacing of 8B between consecutive lines is observed instead of 4B.

(ii) Symmetric Top molecules :-

In symmetric top molecules, the rotation about the top axis does not produce a change in the polarizability whereas end over end rotation produces a change. The rotational energy levesl of a symmetric top molecule in given by

$$\varepsilon_{J_1K} = BJ(J+1)+(A-B)K^2, \quad J=0,1,2....., \; K=0,\pm1,\pm2, \tag{3.15}$$

The seletion rules are

$$\Delta K = 0, \; \Delta J = 0, \pm1, \pm2 \; (\text{for } k=0 \text{ states}, \; \Delta J = \pm 2 \text{ only})$$

Again $\Delta J = 0$ corresponds to Rayleigh scattering. As K represents the angular momentum about the top axis, $\Delta k = 0$ implies that rotations about the top axis are Raman inactive. Since $k = 0$ for the ground state, it is governed by the selection rule $\Delta J = \pm 1$ transitions are allowed.

We shall next consider the frequencies of the transitions. Consider $\Delta J = J^1 - J^{11} = 1$ only.

$$\varepsilon_{J+1,\,k} - \varepsilon_{J_1k} = B\,(J+1)(J+2)+(A-B)\,K^2 - B\,J\,(J+1)-(A-B)\,K^2$$

$$= 2B(J+1)\,cm^{-1}$$

When the molecules gain rotational energy from the photon we get stoke lines of frequencies

$$\bar{\gamma} = \bar{\gamma}_0 - 2B(J+1)\,cm^{-1}$$

and when molecules losses energy to photon we get anti- stokes lines frequencies.

$$\bar{\gamma} = \bar{\gamma}_0 + 2B(J+1)\,cm^{-1}$$

Hence, for $\Delta J = \pm 1$(R-branch), we have the frequencies of anti-stokes and stokes lines as

$$\overline{\gamma_R} = \bar{\gamma}_0 \pm 2B(J+1)\,cm^{-1}$$

The R branch lines appear at $4B, 6B, 8B, 10B.....cm^{-1}$ from the exciting line. Similar calculations for $\Delta J = \pm 2$ (S-branch) leads to anti-stokes and stokes lines of frequencies.

$$\overline{\gamma_S} = \bar{\gamma}_0 \pm B(4J+6)\,cm^{-1}$$

These lines appear at $4B, 6B, 8B, 10B.....cm^{-1}$, from the exciting line. The complete spectrum is illustrated in Fig.3.5

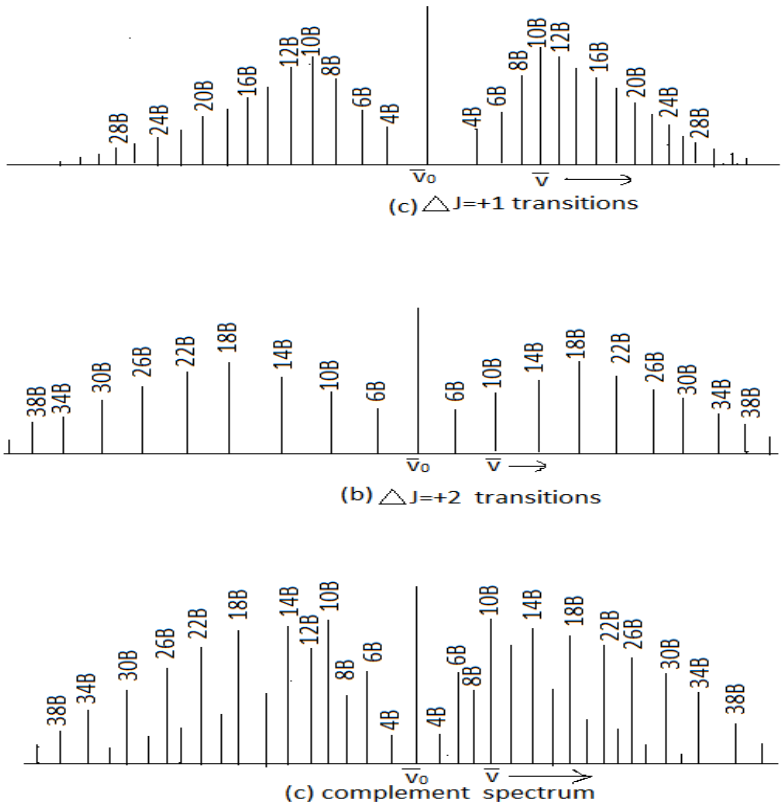

Fig.3.5 Rotational Raman spectrum.

3.5 Vibrational Raman Spectra:-

The vibrational energy of an anharmonic oscillator is given by

$$\varepsilon_V = \left(V+\frac{1}{2}\right)\ \bar{\gamma}_e - \ \left(V+\frac{1}{2}\right)^2 x_e\ \ \bar{\gamma}_e\ \ cm^{-1} \qquad (3.16)$$

$$V = 0,1,2,.....$$

Where $\bar{\gamma}_e$ is the equilibrium oscillation frequency of the anharmonic system and x_e is the anharmonicity constant. The selection rule Raman transition is

$$\Delta V = \pm 1, \pm 2, \pm 3,..... \qquad (3.17)$$

We need to consider only the $V = 0 \rightarrow V+1$ transition as the population in the $V = 1,2,3.....$ levels will be negligible. Also, since Raman scattering is very weak, overtones and combinations appear seldom in Raman spectra.

$$\varepsilon_1 - \varepsilon_0 = \left(\frac{3}{2}\bar{\gamma}e - \frac{9}{4}x_e \ \bar{\gamma}_e \right) - \left(\frac{1}{2}\bar{\gamma}e - \frac{1}{4}x_e \ \bar{\gamma}_e \right)$$

$$= \bar{\gamma}e(1-2x_e) \tag{3.18}$$

Corresponding to each active normal mode of vibration we will have the Raman frequencies.

$$\bar{\gamma} = \bar{\gamma}_0 \pm \bar{\gamma}_e(1-2x_e) \tag{3.19}$$

Again the minus sign corresponds to stokes lines and plus sign to anti – stokes lines. The rotational fine structure of vibrational Raman spectrum is resolved only in the case of light diatomic molecules. The vibration–rotation energy equation gives

$$\varepsilon_{V,J} = \left(V+\frac{1}{2}\right) \bar{\gamma}_e - \left(V+\frac{1}{2}\right)^2 x_e \ \bar{\gamma}_e + BJ(J+1)cm^{-1} \tag{3.20}$$

$$V = 0,1,2,3..... \quad J = 0,1,2,3.....$$

The rotational selection rule is $\Delta J = 0, \pm 2, \ V = 0 \rightarrow V = 1,$ $\Delta J = 0$ gives,

$$\Delta\varepsilon_{V,J} = \bar{\gamma}_e(1-2x_e)$$

This gives the Q-branch stokes lines

$$\overline{\gamma_Q} = \bar{\gamma}_0 - \bar{\gamma}_e(1-2x_e) \tag{3.21}$$

$V = 0 \rightarrow V = 1,$ $\Delta J = +2$

$$\Delta\varepsilon_{V,J} = \bar{\gamma}_e(1-2x_e) + B(J+2)(J+3) - BJ(J+1)$$

$$= \bar{\gamma}_e(1-2x_e) + B(4J+6)cm^{-1}, \quad J = 0,1,2...$$

This corresponds to energy gain by the molecule. Hence the frequency of the corresponding stokes lines will be

$$\bar{\gamma}_s = \bar{\gamma}_0 - \bar{\gamma}_e(1-2x_e) - B(4J+6)cm^{-1} \tag{3.22}$$

Where the subscript S stands for S branch ($\Delta J = +2$)

$V = 0 \rightarrow V = 1, \Delta J = -2$, gives,

$$\Delta\varepsilon_{V,J} = \bar{\gamma}_e(1-2x_e) + B(J^{11}-2)(J^{11}-1) - BJ^{11}(J^{11}+1)$$

$$\Delta\varepsilon_{V,J} = \bar{\gamma}_e(1-2x_e) - B(4J^{11}-2) \qquad J^{11} = 2,3.....$$

$$= \bar{\gamma}_e(1-2x_e) - B(4J-6) \qquad J = 0,1,2.....$$

In this case also there is gain of energy by the molecule, since the second term is very small compared to the first term. This also gives rise to the stokes lines.

$$\bar{\gamma}_{O,b} = \bar{\gamma}_0 - \bar{\gamma}_e (1-2x_e) - B(4J+6) \quad cm^{-1} \quad J = 0,1,2, \tag{3.23}$$

where the subscript O,b stands for O branch. The resulting spectrum is illustrated in Fig.3.6.

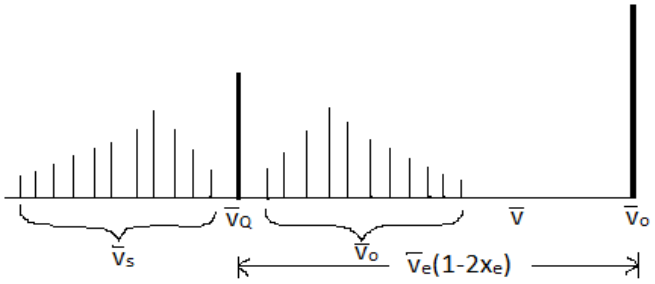

Fig 3.6: Rotaional structure of a stokes Raman line of a diatomic molecule having a vibrational frequency $\bar{\gamma}_e(1-2x_e)$.

3.6 Raman Spectrometer

(i) Source :- The first Raman spectrum of an organic compound was observed using sun as the source, a telescope as the receiver and human eye as the detector.

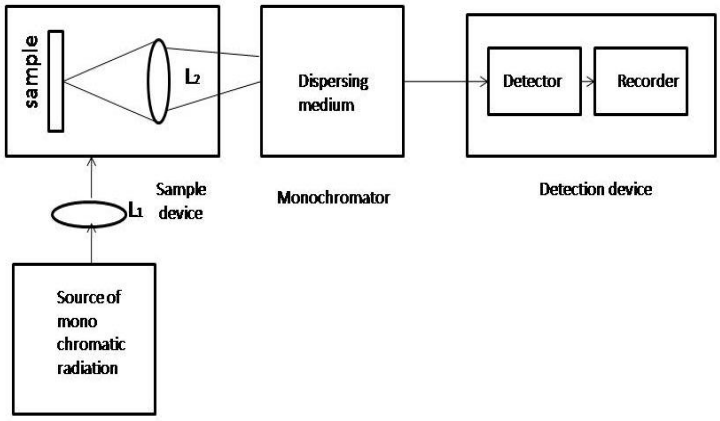

Fig.3.7 The schematics of Raman spectrometer

In the prelaser days, the commonly used sources were the 435.8 nm (blue) and the 253.6 nm (uv) emission lines of mercury vapour. These sources has some disadvantages. With the discovery of lasers, these disadvantages are minimized since laser is a highly–directional and intense laser. The schematics of a Raman spectrometer with a laser source are shown in Fig.3.7. The commonly used sources are He-Ne laser, (632.8nm), Argon ion laser (488 and 514.5 nm),

krypton (647.1, 568.2, 530.8, 520.8, 482.5, 476.2nm) and Argon krypton mixed laser (488.0, 514.5, 647.1 nm).

(ii) Sample device :-

A laser beam may be focussed to produce a beam of much smaller diameter using a lens. The sample illumination geometry is illustrated in Fig.3.8. Two additional concave mirrors used in the illumination system increases the observed intensity of scattering by 8-10 times. Filters and optical devices such as polarizer, polarization analyzer etc., may be inserted into the incident laser beam or into the scattered beam.

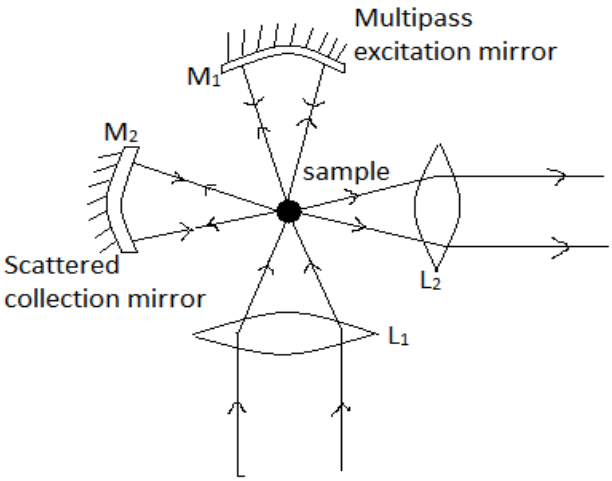

Fig.3.8 Sample illumination geometry

(iii) Monochromator

The monochromator used often is the one based on grating. The most important property of any monochromator is its ability to distinguish lights of nearby wavelengths forming neighbouring line images. This depends essentially upon factors like resolving power, slit width etc. Essentially a single monochromator can have a high enough resolution for Raman spectroscopy but it may not have good enough stray light rejection. However, if two monochromators are used in series the situation will be much better but only at the expense of efficiency. For the study of vibrational bands, a double monochromator is often sufficient. For high resolution work (rotation and rotation- vibration studies) a triple moochromator is preferred.

(iv) Detection device :-

The dispersed radiation is detected photo electrically. The exit slit allows only a narrow band to reach the photomultiplier tube and the rotation of the grating allows the successive bands to reach the detector. To reduce the thermal emission contributing a noise element in the signal, the photomultiplier is cooled. The photomultiplier has a high efficiency and uniform response over the 4000 to 8000 A° range. The output of the photomultiplier tube is amplified and fed to the strip chart recorder which can be operated in the photon counting mode or direct current mode. The direct current mode is used at higher signal level.

3.7 Structure determination using IR and Raman spectroscopy

Determination of molecular structures using IR and Raman spectroscopies is mainly based on the application of symmetry, the vibrational selection rules, state of polarization of the lines and the observed frequencies.

For diatomic molecules, there will be one totally symmetric stretching mode which is active in IR if the molecule is heteronuclear and inactive if it is homonuclear. On the contrary, it is allowed as a polarized line in Raman effect. The observation of the rotational fine structure of these helps one to determined the moment of inertia and the bond length of the molecule.

(i) Molecules of type XY_2

The next simplest type is the triatomic which has linear symmetric, bent symmetric and linear asymmetric modes.

If it is the linear symmetric model, it has to obey the rule of mutual exclusion as centre of symmetry is present in the molecule. If it is the bent symmetric or linear asymmetric type, all the three distinct modes are active in both IR and Raman. In addition, if the molecule is nonlinear it cannot give rise to infrared bands with P,R contours. As an example, the details of the observed IR and Raman spectra are listed in table 3.1.

Frequency $\bar{\gamma}(cm^{-1})$	**IR**	**Raman**	**Assignment**
1285	Very strong, PR contour	very strong, polarized	Symmetric stretching
589	Strong, PQR Contour	------	Bonding mode
2224	Very strong ,PR contour	Strong ,depolarized	Asymmetric stretching

(iii) Molecules of type XY_3.

XY_3 type molecules will have six fundamentals, some of them may become degenerate depending on the symmetry. The simplest of them are the planar D_{3h} point group and the pyramidal C_{3V} point group. The predictions of fundamentals of symmetric Xy_3 molecules are summarized in table.3.2.

Table – 3.2

Predictions of Fundamental of Symmetric XY_3 molecules

Model	Number of distinct fundamentals	No of fundamentals predicated in IR	Number Premitted in Raman	Number of Polarized Raman lines.
Planar (D_{3h})	4	3	3	1
Pyramidal (C_{3V})	4	4	4	2

(iv) Molecules of type XY_4.

The common models in the category are the square planar (point group D_{4h}) and the tetrahedral (point group T_4) ones. The number of distinct fundamental for them are seven and four respectively. The predictions based on selection rules and polarization for these two types are given in table 3.3.

Table –3. 3

Predictions of Fundamental of Symmetric XY_4 molecules

Model	Number of distinct fundamentals	No of fundamentals active in IR	Number of fundamental active in Raman	Number of Polarized Raman lines.
Square Planar (D_{4h})	7	3	3	1
Tetrahedral (T_4)	4	2	4	1

3.8 Nonlinear Raman Phenomena :-

Lasers have been developed in the early 1960s and since then they have been used in spectroscopic experiments of one form or another. Its use as an excitation source for spectroscopy become apparent when it was used as a Raman source. The development of tunable laser systems soon began to open up new possibilities for spectroscopic applications. The large intensity possessed by lasers leads to a nonlinear polarization of the medium which is responsible for the observation of number of nonlinear phenomena such as nonlinear Raman Spectroscopy, multiphoton spectroscopy, saturation spectroscopy, harmonic generation etc. When light propagates through an optically dense medium the electric field associated with wave (E) induces dipole in the medium. The polarization P thus induced is directly proportional to E.
That is,

$$P = \alpha E$$

Where α , called the polarizability, is a property of the material. In general, it is a tensor.
A more general relation connecting P and E at extra high electric intensities is,

$$P = \alpha E + \frac{1}{2}\beta E^2 + \frac{1}{6}\gamma E_3 + \ldots\ldots\ldots\ldots \quad (3.24)$$

Where β, γ.....are respectively the hyperpolarizailities tensor, second hyperpolarizability tensor and so on. Thus tensors measure the amount of distortion of electrons to a molecular system and their values depend on the nuclear and electron configuration. Alternately, Eq.(3.24) is sometimes written as

$$P = \chi_1 E + \chi_2 E^2 + \chi_3 E^3 + \ldots\ldots\ldots\ldots \quad (3.25)$$

Here χ_1 is the linear polarizability and χ_2, χ_3 are called the nonlinear polarizabilities.

3.9 Hyper Raman effect :

When a molecule is illuminated with radiation of frequency γ_0 from a focussed giant pulse laser, it gives rise to scattered radiations at frequencies $\gamma_0, (\gamma_0 + \gamma_m)$, $(\gamma_0 - \gamma_m)$, $2\gamma_0$, $(2\gamma_0 + \gamma_m)$, $(2\gamma_0 - \gamma_m)$, and so on, where γ_m corresponds to Raman – active vibration of the molecule. These are respectively called Rayleigh, anti – stokes Raman, Stokes Raman, hyper Rayleigh, hyper – Raman anti – stokes and hyper – Raman stokes scatterings. If the electric field E associated with the incident radiation is extremely high, one can observe the additional

scattered radiations at frequencies , $3\gamma_0$, $(3\gamma_0 - \gamma_m)$ and $(3\gamma_0 + \gamma_m)$. Hyper – Rayleigh and hyper – Raman scattering are three photon processes with two incident photons and one scattered photon as illustrated in Fig.3.9. The vibration selection rules for hyper – Raman scattering are different from those for linear Raman scsattering and for infrared absorption. In general, the hyper – Raman selection rules have the following characteristics.

1. All infrared – active hands are hyper – Raman active.
2. All Raman – active bands are not hyper – Raman active.
3. Vibrations which are both IR and Raman active are hyper – Raman active.
4. Hyper Raman active vibrations which are IR active are always polarized.

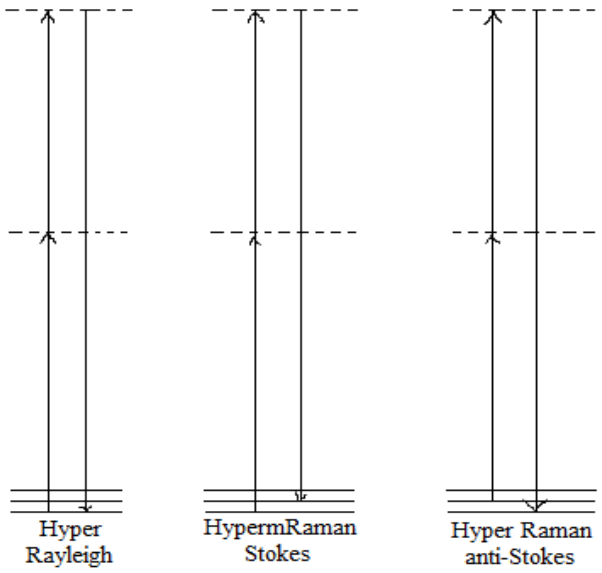

Fig.3.9. Schematic representation of Hyper – Rayleigh and hyper – Raman scattering

3.10 Classical treatment of Hyper–Raman effect :-

The time dependence of the electric filed E associated with the incident radiation can be written as

$$E = E_0 \cos 2\pi\gamma_o t \qquad (3.26)$$

For simplicity, we shall consider the vibrational case of a system. Let Q be the normal coordinate associated with the vibrational frequency γ_m. In the harmonic approximation

$$Q = Q_0 \cos 2\pi\gamma_m t \qquad (3.27)$$

Already we know that, the expression for polarization (P)

$$P = \chi_1 E + \chi_2 E^2 + \chi_3 E^3 + \ldots\ldots\ldots\ldots \tag{3.28}$$

Expanding χ_1 and χ_2 as a Taylor series in the normal coordinate Q.

$$\chi_1 = \chi_{10} + \left(\frac{\partial \chi_1}{\partial Q}\right)_0 Q + \text{higher order terms} \tag{3.29}$$

$$\chi_2 = \chi_{20} + \left(\frac{\partial \chi_2}{\partial Q}\right)_0 Q + \text{higher order terms} \tag{3.30}$$

Neglecting the higher order terms and substituting χ_1 and χ_2 in Eq. (3.28)

$$P = \left[\chi_{10} + \left(\frac{\partial \chi_1}{\partial Q}\right)_0 Q_0 \cos 2\pi\gamma_m t\right] E_0 \cos 2\pi\gamma_o t +$$

$$\left[\chi_{20} + \left(\frac{\partial \chi_1}{\partial Q}\right)_0 Q_0 \cos 2\pi\gamma_m t\right] E_0^2 \cos^2 2\pi\gamma_o t$$

Replacing $\cos^2 2\pi\gamma_o t = (1 + \cos 4\pi\gamma_o t)/2$ and using simple trigonometric identities.

$$P = \chi_{10} E_0 \cos 2\pi\gamma_o t + \frac{1}{2} E_0 Q_0 \left(\frac{\partial \chi_1}{\partial Q}\right)_0 \cos 2\pi(\gamma_0 - \gamma_m)t + \frac{1}{2}$$

$$Q_0 E_0^2 \left(\frac{\partial \chi_1}{\partial Q}\right)_0 \cos 2\pi\gamma_m t + \frac{1}{2} E_0 Q_0 \left(\frac{\partial \chi_1}{\partial Q}\right)_0 \cos 2\pi$$

$$(\gamma_0 + \gamma_m)t + \frac{1}{2} \chi_{20} E_0^2 + \frac{1}{2} \chi_{20} E_0^2 \cos 4\pi\gamma_o t +$$

$$\frac{1}{4} Q_0 E_0^2 \left(\frac{\partial \chi_2}{\partial Q}\right)_0 \left[\cos 2\pi (2\gamma_0 + \gamma_m)t + \cos 2\pi(2\gamma_0 - \gamma_m)t\right]$$

Thus, the polarizability contains eight distinct frequency components, They are :

i. $\gamma = 0$ the d.c field term $\frac{1}{2}\chi_{20} E_0^2$.

ii. $\gamma = \gamma_0$ the Rayleigh scattering

iii. $\gamma = \gamma_0 - \gamma_m$ Raman stokes.

iv. $\gamma = \gamma_0 + \gamma_m$ Raman anti – stokes

v. $\gamma = \gamma_m$ molecular frequency

vi. $\gamma = 2\gamma_0$ Hyper – Rayleigh

vii. $\gamma = 2\gamma_0 - \gamma_m$ hyper – Raman stokes

viii. $\gamma = 2\gamma_0 + \gamma_m$ Hyper – Raman anti – stokes

Five of these eight arise from the nonlinear susceptibility $\chi_{2.}$

3.11 Experimental techniques for Hyper – Raman effect :

Only giant pulse lasers is used as a source for observing the hyper – Raman effect. A typical nano-second pulse from a giant pulse laser would deliver about 10^{17} photons to the sample at frequency γ_0 but the number of photons of frequency $2\gamma_0 - \gamma_m$ which the detector would receive ranges from a few photons per laser pulse down to 1 photon for every 100 laser pulses depending on the sample.

There are two methods of observing the scattered radiations of such low intensities.

(i) Single channel detection and

(ii) Multichannel detection.

In both cases, radiations from a giant pulse laser is focussed on to the sample and the radiations scattered at right angles to the laser beam is collected with a wide single lens and fed to a grating system which disperses the radiation.

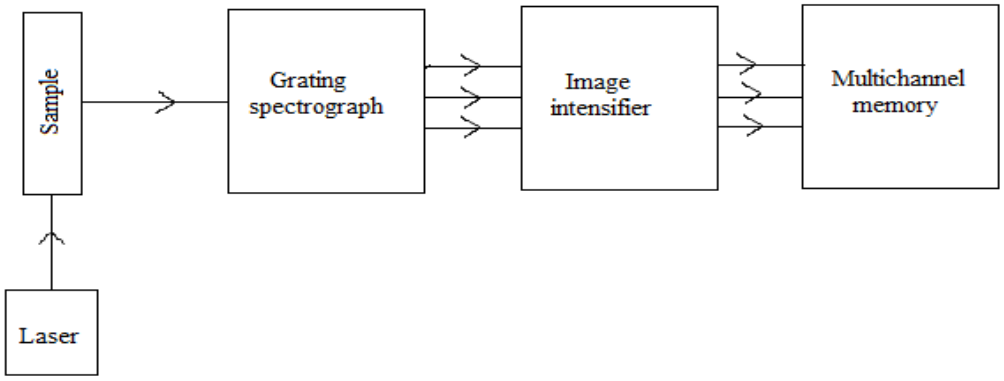

Fig.3.10 Block diagram of multichannel Raman spectrometer

In single channel detection, the grating dispersion system works as a monochromator. The monbochromator is set to pass radiation over a narrow frequency range. This method is very time consuming and very hard on the laser and observer.

In the multichannel method, the grating dispersion system operates as a spectrograph. The exit slit and photomultiplier are replaced by an image intensifier which intensity the complete spectrum to a level at which it can be scanned by a television camera. The information is stored in the digital form so that it can easily be combined with information from other laser shots and then averaged. At the end of the experiment, the stored data can be displayed in analogue form on an oscilloscope or plotter. Fig.3.10 gives the block diagram of a multichannel instrument.

3.12 Stimulated Raman scattering

When a giant pulse laser is focused into a sample and the scattered radiation is observed along the laser beam direction and at small angles to it, it is found to consist of the incident frequency γ_0 and the stokes and anti-stokes lines at $\gamma_0 \mp n\gamma_m, n-1,2,3...$where γ_m corresponds to one Raman – active vibration of the scattering molecule. This phonomeum is called *stimulated Raman scattering* . The stimulating process is schematically represented in Fig.3.11. In stimulated Raman scattering there is no need for population inversion of the stats. This non – linear Raman technique is associated with the third order non – linear polarizatbility.

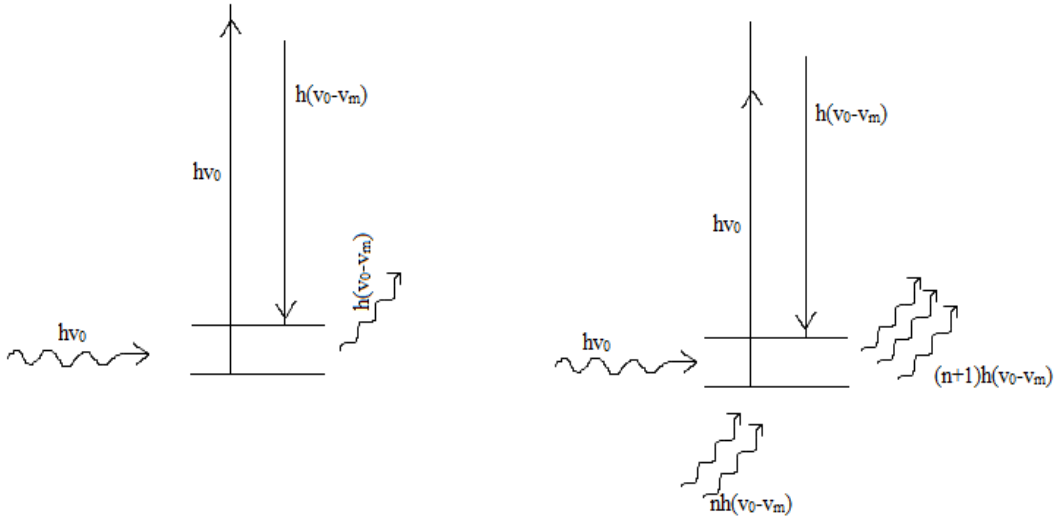

Fig.3.11 Schematic illustration of (a) spontaneous Raman stokes scattering (b) stimulated Raman stokes, scattering

Investigations here shown that the mechanism responsible for the enhancement of the stimulated Raman stokes is that of parametric amplification. The stokes line produced by spontaneous Raman scattering at frequency $(\gamma_0 - \gamma_m)$ becomes intense enough quickly, to act as a powerful

source to produce a stokes line at $\gamma_0 - 2\gamma_m$. This is illustrated in Fig.3.12. As this line gains in intensity, it acts another source and so on.

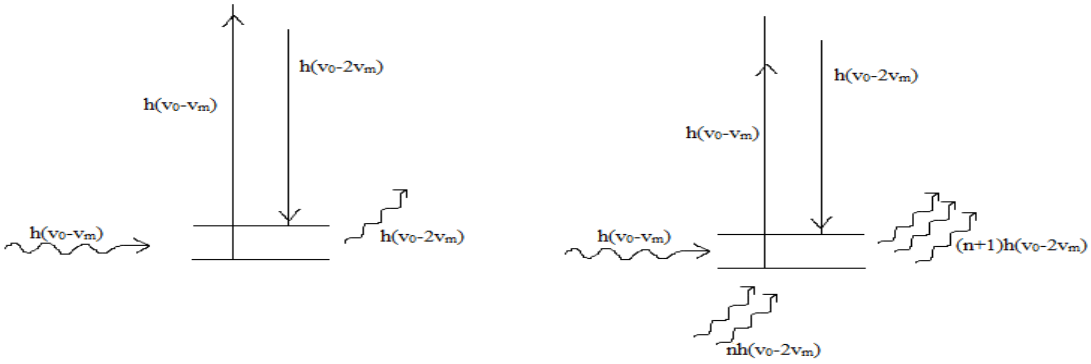

Fig.3.12 Illustration of (a) spontaneous Raman scattering at (γ_0 - $2\gamma_m$), (b) stimulated Raman scattering at (γ_0 - $2\gamma_m$).

A typical experimental arrangement for the observation of stimulated Raman scattering (SRS) is shown in Fig.3.13(a). The laser radiation from a giant pulse ruby laser is focussed into the cell containing the benzene sample and the scattering is observed along the laser beam direction and at small angles to this direction. When the forward scattered radiation is photographed on a colour–sensitive film, a system of concentric coloured rings as shown in Fig.3.12(b). The red spot at the centre corresponds to the ruby laser output and the stokes bands which are emitted almost along the laser beam direction. The coloured rings corresponds to successive anti-stokes

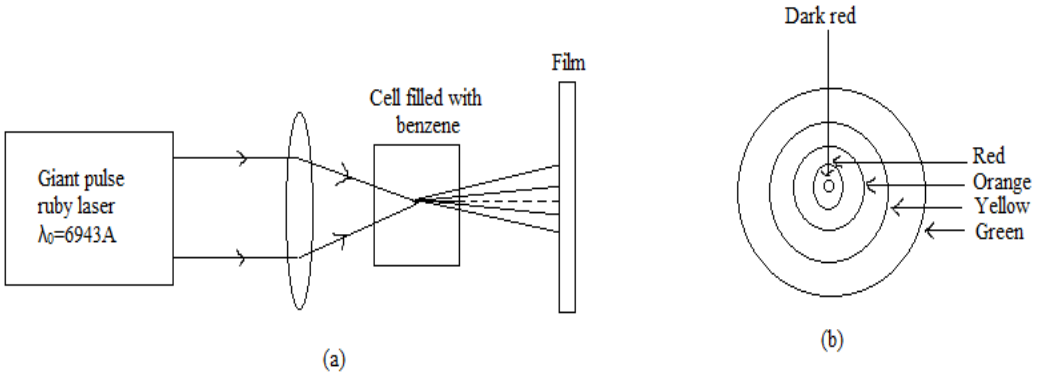

Fig.3.13 (a) Schematic representation of SRS experimental set-up, (b) observed pattern for benzene

lines at higher wavenumbers which are emitted along directions making definite small angles with laser beam direction.

SRS can also be done by mixing two lasers at frequencies γ_1 and γ_2 $(\gamma_1 > \gamma_2)$. The second laser stimulates the scattering at γ_2 which equals $\gamma_1 - \gamma_2$ as illustrated in Fig.3.14. The generated Raman frequency at γ_2 has the same properties as the γ_2 laser. During the process of gain is produced at the frequency γ_2 where photons of frequency γ_1 are annihilated. Therefore, then are two ways to perform the experiment either by measuring the gain at the frequency γ_2 or by measuring losses at frequency γ_1. These two are sometimes referred to as Raman gain spectroscopy and Raman loss spectroscopy respectively. Generally a pulsed laser serves as the pump beam and a CN laser as the probe beam.

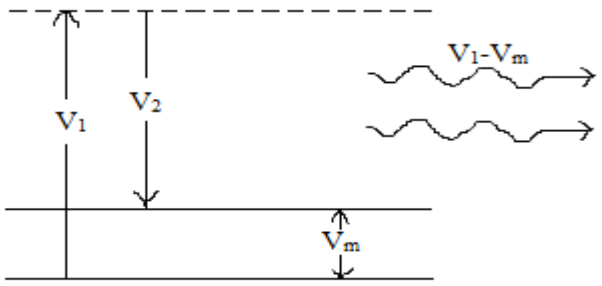

Fig. 3.14. Stimulated Raman process with two lasers having frequencies γ_1 and γ_2

3.13 Inverse Raman Scattering.

Raman scattering is inelastic scattering of photons of energy $h\gamma_0$ by molecules. If the scattered photon has an energy $h(\gamma_0 + \gamma_m)$, the incident photon gained an amount of energy $h\gamma_m$ from the molecule. The energy balance equation for this normal anti-stokes Raman is illustrated in Fig.3.15(a). If this process is inverted, the scattering molecule absorbs radiation of frequency $(\gamma_0 + \gamma_m)$ resulting in the molecule going to a higher energy level and the emission of radiation of frequency γ_0. This phenomenon is called the inverse anti-stokes Raman effect which is illustrated in Fig.3.15(b)

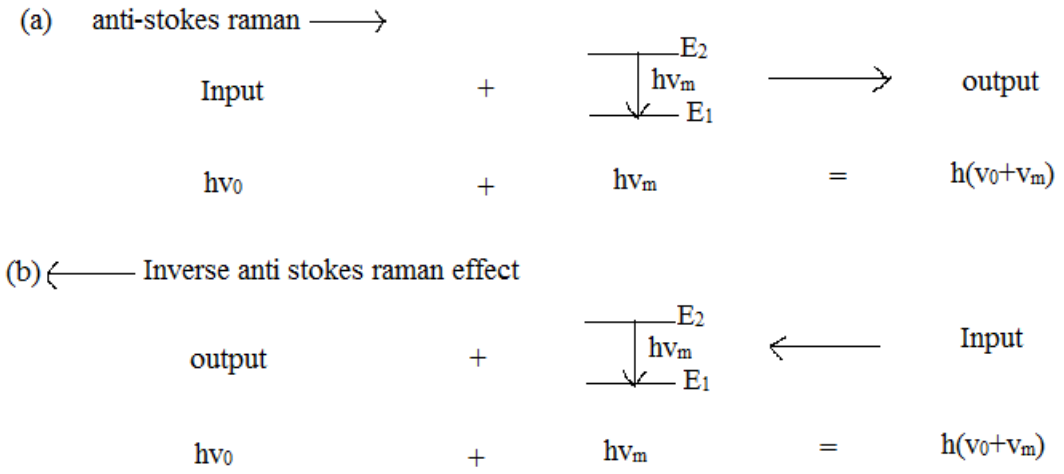

. **Fig.3.15 (a) Anti-stokes Raman scattering , (b) inverse anti-Stokes Raman scattering**

The absorption of radiation of frequency $\gamma_0 - \gamma_m$ by the molecule would result in a decrease in the energy of the scattering molecule by $h\gamma_m$ and emission of radiation of energy $h\gamma_0$. This process is inverse stokes Raman scattering. It is found that absorption at frequencies $\gamma_0 \pm \gamma_m = \gamma_L$ can occur only in the presence of very intense radiation at frequency γ_0. Thus, the essential requirements for the observation of inverse Raman scattering are the simultaneous irradiation of the sample with a giant pulse laser beam of frequency γ_0 and a strong continuum covering the stokes and anti – stokes regions in which absorption are expected.

Fig.3.16 shows the experimental arrangement for the observation of inverse Raman effect. A giant pulse ruby laser is frequency doubled in a KDP crystal. The second harmonic which pumps a dye laser is separated from the fundamental by mirror M1. The dye laser cavity is formed by partially transmitting mirror M_3 and a totally reflecting mirror M_6. The dye laser output is direct to the sample cell by M_2. The ruby fundamental output (γ_0) is combined with the dye laser output (γ_1) by M_4 and M_5 so that spatial overlap is achieved.

Temporal overlap is a certainty since the duration of the dye laser pulse in 7ns and that of the ruby pulse 25ns. The dye laser output is the continuum which has a width of about $200cm^{-1}$. By recording this in a spectrograph, the different portions of the Raman spectrum can be covered, depending on the dye and its concentration. The region below $800cm^{-1}$ can be recorded with a slightly different arrangement. In this region pumping by frequency doubled ruby is not reliable.

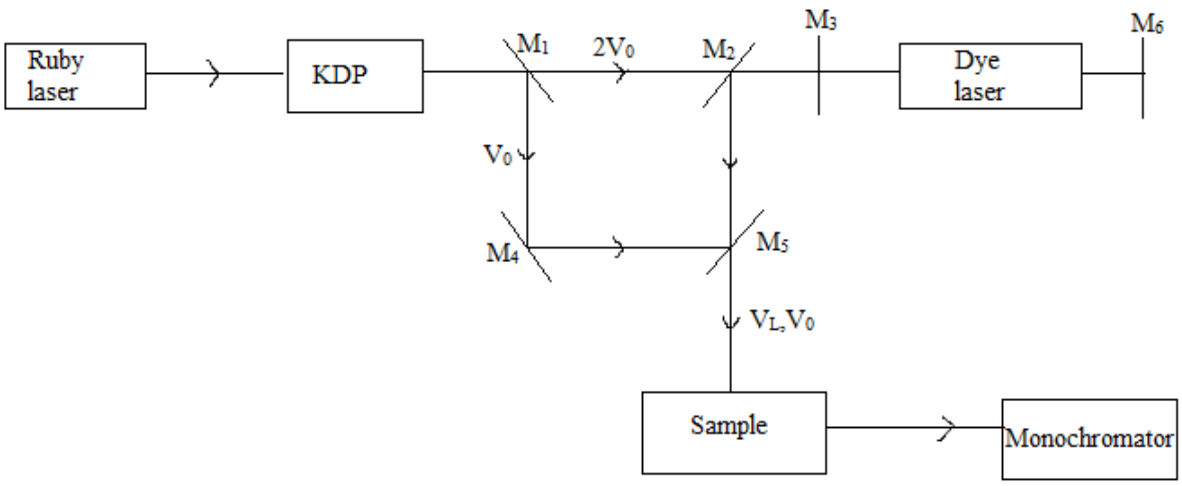

Fig.3.16: Schematic arrangement of the experimental set up for inverse Raman scattering, m_1, m_2, m_3, m_4, m_5, m_6 are dichotic mirrors.

3.14 Coherent Anti–stokes Raman Scattering (CARS).

The coherent Anti-stokes Raman Scattering (CARS) combines the advantages of stimulated Raman scattering and the general applicability of normal Raman scattering. When coherent radiation of frequency γ_1 is mixed with coherent radiation of frequency γ_2 $(\gamma_1 > \gamma_2)$ in a molecular medium, coherent radiation of frequency

$$\gamma_3 = 2\gamma_1 - \gamma_2 = \gamma_1 + (\gamma_1 - \gamma_2)$$

is generated, if the irradiances of the two radiations are sufficiently large. Here mixing implies spatial and temporal coincidence of the two beams. If γ_1 is fixed and γ_2 is varied so that $\gamma_1 - \gamma_2 = \gamma_m$ a Raman active vibration of the molecule under investigating them $\gamma_3 = \gamma_1 + \gamma_m$ which is an anti- stokes Raman frequency. Radiation produced in this way is formed CARS, which is also associated with the third order nonlinear susceptibility.

Experimental arrangement for CARS :

Different experimental arrangements are available depending on the purpose for which it is used. Figure 3.17 illustrates a typical CARS set up where the two incident radiations are provided by the 514.5nm argon laser line (γ_1) and a CW dye laser (γ_2) pumped by the same argon laser.

With CARS, the conversion efficiency to $\gamma_3 = \gamma_1 + \gamma_m$ is several orders of magnitude greater them conversion coefficients with normal Raman scattering. The radiations resulting from CARS

form a highly coherent collimated beam whereas normal Raman scattering is incoherent and extends over a solid angle 4π .

Since CARS is highly collimated, fluorescence and thermal radiation from hot samples can effect by filtered by placing a screen with a hole of few mm diameter between the detector and the sample, which just passes only the CARS beam. Moreover, in principle no dispersing medium is needed for CARS experiment. The fluorescence – free nature of CARS makes it an ideal tool for high resolution spectroscopy studies and analysis of biological samples.

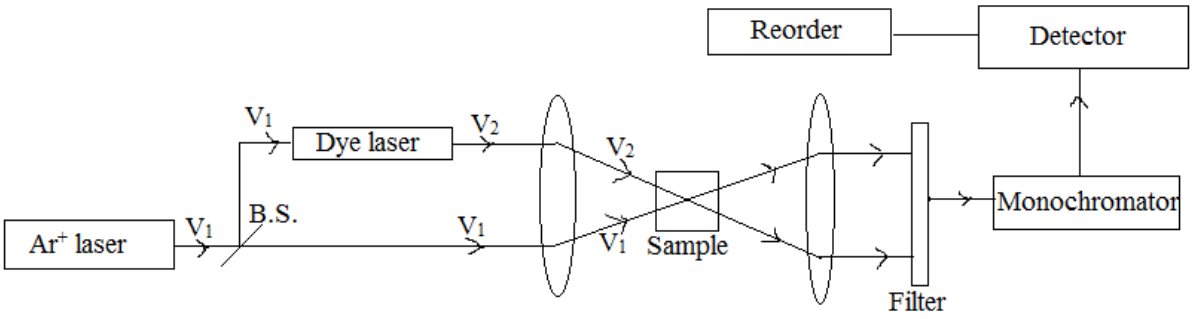

Fig.3.17 Experimental arrangement for CARS (monochromator optical)

3.15 Photoacoustic Raman Scattering (PARS) :

This phenomenon requires the simultaneous illumination of the sample by two laser beams γ_p *and* γ_s such that $\gamma_p - \gamma_s = \gamma_m$ a Raman active transition frequency.

The PARS process is illustrated schematically in Fig.3.18. The frequency γ_s is tunable to satisfy the above condition.

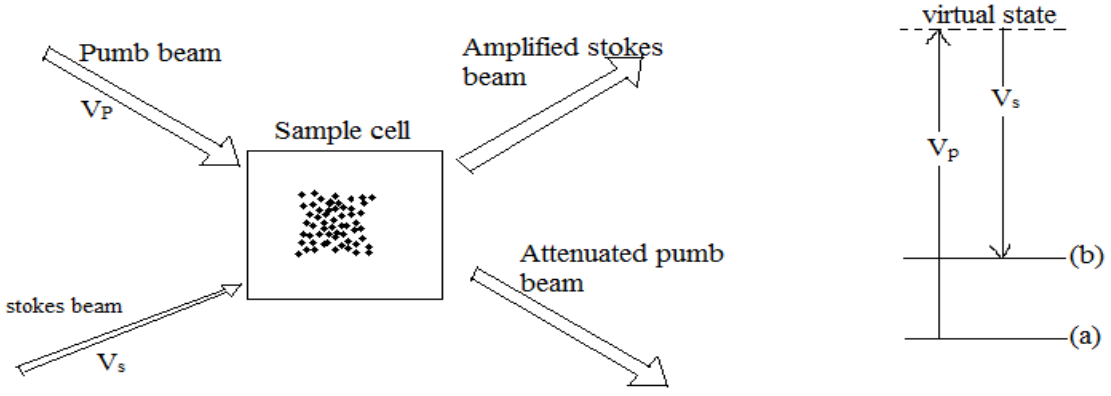

Fig.3.18 Photoacoustic Raman process

The incident laser beams with frequencies γ_p (pump beam) and γ_s (stokes beam) interact with two energy states $|a>$ and $|b>$ of a molecule. By stimulated Raman scattering, the intensity of the stokes beam increases and that of the pump beam decreases. This causes an increase in the molecular population of the upper state $|b>$. For this to happen, the pump and stokes beams must mix spatially and temporally in the gas sample. During this collision, the excited molecules produces a pressure change in the sample, causing an acoustic wave which is detected by a microphone. If the input lasers are modulated chopped at a rate which is slow compared to the vibrational to translational relaxation rate, then the temperature and hence the gas pressure will very at the modulation frequency. The modulated pressure wave is the sound wave which is detected. Fig.3.19 gives the schematic representation of the experimental arrangement used for obtaining PARS signal with CW laser source.

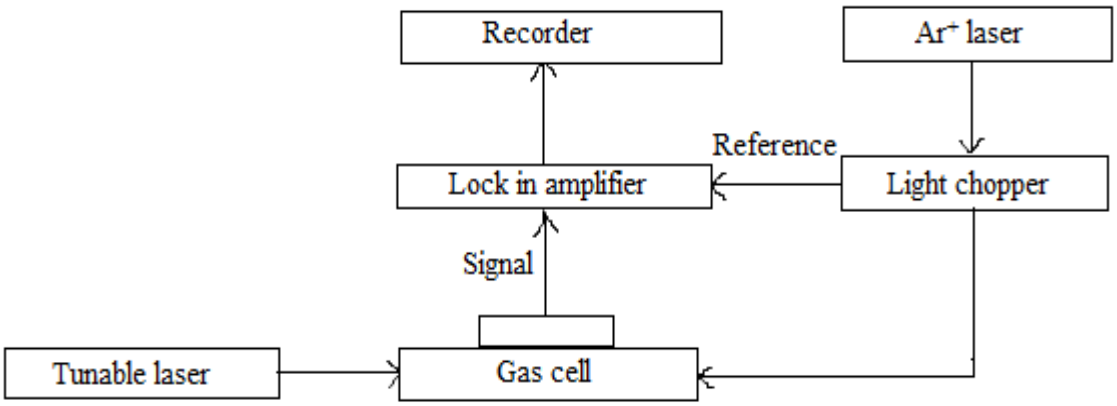

Fig.3.19 Schematic representation of the experimental set up used for PARS

Uses :-

1. It is used to study pure rotational Raman transition.
2. The absence of the Rayleigh component is helpful in recording the low- lying vibrational and rotational transitions.
3. The high sensitivity of this technique provides a new method for the problem of trace analysis of gaseous mixtures with a detection capability of about one part per million.

3.16 Surface Enhanced Raman Sacttering (SERS):-

The SERS Phenomenon is accompanied by quenching of fluorescence associated with Raman bands which extends the range of molecules, crude mixtures and extract that can be investigated. The magnitude of the enhancement in Raman Scattering cross – section depends on

i. the chemical nature of the absorbed molecules
ii. the roughness of the surface and
iii. optical properties of the absorbant.

SERS offers the possibility of overcoming many of the problems in conventional Raman spectroscopy.

(i) **Surfaces for SERS study**

Silver is the most widely used materials for SERS investigations. Reports of SERS are also available from lithium, sodium, aluminium, indium, nickel, copper and gold surfaces etc., Three types of metal surfaces are commonly used in SERS experiments.

1. Cold – deposited metal films
2. Metal electodes
3. Metal sol.

(ii) Enhancement mechanisms:

Though number of mechanisms have been suggested for the SERS phenomenon, the generally accepted mechanisms are.

1. Electromagnetic enhancement mechanism.
2. Chemical enhancement mechanism.

(iii) Applications of SERS

SERS is a useful tool for probing the behaviour of molecules absorbed on metal surfaces. Some of the applications are

(i) SERS is used to study the functional characteristics of bio molecules.

(ii) Medical applications of SERS as a diagnostic or analytical tool. Now SERS used as an active tool to study the anti-tumour activity of certain drugs used for the treatment of cancer.

UNIT – IV

Electronic Spectroscopy

4.1 Introduction :-

The term electronic spectroscopy is used for transitions between electronic states which fall in the visible and ultra – violet regions of the electromagnetic spectrum. During an electronic transition, vibrational and rotational energy changes can also occur. The vibrational changes produce what is called the vibrational coarse structure whereas the rotational change give rise to the rotational fine structure on the electronic spectra. The separation between electronic levels is of the order is 10^6 cm^{-1} or more.

Molecules possessing permanent electric dipole moment give pure rotational spectra. Vibrational spectra require a change of dipole moment during its normal mode of vibration. However, electronic spectra are given by all molecule since changes in the electron distribution in a molecule are always accompanied by a dipole moment change. Therefore homonuclear diatomic molecules, though possesses no permanent dipole moment, show an electronic spectra with rotational and vibrational structures.

4.2 Vibrational coarse structure :-

According to Born and Oppenheimer, the various forms of energies of a molecule are independent of each other. Hence leaving the translational contribution, the total energy E is given by

$$E_{total} = E_l + E_v + E_r \tag{4.1}$$

The rotational, vibration and electronic separations are of the order of $1-30 cm^{-1}$, $300-4000\, cm^{-1}$ and $10^6 cm^{-1}$ respectively. To understand the vibrational coarse structure, we drop the rotational energy term ε_r from the expression for total energy.

$$\varepsilon_t = \varepsilon_{el} + (V+\frac{1}{2})\,\bar{\gamma}_e - (V+\frac{1}{2})^2\,\bar{\gamma}_e\, x_e + (V+\frac{1}{2})^3\, y_e\, \vec{\gamma}_e + \ldots . cm^{-1}$$

for $V = 0,1,2,3$.....

The energy levels corresponding to the above equation are shown in Fig.4.1.

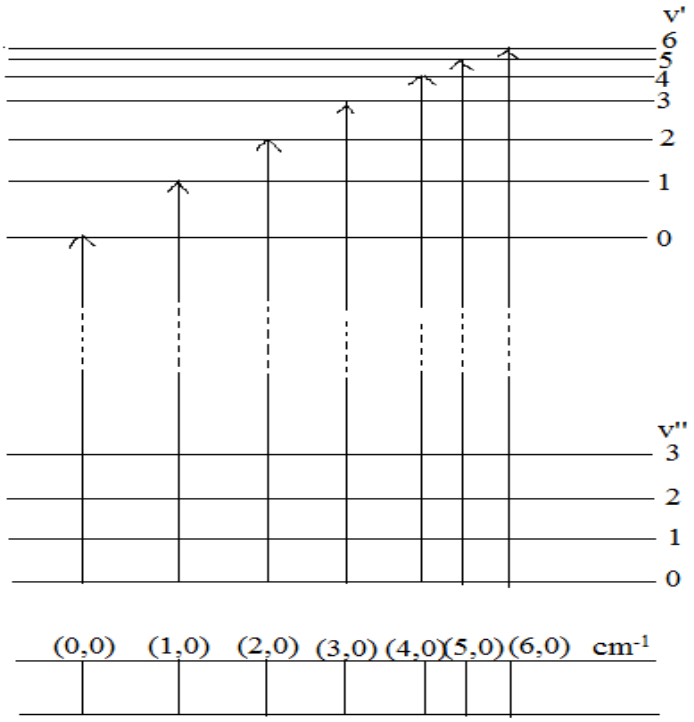

Fig.4.1 The vibrational coarse structure of electronic absorption from the ground state

The wave number of a spectral line can be written as

$$\bar{\gamma}_{V^1V^{11}} = (\varepsilon_{el}' - \varepsilon_{el}'') + \left[(V'+\frac{1}{2})\,\bar{\gamma}_e - (V'+\frac{1}{2})^2\,\bar{\gamma}_e' x_e' \right] - \left[(V''+\frac{1}{2})\,\bar{\gamma}_e'' - (V''+\frac{1}{2})^2\,\bar{\gamma}_e^{11} x_e'' \right] \quad (4.3)$$

The transitions which are of considerable intensity are those originating from the state $V^{11} - 0$. It is labelled according to their (V^1, V^{11}) values as $(0,0),(1,0),(2.0),(3,0)$. The set of lines corresponding to these transitions is called a V^1 *progression* since the value of V^1 increases by unity for each line in the set. The wave number of the (0,0) transition is then,

$$\bar{\gamma}_{00} = (\varepsilon_{el}' - \varepsilon_{el}'') + \frac{1}{2}\bar{\gamma}e^1 - \frac{1}{4}x_e^1\,\bar{\gamma}_e^1 - \frac{1}{2}\bar{\gamma}e'' + \frac{1}{4}x_e''\,\bar{\gamma}e'' \quad (4.4)$$

4.3 Vibrational analysis of band systems:

In the energy scale, taking the minimum of the potential energy curve as zero, the vibrational term value $E(V)$ is given by,

$$E(V) = \varepsilon_V + (V+\frac{1}{2})\,\bar{\gamma}_e - (V+\frac{1}{2})^2\,\bar{\gamma}_e x_e + (V+\frac{1}{2})^3\,y_e\vec{\gamma}_e + \ldots . cm^{-1} \quad (4.5)$$

In vibration analysis of the spectrum of a band system, the energy of the $V=0$ vibrational level is taken as zero. That is, in the modified system the vibrational term,

$$E(0) = \frac{1}{2}\bar{\gamma}_e - \frac{1}{4}\bar{\gamma}_e x_e + \frac{1}{8}\bar{\gamma}_e y_e \qquad (4.6)$$

is taken as the zero and the modified vibrational term is written as $E_o(V)$. Then,

$$E_0(V) = V\,\bar{\gamma}_e - V^2 x_e\,\bar{\gamma}_e - V x_e \vec{\gamma}_e + V^3\, y_e \vec{\gamma}_e + \frac{3}{2}V^2 y_e\,\bar{\gamma}_e + \frac{3}{4}V y_e\,\bar{\gamma}_e$$

$$= V\left(\bar{\gamma}_e - x_e\,\bar{\gamma}_e + \frac{3}{4}y_e \vec{\gamma}_e + \ldots\ldots\right) - V^2\left(x_e\,\bar{\gamma}_e - \frac{3}{2}y_e\,\bar{\gamma}_e + \ldots\ldots\ldots\right) + V^3\left(y_e\,\bar{\gamma}_e + \ldots\ldots\ldots\right)$$

$$= V\,\bar{\gamma}_0 - x_0\,\bar{\gamma}_0 V^2 + y_0\,\bar{\gamma}_0 V^3 + \ldots\ldots\ldots \qquad (4.7)$$

Where

$$\bar{\gamma}_0 = \bar{\gamma}_e - x_e\,\bar{\gamma}_e + \frac{3}{4}y_e\,\bar{\gamma}_e + \ldots\ldots\ldots \qquad (4.8)$$

$$x_0\,\bar{\gamma}_0 = x_e\,\bar{\gamma}_e - \frac{3}{2}y_e\,\bar{\gamma}_e + \ldots\ldots\ldots\ldots \qquad (4.9)$$

$$y_0\,\bar{\gamma}_0 = y_e\,\bar{\gamma}_e + \ldots\ldots\ldots\ldots \qquad (4.10)$$

In the modified form, the wavenumber of a spectral line can be written from Fig.4.2 as

$$\bar{\gamma}_{V'V''} = \bar{\gamma}_{00} + E'_0(V') - E''_0(V''). \qquad (4.11)$$

where $\bar{\gamma}_{00}$ is the wavenumber of the (0,0) band.

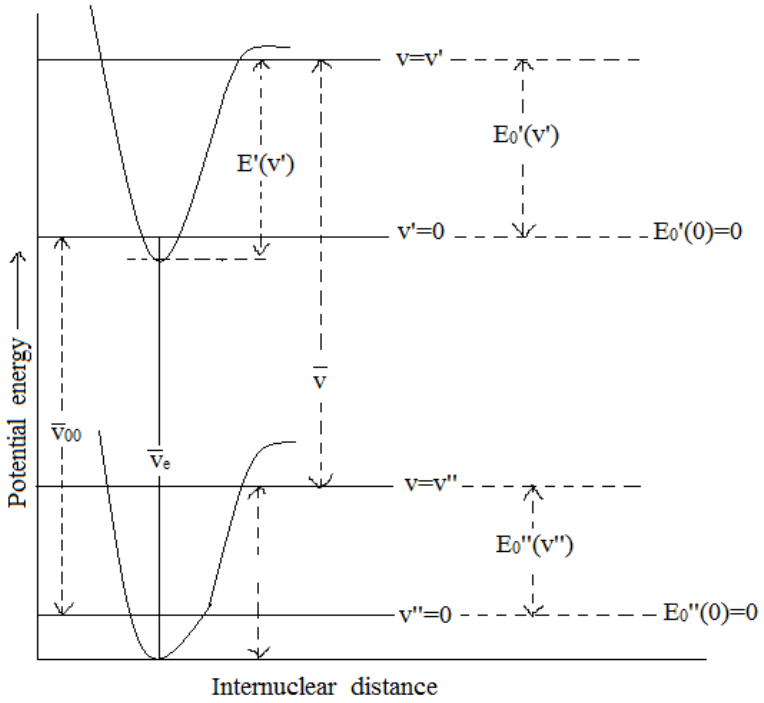

Fig.4.2 Symbols used in the vibrational analysis of a band system.

The wavenumbers of each of the (V',V'') band are then arranged in the form of table called *Deslandre's table.* In table the wave number of each band is given on the basis of Eq.(4.11). The wavenumber separation of two successive vibration levels in an electronic state is given by $E_0(V+1)-E_0(V)$ and is called the *first difference* denoted by $\Delta E(V+\frac{1}{2})$ using Eq.(4.7).

$$\Delta E(V+\frac{1}{2}) = \bar{\gamma}_0 - \bar{\gamma}_0 x_0 - 2x_0 \bar{\gamma}_0 V \qquad (4.12)$$

In deriving, Eq.(4.12), higher order terms have been neglected.

The first difference can be obtained from table 1 by subtracting a V' value from the V' value vertically below it or by subtracting horizontal numbers in the V'' column from the ones in the previous V'' column. Thus $\Delta E'(\frac{1}{2})$ is obtained by subtracting V$^{'}$ = 0 value from V$^{'}$ = 1 value vertically below it. Four values of $\Delta E'(\frac{1}{2})$ would be possible as per table 1 and their average is taken as $\Delta E'(\frac{1}{2})$. By a similar procedure $\Delta E'(1\frac{1}{2}), \Delta E'(2\frac{1}{2})$ and $\Delta E'(3\frac{1}{2})$ are also estmiaed. The value of $\Delta E''(\frac{1}{2})$ is obtained by subtracting horizontal numbers in the $V^{11}=1$ column from the one in the $V^{11}=0$ column. Their mean is $\Delta E^{11}(\frac{1}{2})$. By a similar procedure $\Delta E^{11}(1\frac{1}{2}), \Delta E^{11}(2\frac{1}{2})$ and $\Delta E^{11}(3\frac{1}{2})$ are also estimated. According to Eq.(4.12), $\Delta E^{1}(V+\frac{1}{2})$ plotted against V should give a straight line with slope - $-2x_0^{\,1}\,\bar{\gamma}_0^{\,1}$ and intercept $\bar{\gamma}_0 - \bar{\gamma}_0 x_0$. Similarly $\Delta E^{11}(V+\frac{1}{2})$ against V would give $-2x_0^{\,11}\,\bar{\gamma}_0^{\,11}$. From these the values of $x_0^{\,1}$, $\bar{\gamma}_0^{\,1}, x_0^{\,11}$ and $\bar{\gamma}_0^{\,11}$ can easily be obtained. Substituting these values in Eqs.(4.8) and (4.9) and neglecting terms in y_e, the values of $x_e^{\,1}$, $\bar{\gamma}_e^{\,1}\, x_e^{\,11}$ and $\bar{\gamma}_e^{\,11}$ can be evaluated.

The second difference $\Delta^2 E(V+1)$, defined by

$$\Delta^2 E(V+1) = \Delta E(V+1\frac{1}{2}) - \Delta E(V+\frac{1}{2}) \qquad (4.13)$$

can be used as a check on the assignment. Substitution of Eq.(4.12) in Eq(4.13) gives,

$$\Delta^2 E(V+1) = \left[\bar{\gamma}_0 - x_0 \bar{\gamma}_0 - 2x_0 \bar{\gamma}_0 (V+1)\right] - \left(\bar{\gamma}_0 - x_0 \bar{\gamma}_0 - 2x_0 \bar{\gamma}_0 V\right)$$

$$= -2x_0 \bar{\gamma}_0 \qquad (4.14)$$

If the analysis is correct, the second difference for the lower electronic state should also lead to the same value for $-2x_0^{11}\bar{\gamma}_0^{11}$ as that obtained from the first difference. Similar in the case for the upper electronic state.

Table – 4.1: Arrangements of wavenumbers (based on Eq.(4.11) of the band orgins in a band system in terms of their (V^1, V^{11}) values.

V'/V''	0	1	2	3	4	$\Delta E^1\left(V+\frac{1}{2}\right)$
0	$\bar{\gamma}_{00}+E^1_0(0)-E^{11}_0(0)$	$\bar{\gamma}_0+E^1_0(0)-E^{11}_0(1)$	$\bar{\gamma}_0+E^1_0(0)-E^{11}_0(2)$	$\bar{\gamma}_{00}+E^1_0(0)-E^{11}_0(3)$	$\bar{\gamma}_{00}+E^1_0(0)-E^{11}_0(4)$	
1	$\bar{\gamma}_{00}+E^1_0(1)-E^{11}_0(0)$	$\bar{\gamma}_{00}+E^1_0(1)-E^{11}_0(1)$	$\bar{\gamma}_{00}+E^1_0(1)-E^{11}_0(2)$	$\bar{\gamma}_{00}+E^1_0(1)-E^{11}_0(3)$	$\bar{\gamma}_{00}+E^1_0(1)-E^{11}_0(4)$	$\Delta E^1\left(\frac{1}{2}\right)$
2	$\bar{\gamma}_{00}+E^1_0(2)-E^{11}_0(0)$	$\bar{\gamma}_{00}+E^1_0(2)-E^{11}_0(1)$	$\bar{\gamma}_{00}+E^1_0(2)-E^{11}_0(2)$	$\bar{\gamma}_{00}+E^1_0(2)-E^{11}_0(3)$	$\bar{\gamma}_{00}+E^1_0(2)-E^{11}_0(4)$	$\Delta E^1\left(1\frac{1}{2}\right)$
3	$\bar{\gamma}_{00}+E^1_0(3)-E^{11}_0(0)$	$\bar{\gamma}_{00}+E^1_0(3)-E^{11}_0(1)$	$\bar{\gamma}_{00}+E^1_0(3)-E^{11}_0(2)$	$\bar{\gamma}_{00}+E^1_0(3)-E^{11}_0(3)$	$\bar{\gamma}_{00}+E^1_0(3)-E^{11}_0(4)$	$\Delta E^1\left(2\frac{1}{2}\right)$
4	$\bar{\gamma}_{00}+E^1_0(4)-E^{11}_0(0)$	$\bar{\gamma}_{00}+E^1_0(4)-E^{11}_0(1)$	$\bar{\gamma}_{00}+E^1_0(4)-E^{11}_0(2)$	$\bar{\gamma}_{00}+E^1_0(4)-E^{11}_0(3)$	$\bar{\gamma}_{00}+E^1_0(2)-E^{11}_0(4)$	$\Delta E^1\left(3\frac{1}{2}\right)$
	$\Delta E^{11}(V+\frac{1}{2})$	$\Delta E^{11}(\frac{1}{2})$	$\Delta E^{11}(1\frac{1}{2})$	$\Delta E^{11}(2\frac{1}{2})$	$\Delta E^{11}(3\frac{1}{2})$	

4.4 Progressions and sequences :-

The bands in a particular column where V^1 varies and V^{11} is constant are called V^1 *progressions* while those in a row where V^{11} varies and V^1 is constant are called V^{11} *progressions.* Fig.4.3 illustrates transitions in some V^1 and V^{11} progressions. As V increases the spacing of the vibrational levels decreases, progressions with constant V^1 (V^{11} progressions) appear as bands whose wavenumber separations decrease towards shorter wavelengths.

Bands which fall in diagonal rows such as (0,0), (1,1), (2,2), (3,3) ..... (0,1), (1,2), (2,3), (3,4), ... (0,2), (1,3), (2,4) ..... of the Deslandres table are called *sequences*. The wave numbers of the bands in a sequence do not differ considerably.

4.5 Franck – Condon Principle:

According to Franck – Condon Principle, an electronic transition takes place so rapidly that a vibrating molecule does not change its internuclear distance appreciably during the transition. That is, during an electronic transition, the internuclear distance remains the same. Internuclear distance remains the same means straight line representing a transition between electronic stats will be veritical. Alternately Franck Condon Principle can be stated thus : transition between electronic states occur vertically in a potential energy diagram.

The intensity variations are readily explained on the basis of Franck Conon Principle. The anharmonic model of a diatomic molecule has a potential energy curve represented by the Morse function.

Consider a diatomic molecule undergoing transition from E_e^{11} to E_e^{1}. Fig.4.3 illustrates three different cases. In case (1), the bond length of the lower and upper electronic states are assumed to be equal. If the molecule is initially in the $V = 0$ of the lower electronic state, the probability of finding the atom is greatest at the equilibrium distance. Since the vertical from the maximum of $V^{11} = 0$ meets the maximum of $V^{1} = 0$, the most intense line will be (0,0) transition, Figure.4.3(a).

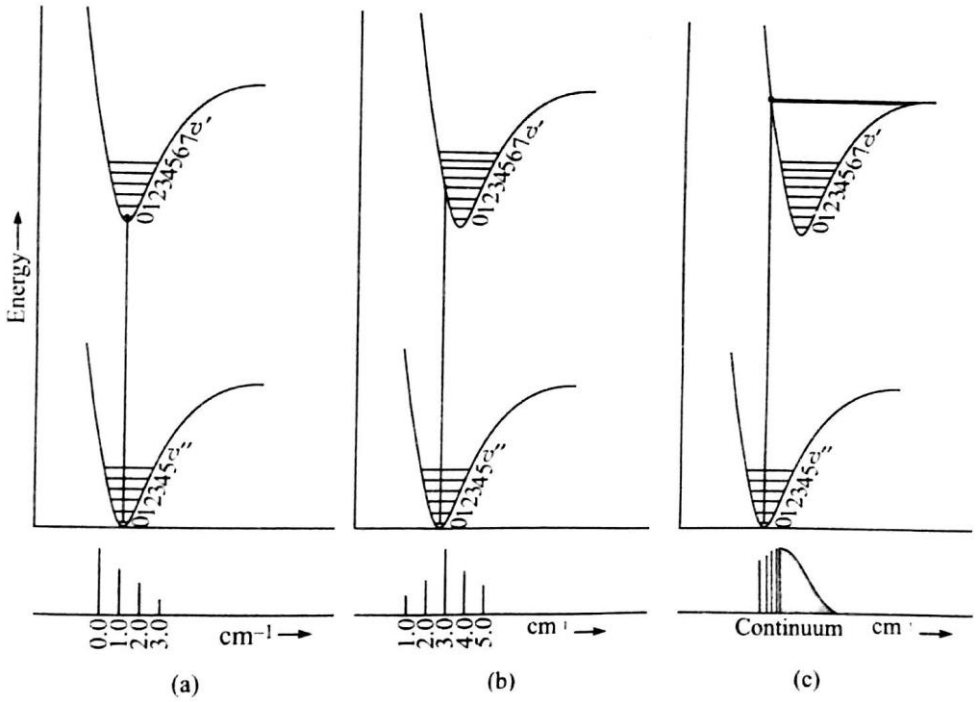

Fig.4.3 The operation of Franck-Condon principle for (a) upper and lower states having the same internuclear distance , (b) upper state inetrnuclear distance slightly greater than that in the lower state, (c) upper state distance greater than that in the lower state.

In the same way, in Figure 4.3(b), the (3,0) transition will be the most intense one. In figure 4.3(c) the vertical from the maximum of $V^{11}=0$ goes straight to the continuum of states and hence a continuum results. Franck – Condon Principle is thus able to account for the intensities of lines in vibrational electronic spectra.

4.6 Rotational fine structure of electronic – vibration.

Under high resolution each line in the spectrum consists of a set of closely spaced lines caused by the rotational fine structure of electronic – vibration transitions. Taking rotational energy into account,

$$\varepsilon_t' = \varepsilon_{el}' + \varepsilon_V' + B'J'(J'+1)\,cm^{-1} \qquad J' = 0,1,2.....$$

$$\varepsilon_t'' = \varepsilon_{el}'' + \varepsilon_V'' + B''J''(J''+1)\,cm^{-1} \qquad J'' = 0,1,2.....$$

Then the frequency of the transitions are :

$$\bar{\gamma} = \left(\varepsilon_{el}' - \varepsilon_{el}''\right) + \left(\varepsilon_V' - \varepsilon_V''\right) + B'J'(J'+1) - B''J''(J''+1)$$

Replacing the first two terms by $\bar{\gamma} V', V''$ the wavenumber of an electronic vibrational transition,

$$\bar{\gamma} = \bar{\gamma}_{V',V''} + B'J'(J'+1) - B''J''(J''+1) \qquad (4.15)$$

$\bar{\gamma}_{V',V''}$ could by any one of the (0,0), (1,0), (2,0), (3,0) ..... transitions. The selection rule for J is

$$\Delta J = \pm 1 \qquad (4.16)$$

This leads to the presence of both P and R branches. For all other transitions.

$$\Delta J = 0, \pm 1 \qquad (4.17)$$

In such cases, Q branch will also be there in addition to P and R branches.

For P branch, $\Delta J = -1$ (or) $J^1 - J^{11} = -1$

The rotational contribution,

$$B'J'(J'+1) - B''J''(J''+1) = B''(J''-1)\;\; J'' - B''J''(J''+1)$$

$$= -\left(B' + B''\right)J'' + \left(B' - B''\right)J''^2\; cm^{-1} \qquad J'' = 1,2,3$$

$$\therefore \bar{\gamma}_p = \bar{\gamma}_{V',V''} - \left(B' + B''\right)(J'+1) + \left(B' - B''\right)\left(J'+1\right)^2, \quad J' = 0,1,2,3 \qquad (4.18)$$

For R branch,

$$\Delta J = +1,\ J^{1} - J^{11} = +1$$

$$\therefore \bar{\gamma}_R = \bar{\gamma}_{V',V''} + (B' + B'')(J''+1) + (B' - B'')(J''+1)^2 \ ;\ J'' = 0,1,2,3 \tag{4.19}$$

For Q branche

$$\bar{\gamma}_Q = \bar{\gamma}_{V',V''} + (B' - B'')J''^2 + (B' - B'')\ J'' = 1,2,3 \tag{4.20}$$

The frequency $\bar{\gamma}_{V^1,V^{11}}$ is referred to as *band orgin*. Eqns (4.18) and (4.19) can be combined into a single equation as

$$\bar{\gamma}_{P,R} = \bar{\gamma}_{V',V''} - (B' + B'')m + (B' - B'')m^2 \ cm^{-2} \tag{4.21}$$

$$m = \pm 1, \pm 2, \pm 3 \ldots\ldots$$

Where m replaces $(J^1 + 1)$ in Eq (4.18) and $(J^{11} + 1)$ in Eq.(4.19). For R branch lines, m takes +ve values whereas it takes –ve values for P branch lines.

In general the equilibrium internuclear distance of the upper electronic state will be larger than that of the lower. Consequently, the rotational constant B^1 will be less then B^{11}. In such a case the P branch lines occur on the low wavenumer side of the band origin and th line spacing increases as the involved quantum number increases. The R branch appears on the high wavenumber side of the band origin, the line spacing decreases with increasing quantum number. The R branch converges to a line called the band head and then begins to return to the low wavenumber side with increasing spacing. The Q branch lines also lie on the wavenumber side of the origin with an increase in spacing with increasing J^{11}. The rotational fine structure of all the branches are shown in Fig.4.4. The complete spectrum will be superposition of all the three branches. When $B' < B''$, the band head appears on the high wave number (violet) side of the spectrum and the band is said to be shaded on degraded towards the red. If $B' > B''$ the above situation will be reversed completely. When $B' = B''$ the spectrum resembles that of a pure vibration rotation spectrum with no band head.

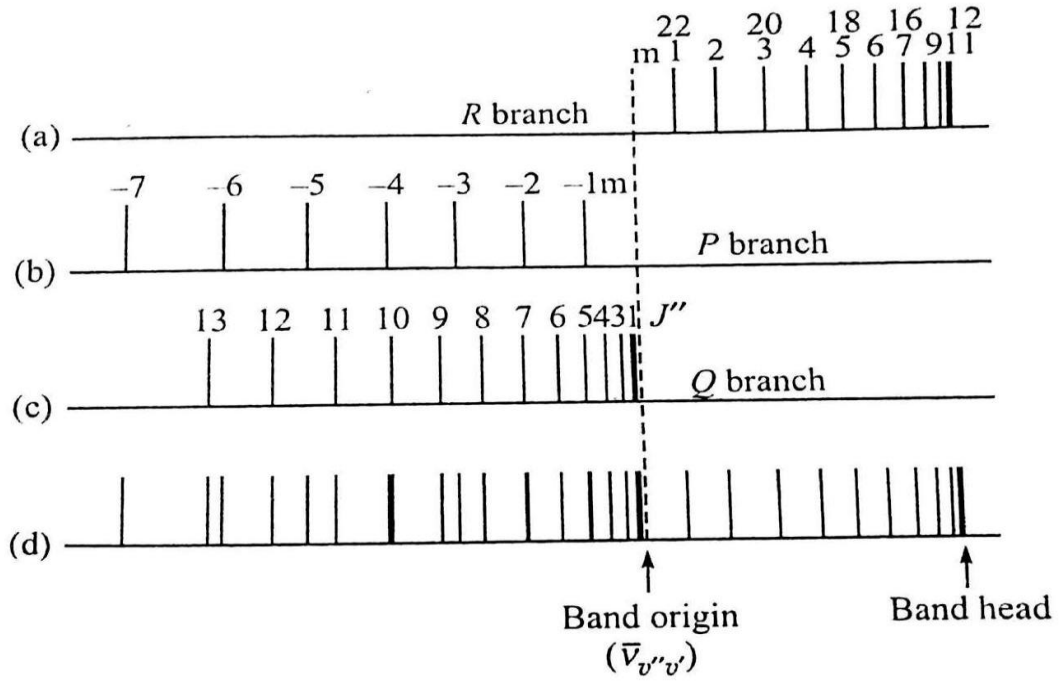

Fig.4.4: The rotational fine structure of a electronic – vibration transition for a diatomic molecule $(B' < B'')$ **(a) R branch, (b) (P-branch) (c) Q branch (d) complete spectrum**

4.7 The Fortrat Parabolae

Frequencies of the lines in Q, P and R branch Eqs. (4.20) and (4.21) can be written with continuous variable p and q as

$$\bar{\gamma}_{P,R} = \bar{\gamma}_{V',V''} + (B' + B'')p + (B' - B'')p^2 \qquad (4.22)$$

$$\bar{\gamma}_{Q} = \bar{\gamma}_{V',V''} + (B' - B'')q + (B' - B'')q^2 \qquad (4.23)$$

Where p takes both +ve and –ve values and q takes only +ve values. Equations (4.22) and (4.23) are equations to parabolae and are illustrated in Fig.4.5. These parabola are referred to as Fortrat parabolae. The PR parabola intersects the axis at N, the band origin. Its vertex H is the band head. As we have a turning point at the vertex

$$\frac{d\bar{\gamma}_{P,R}}{dp} = 0 = B' + B'' + 2(B' - B'')p \qquad (4.24)$$

Therefore, the position of the band head corresponds to

$$P_{head} = -\frac{(B' + B'')}{2(B' - B'')} \qquad (4.25)$$

Substitution of Eq. (4.25) in Eq.(4.22) gives,

$$\bar{\gamma}_{P,R} - \bar{\gamma}_{V',V''} = -\frac{(B'+B'')^2}{4(B'-B'')} \qquad (4.26)$$

The right hand side is +ve if $B' < B''$. That is, the band head is at a higher frequency than the band origin (Fig.4.5). This means the band head appears in the R branch with +ve P values. If $B' > B''$, the band head occurs in the P branch with –ve P values.

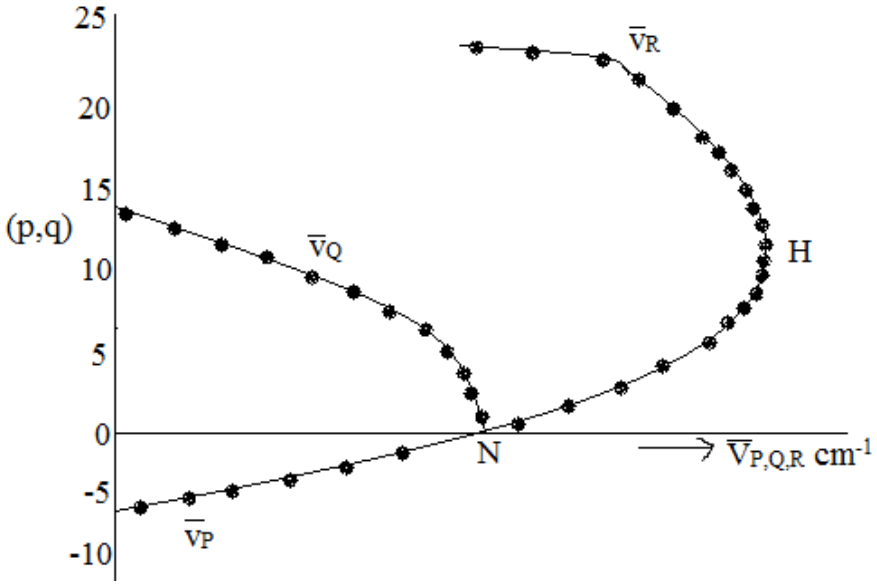

Fig.4.5 The Fortrat parabolae in B' < B" (H-band head, N- band origin)

4.8 Dissociation

The energy required to separate a stable diatomic molecule AB in the $V = 0$ vibrational state into the two unexcited atoms A and B is known as the *dissociation energy* D_0. The different dissociation energies are illustrated in Fig.4.6. D_0^{11} and D_0^{1} are the dissociation energies of the normal and excited molecules respectively. From D_0 and is given by

$$D_e = D_0 + \varepsilon_0 \quad cm^{-1} \qquad (4.27)$$

Where ε is the zero point energy.

Normally, a molecule in the state corresponding to the continuum limit dissociates into a normal atom and an excited atom with an excitation energy E_{ex}. Energy (Fig.4.6) is the total energy of the dissociation products in the upper state minus the total energy of dissociation products in the upper state minus the total energy of dissociation produces in the lower state. If the molecule dissociates from one of the continuum states, the energy in excess of the continuum limit will be appearing as K.E. of the separated atoms.

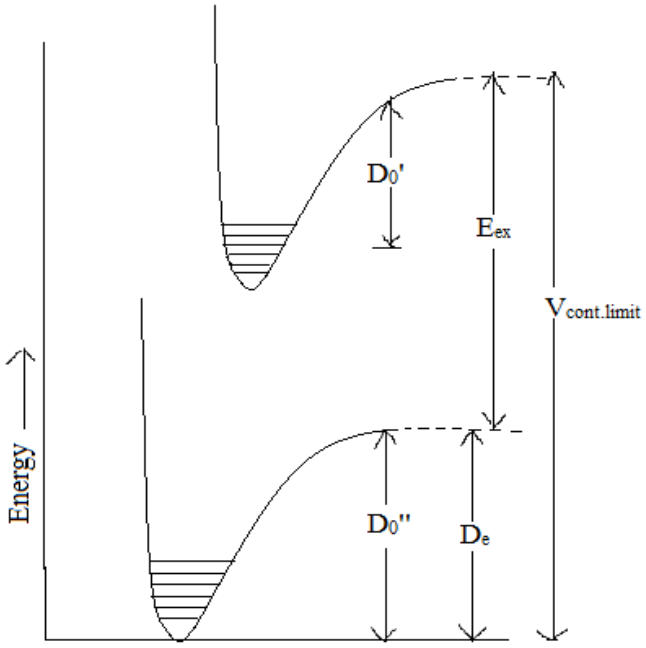

Fig.4.6 Illustration dissociation

Energy balance requires,

$$\bar{\gamma}_{\text{cont.limit}} = D_0^{11} + E_{ex} \ \ cm^{-1} \tag{4.28}$$

Also,

$$\bar{\gamma}_{\text{cont.limit}} = \gamma_{00} + D_0^{1}$$

Hence,

$$D_0^{11} = \bar{\gamma}_{00} + D_0^{1} - E_{ex} \tag{4.29}$$

The value of $\bar{\gamma}_{\text{cont.limit}}$ is known accurately from electronic spectroscopy and E_{ex} is available from atomic spectroscopy. Using these values one can estimate the dissociation energy.

The vibrational energy ε_V of a diatomic molecule is given by

$$\varepsilon_v = \left(V + \frac{1}{2}\right)\bar{\gamma}_e - \left(V + \frac{1}{2}\right)^2 \ \bar{\gamma}_e \ x_e$$

The separation between successive vibrational levels $\Delta\varepsilon$ is

$$\Delta\varepsilon = \varepsilon_{V+1} - \varepsilon_V + \bar{\gamma}_e \left[1 - 2x_e (V+1)\right] cm^{-1}$$

This separation decreases linearly with increasing V and tends to zero when the dissociation limit is reached. Denoting the value of the corresponding to dissociation limit $(\Delta\varepsilon = 0)$ by $V_{\max}$ We have,

$$\bar{\gamma}_e\left[1-2x_e\left(V_{\max}+1\right)\right]=0$$

$$V_{\max}=\frac{1}{2x_e}-1$$

The vibrational energy for $V=V_{\max}$ is the equilibrium dissociation energy D_e.

$$D_e=\left(\frac{1}{2x_e}-\frac{1}{2}\right)\bar{\gamma}_e-\left(\frac{1}{2x_e}-\frac{1}{2}\right)^2 x_e\bar{\gamma}_e$$

$$=\frac{\bar{\gamma}_e}{4x_e}-\frac{1}{4}x_e\bar{\gamma}_e\simeq\frac{\bar{\gamma}_e}{4x_e}\ cm^{-1} \qquad (4.30)$$

The value of D_e may be estimated from the known values of the $\bar{\gamma}_e$ and x_e from which the value of D_0[11] can be evaluated.

4.9 Predissociation :-

In electronic spectra, a continuum at the high wavenumber side correspond to ordinary dissociation. However, in certain cases, the rotational fine structure is diffused or a complete continuum is observed for intermediate changes. Occurrence of such diffuse structure or complete continuum below the true dissociation limit is referred to as p*redissociation* which was first observed in the electronic spectrum of S_2.

A simple case of predissociation is explained with respect the Morse curve, A, B and C in Fig.4.7. The excited state C is not stable as it has no minimum. Consider a transition taking place from curve A to curve B. If it is into the levels labelled $V^1=0,1,2$ a normal vibrational electronic spectrum with rotational fine structure occurs. However if it is to $V^1=3$ there is a possibility that the molecule will 'cross – over' to the continuous curve C and dissociate. When this radiationless transition from curve B to curve C takes place there will not be any rotation of the molecule as the time required for a molecular rotation is $\approx 10^{-14}$ sec.

Transitions to the levels 4,5,6,7 will also give rise to normal vibrational electronic spectrum with rotational fine structure the molecule spends more time at the extreme ends of the vibrational motion and minimum time near the crossing points. It may be remembered that the crossing over from curve B to curve C may take place even if the transition is to $V^1=2$ and 4, the nearby levels of $V^1=3$.

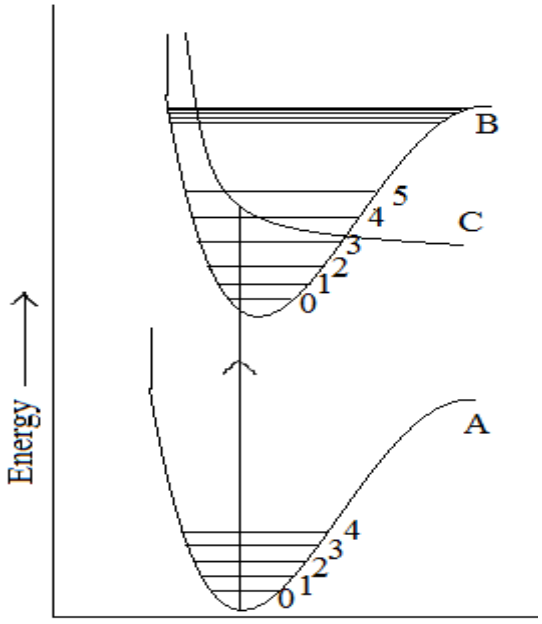

Fig. 4.7: Pre dissociation during transition to a stable upper state intersected by a continuums state

4.10 Photoelectron Spectroscopy :

(i) Principle :-

It is based on the well known photoelectric effect first explained by Einstein in 1905. If a sample is irradiated with high energy photons of energy $h\gamma$, electrons are emitted and part of the energy of the incident radiation is carried off as K.E. of the emitted electrons. Energy conservation requires,

$$h\gamma = I + E_{el} + E_{ion} \qquad (4.31)$$

Where I is one of the ionization energies, E_{el} is the K.E. of the emitted electron and E_{ion} is the K.E of the ion plus any internal energy of the ion. In photo electron spectroscopy (PES), a monochromatic radiation is used to ionize the atoms, A schematic representation of the energetics of PES is shown in Fig.4.8.

Two techniques have been developed, namely ultraviolet photoelectron spectroscopy (VPS) and X-ray photoelectron spectroscopy (XPS), depending upon the radiations used in exciting photoelectrons. VPS usually probes the values orbital electrons in an atom or molecule or solid and XPS the core orbital electrons.

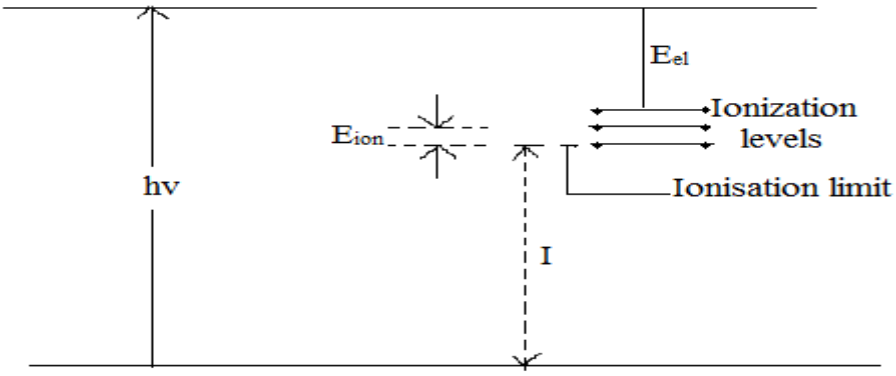

Fig.4.8 Schematic representation of energetic of PES

(ii) Instrumentation :-

A typical photo electron spectrometer requires four components and Fig.4.9 gives a schematic diagram.

i. A suitable source of electromagnetic radiation of high intensity.
ii. A sample chamber to hold the sample in the required physical state.
iii. An electron energy analyzer to analyze the energy distribution of electrons emitted from the sample.
iv. A suitable detection system to detect the electrons whose energy has been measured by the electron analyzer.

Most frequently used UV source is either the 58.4nm (21.21 ev) line of He-I or the 30.39nm (40.81 ev) line of He-II. The width of these lines are ~ 0.1 ev. Other less monochromatic sources Ne-I at 73.58nm (16.85ev) and they Lyman line of atomic hydrogen at 121.55nm (10.2ev) are also used. A typical X-ray source consist of a twin anode of aluminium and magnesium giving Al K_α (0.834nm, 1486.6ev) and Mg K_α (0.989 nm 1253.6 ev). The large line width of X-ray sources can be reduced by the use of monochromators.

The resolving power of the instrument decreases as the line width of the source increases. With the use of synchrotron radiation this problem is solved to a very great extent.

Electron energy analyzers of different types are available. All of them are either of the magnetic type or the electrostatic type. In either case the analyzer must be shielded from the earth's magnetic field to avoid its effect on the motion of the electrons. Shielding of the electrostatic analyzer is easier than that of magnetic analyzer. When photo electrons emitted they should reach the detector without being scattered by gas molecules. Also the excitation source and the sample should be kept under clear conditions. Hence the experimental chamber is usually made up of stainless steel and equipped with the source, sample manipulator, electron energy analyzer and arrangement for the detection of photo electrons.

The photoelectron signal is amplified and fed to a recorder or the data is stored in a computer. The whole set up except the recording system is kept in ultra high vaccum.

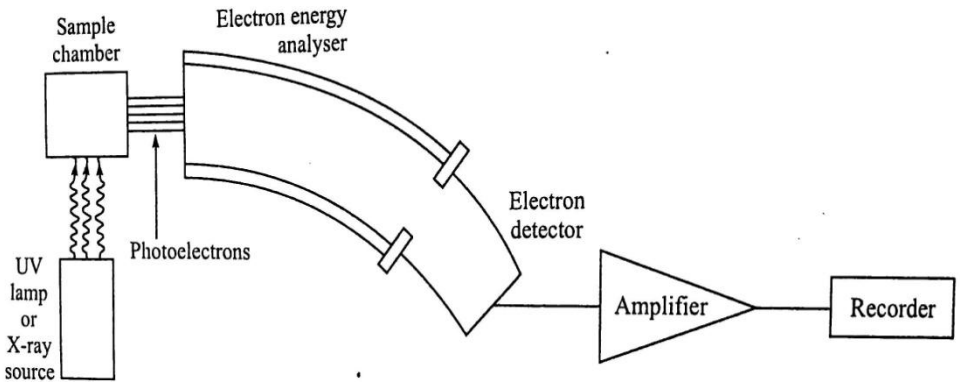

Fig.4.9 Schematic diagram of a photoelectron spectrometer.

4.11 Information from Photoelectron spectra

Measurement of the kinetic energy of the photoelectrons can give values for the binding energies of all the electrons in an atom or molecule.

1. Orbital energies of atoms :

In the simplest case hydrogen, when a helium lamp is used to give photons of energy 21.2 ev, the kinetic energy spectrum showed a single peak at $E_{el} = 7.6ev$.

As the next example, consider the spectrum of electron kinetic energies of the rare gas atoms studied using the excitation energy $h\gamma = 40.81\, ev.$ In each case the spectrum is a doublet with 2:1 relative intensity. The doubling is due to the formation of two internal energy states of the ion. Fig .4.10 shows the photoelectron spectra of some rare gas atoms.

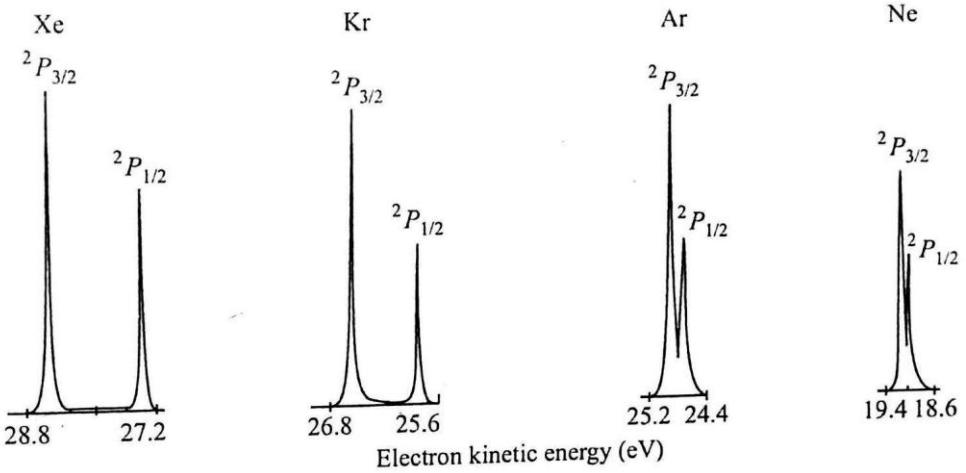

Fig. 4.10 Photoelectron spectra of rare gas atoms

2. Orbital energies of molecules

In the case of molecules, the nature of the ionization bands produced by the emission of electrons from nonbonding, bonding and anti-bonding orbitals follow certain pattern as follows. This helps very much the assignment of the ionization bands to orbitals.

(i) If the ionized electron comes from a non-bonding orbital, the potential energy curve for the ion is almost the same.

(ii) If a bonding electron is removed, the bonding in the ion is expected to be weaker then that in the molecule. Hence the potential energy curve of the ion will be shifted to the direction of longer equilibrium bonds.

(iii) If an electron in an antibonding orbital is removed the opposite of the above is expected.

3. Binding energy of core - electron

The binding energy of core electron varies depending on the electronic environment of the atom in the molecule. Consider the molecule ethyl chloroformate which shows 3 lines for the 1s ionization energy of the of carbon atoms. In the molecule the electronic environment of each carbon atom is different and hence each one gives a different. 1s ionization peak at slightly different energies. Binding energy difference of core electrons for nonequivalent atoms of the same kind in a compound is called *chemical shift.* Photoelectron spectroscopy of core electrons has become a very powerful to technique for structure determination.

UNIT – V

NMR , ESR, NQR and Mossbauer Spectroscopy

5.1 Introduction :-

The phenomenon of nuclear magnetic resonance (NMR), first observed in 1946, deals with transitions between energy levels that arise because of the different orientations of magnetic moment of nuclei placed in a magnetic field. These transitions are studied by means of a resonance method. Hence the name nuclear magnetic resonance.

5.2 Magnetic properties of Nucleus :-

One of the most important properties of a nuclei is its spin I or intrinsic spin angular momentum $I\hbar$. This gives rise to a magnetic moment to the nucleus. The following rules are useful in determining the value of nuclear spin I.

(i) If mass number A is odd and atomic, number Z is even or odd, I is half integer.

Examples : ${}_{1}H^{1}$, ${}_{6}C^{13}$, ${}_{7}N^{15}$, ${}_{9}F^{19}$,.....,

(ii) If A and Z are both even, I is zero.

Examples : ${}^{4}_{2}He$, ${}^{12}_{6}C$, ${}^{16}_{8}O$, ${}^{32}_{16}S$,.....,

(iii) If A is even and Z odd, I is integer.

Examples : ${}^{2}_{1}H$, ${}^{10}_{5}B$, ${}^{14}_{7}N$,

The projection of the spin vector I on any direction can have the values

$$m_I = -I, (-I+1).....,(I-2), (I-1), I$$

There are $(2I+1)$ in number, and all are degenerate in absence of an external magnetic field. In a magnetic field it splits up into $(2I+1)$ States. The Magnetic moment μ associated with the spin angular momentum is given by

$$\mu = \gamma I \hbar$$

Here γ is a scalar called the *gyromagnetic ratio* and may take +ve or –ve values. An alternate expression for the magnetic moment is given by

$$\mu = g_N \mu_N I$$

Where g_N, the nuclear *g* factor, μ_N is the nuclear magnetic field and is defined by

$$\mu_N = \frac{e\hbar}{em_p} = 5.51 \text{x} 10^{-27} \quad JT^{-1} (NM^2)$$

Where m_P in the proton mass.

5.3 Resonance condition :-

When a nucleus of magnetic moment μ is placed in a magnetic field B_0, the interaction energy.

$$E = -\mu.B_o = -\mu B_o \cos\theta = -\frac{\mu B_o m_I}{I} \qquad (5.1)$$

Since m_I can have 2I+1 values, we will have 2I+1 equally spaced energy levels. The energy separation between any two adjacent levels is given by

$$|\Delta E| = \mu B_o \frac{\Delta m_I}{I} = \frac{\mu B_o}{I} = g_N \mu_N B_o$$

The basis of NMR experiment is to induce a transition from a lower level to the next higher level. If γ is the frequency of the electromagnetic radiation that induces transitions between adjacent energy levels. Bohr's frequency condition is then,

$$h\gamma = \frac{\mu B_o}{I} = g_N M_N B_o \qquad (5.2)$$

Eq. (5.2) is the resonance condition

For a spin ½ system we will have 2 states, one corresponding to $m_I = ½$ and the other for $m_2 = -½$. Their energies are

$$E_{1/2} = -\mu B_o \text{ and } \quad E_{-1/2} = +\mu B_o \qquad (5.3)$$

The resonance condition reduces to

$$h\gamma = 2\mu B_o$$

These are represented in Fig.5.1. For proton, $\mu = 2.79268\,\mu_N$, and therefore,

$$\gamma = \frac{2 \text{ x } 2.79268 \text{ x } 15.051 \text{ x } 10^{-27}}{6.626 \text{ x } 10^{-34}} \quad B_o = (42.5772 \text{ x } 10^6) B_o \qquad (5.4)$$

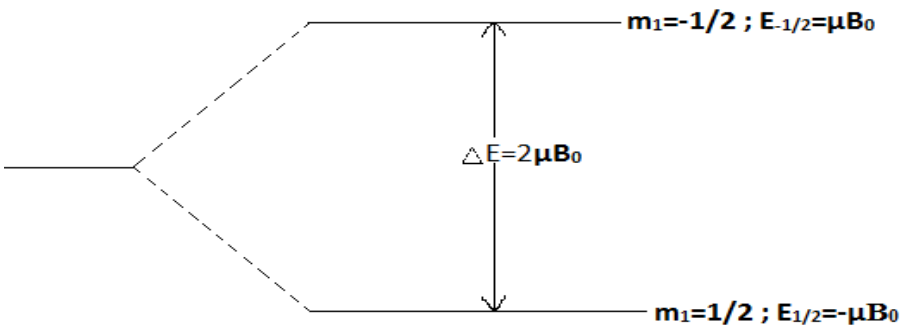

Fig.5.1: Energy levels of a spin ½ system in an external magnetic field B = B_0

Typical external magnetic fields used in NMR experiments are in the range 1 to 5T. The frequencies fall in the radio frequency region of the e.m spectrum and the sources used to induce the transitions are different from those used in the other regions of spectrescopy. The resonance condition is achieved by applying a radio frequency field oscillating at the Larmour frequency perpendicular to the external magnetic field.

Proten is one of the most important nuclei having a spin $I = 1/2$. It is a constituent in almost all organic molecules. The NMR of a proten nucleus is often called Proton magnetic Resonance (PMR). Another nucleus which is present in all organic compounds is carbon. As C^{12} has no magnetic moment it will not show any NMR spectrum. How C^{13} has a magnetic moment and shows resonance. NMR was first discovered in 1946 independently by Purcell, Pound and Torrey in Paraffin and Bloch, Hanson and Packard in water.

5.4 Relaxation Process :

The transfer of energy from the spin system to other degrees of freedom is referred to as *relaxation.* Two different relaxation process are common for the nuclei. In the first, the spins in the upper state transfer the excess energy to the surroundings (lattice). This phenomenon is called *spin-lattice relaxation* and the time required for the population difference to become 1/e times the population difference at t=0 is referred to as the spin-*lattice relaxation time* or *longitudinal relaxation time* T_1. T_1 varies over a large range, being $10^{-2} - 10^{4}$ sec, for solids and $10^{-4} - 10$ sec, for liquids.

In addition to spin-lattice relaxation relaxation of spin can also occur by a direct interaction of two spin states. Consequently, if initially the spins have a common phase, the phase will became random in the course of time. The dephasing time is known as *spin–spin relaxation time (or) transverse relaxation time* T_2. For solids, T_2 is the order of 10^{-4} seconds, while for liquids $T_2 \approx T_1$. The shape of the spectral lines depends significantly on the relaxation time.

For the spin ½ system, let N be the total number of spins, n(o) and n(t) be the population difference at time t=0 and t=t respectively. Then,

$$\frac{dn_1}{dt} = \omega n_2 - \omega n_1 = \omega (n_2 - n_1) = -\omega n \qquad (5.5)$$

Where ω is the transition probability per unit time for induced absorption / emission. Since $n_1 + n_2 = N$ *and* $n_1 - n_2 = n$.

$$n_1 = \frac{1}{2}(N + n), \qquad \frac{dn_1}{dt} = \frac{1}{2}\frac{dn}{dt} \qquad (5.6)$$

From Eqs. (5.5) and (5.6),

$$\frac{dn}{dt} = -2\omega n, \qquad n(t) = n(o)\, e^{-2\omega t} \tag{5.7}$$

The time required for the value of $n(t)$ to become $n(o)/e$ is defined as the spin – lattice relaxation time T_1. Therefore

$$T_1 = \frac{1}{2\omega} \tag{5.8}$$

That is, the spin – lattice relaxation time is inversely proportional to the transition probability per unit time for induced adsorption.

5.5 Bloch Equations:-

Consider a nucleus that possesses a magnetic moment μ and an angular momentum $I\hbar$. The torque experienced by the magnetic moment vector μ in a static magnetic field B is $\mu \times B$. As the rate of change of angular momentum is equal to the torque acting on the system

$$\frac{d}{dt}(I\hbar) = \mu \times B$$

Since $\mu = \gamma I \hbar$

$$\frac{d\mu}{dt} = \gamma(\mu \times B) \tag{5.9}$$

If we rotate the vector μ with an angular velocity ω.

$$\frac{d\mu}{dt} = \omega \text{ x } \mu \tag{5.10}$$

Comparison of Eqs. (5.9) and (5.10) shows that the effect of the magnetic field is exactly equivalent to a rotation with angular velocity.

$$\omega = -\gamma B$$

That is, the magnetic dipole processes about the direction of B with an angular velocity ω. This phenomenon is called the *Larmor precession* and the frequency is called *Larmor frequency*. The nuclear magnetization M is $\sum_i \mu_i$ over all the nuclei in unit volume.

Therefore, Eq.(5.9) summed over all nuclei gives

$$\frac{d\mu}{dt} = \gamma(\mu \text{ x } B) \tag{5.11}$$

If the applied magnetic field B is along z-direction, $B = B_0 \hat{Z}$, where $\hat{Z}$ is the unit vector along Z-axis, under thermal equilibrium the magnetization will be along the Z-axis. That is,

$$M_x = 0,\ M_y = 0,\ M_z = M_0 = \chi_0 B_0 = \frac{CB_o}{T} \tag{5.12}$$

Where *C* is the Curie constant, *T* is the absolute temperature and χ_0 is the volume susceptibility. For a spin ½ system, in the presence of the magnetic field B_0 there will be two energy levels separated by $2\mu B_o$. If N_1 and N_2 be the population per unit volume of the upper and lower levels.

$$M_Z = (N_1 - N_2)\ \mu = N\mu$$

Under thermal equilibrium,

$$\frac{N_2}{N_1} = \exp\left(-\frac{2\mu B_o}{KT}\right)$$

Where K is the Boltzmann constant. Then the equilibrium magnetization can be shown to be equal to

$$\frac{N_2}{N_1} = \exp\left(-\frac{2\mu B_o}{KT}\right)$$

Where K is the Boltzmann constant. Then the equilibrium magnetization can be shown to be equal to

$$M_0 = N_\mu \tanh\left(-\frac{\mu B_o}{KT}\right) \tag{5.13}$$

When M_Z is not in thermal equilibrium, let us assume that the magnetization approaches the equilibrium value M_0 at a rate proportional to the departure from the value M_0.

$$\frac{dM_Z}{dt} = \frac{M_0 - M_Z}{T_1} \tag{5.14}$$

Where T_1 is the spin – lattice relaxation time. Including this Eq. (5.14), the Z – component of the equation of motion becomes,

$$\frac{dM_Z}{dt} = \gamma (M \times B)_x + \frac{M_0 - M_Z}{T_1} \tag{5.15}$$

Eq.(5.15) indicates that the magnetization vector besides precessing about the magnetic field, will relax to the equilibrium value M_0.

In a static magnetic field $B_0 \hat{Z}$, when thermal equilibrium is reached, the *x* and *y* components of magnetization will be zero. Therefore, the M_x and M_y components will be decaying zero, giving the *x* and *y* components of the equation of motion becomes,

$$\frac{dM_x}{dt} = \gamma (M \times B)_x - \frac{M_x}{T_2} \tag{5.16}$$

$$\frac{dM_y}{dt} = \gamma (M \times B)_y - \frac{M_y}{T_2} \tag{5.17}$$

Where T_2 is the spin–spin relaxation time. Expanding the vector product (M x B), we have,

$$\frac{dM_x}{dt} = \gamma (M_y B_z - M_y B_z) - \frac{M_x}{T_2} \tag{5.18a}$$

$$\frac{dM_y}{dt} = \gamma (M_z B_x - M_x B_z) - \frac{M_y}{T_2} \tag{5.18b}$$

$$\frac{dM_z}{dt} = \gamma (M_x B_y - M_y B_x) + \frac{M_0 - M_Z}{T_1} \tag{5.18c}$$

In the NMR experiment, the r-f magnetic field is applied in a direction perpendicular to $B_0 \hat{Z}$ Now we interest to study the behaviour of magnetization in the combined r-f and static fields. An a-c magnetic field polarized along the *x*-axis can be represented by two rotation fields, one in the same sense as the Larmor. precession of the nucleus and the other rotating in the opposite direction. Therefore the effective component of the a-c field which is represented by the vector

$$\hat{B}_1 = B_x \hat{x} + B_y \hat{y} = (B_1 \cos \omega t) \hat{x} - (B_1 \sin \omega t) y \tag{5.19}$$

Including B_1 , the magnetic field components acting on the system are,

$$B_x = B_1 \cos \omega t \tag{5.20a}$$

$$B_y = - B_1 \sin \omega t \tag{5.20b}$$

$$B_Z = - B_0 \tag{5.20c}$$

Substituting the values of B_x, B_y and B_z in Eq.(5.18), we have

$$\frac{dM_x}{dt} = \gamma (M_y B_0 + M_z B_1 \sin \omega t) - \frac{M_x}{T_2} \tag{5.21a}$$

$$\frac{dM_y}{dt} = \gamma (M_z B_1 \cos \omega t - M_x B_0) - \frac{M_y}{T_2} \tag{5.21b}$$

$$\frac{dM_z}{dt} = - \gamma (M_x B_1 \sin \omega t + M_y B_1 \cos \omega t) + \frac{M_0 - M_Z}{T_1} \tag{5.21c}$$

Eqns. (5.21a), (5.21b) and (5.21c) together are called the *Bloch equations*.

5.6 NMR Instrumentation :-

The basic requirements of a typical NMR spectrum are

(i) An electromagnet giving a powerful, stable and homogeneous magnetic field. The field must be a constant over the area of the sample and over the period of time of the experiment.

(ii) A sweep generator which supplies a variable current to a secondary magnet. Then the total applied magnetic field can be varied over a small range.

(iii) The sample container usually a glass tube (5mm OD) spun by an air–driver turbine to average the magnetic field over the sample container. This process is often referred to as the spinning of the sample.

(iv) A r-f oscillator connected to a coil, called the transmitter coil, transmits the energy to the sample.

(v) A r-f receiver connected to the coil, called the receiver coil, encircles the sample. The transmitter and receiver coils and the sample holder are constructed into a single unit called *probe.*

(vi) A read out system consisting of an r-f amplifier, recorder and other accessories to increase the sensitivity, resolution and accuracy.

A schematic representation of the components are shown in Fig.5.2.

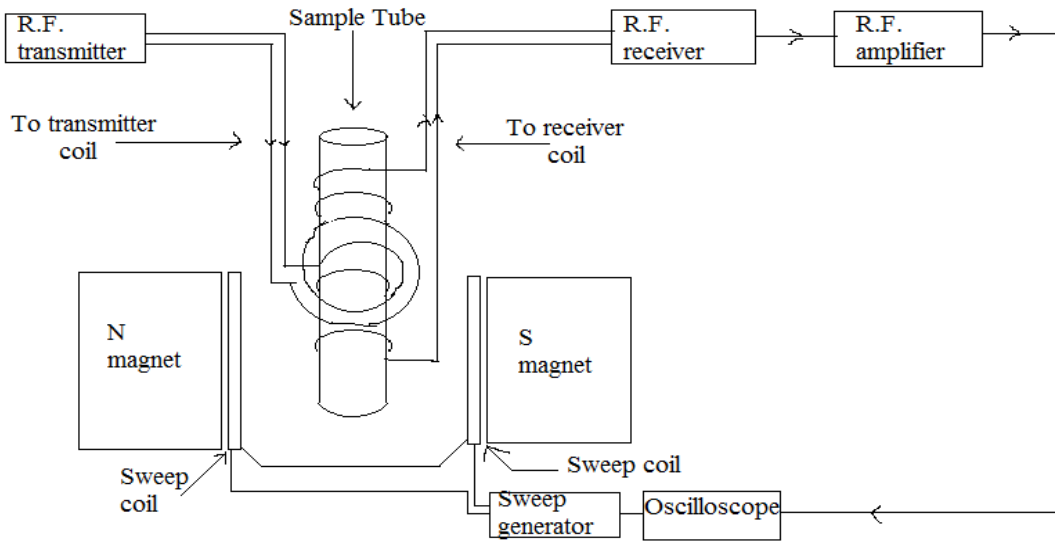

Fig.5.2 Block diagram of a NMR spectrometer

5.7 Chemical shift :-

According to the resonance condition, all protons should absorb energy at the same magnetic field. However it is not the case even under low resolution. The spectrum of acetaldehyde (CH_3CH_0) showed two lines with intensity ratio 1:3 whereas ethanol

(CH_3CH_2OH) showed 3 lines in the ratio 1:2:3 (Fig.5.3). Moving electrons in a molecule constitute effective currents within the molecule and this produces a secondary magnetic field which acts in a direction opposite to the externally applied magnetic field.

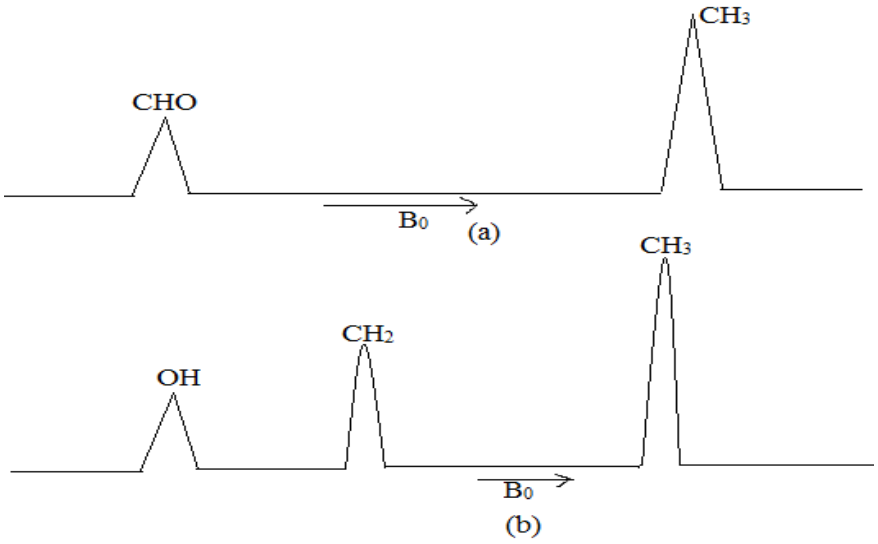

Fig.5.3 The NMR spectrum of (a) CH_3CHO, (b) CH_3CH_2OH under low resolution.

That is, the nucleus finds itself in an effective field less than the actual field applied. In other words, the nucleus is screened by the surrounding electrons. Thus,

$$B_{eff} = B_0 - \sigma B_0 = B_0 (1 - \sigma) \tag{5.22}$$

Where σ is a dimensionless constant called the *screening constant* or *shielding parameter*. The value of σ $(\approx 10^{-5})$ depends on the electron density around the proton. Figure 5.4 illustrates the situation for a shielded spin ½ nucleus.

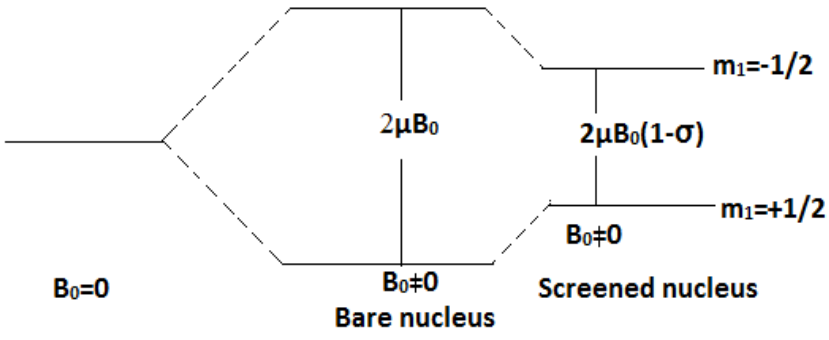

Fig. 5.4: Bare and screened, spin ½ nucleus in a magnetic field B_0.

The shift of the resonance line in a given compound from of a standard reference sample is called the *chemical* shift (δ) of the compound. The absolute magnitude of the sample is

extremely small. Let B_r and B_s be the magnetic field at which resonance occurs for the reference and given compound. Then,

$$B_r = B_0\,(1-\sigma_r),\quad B_S = B_0\,(1-\sigma_s)$$

$$\sigma = \frac{B_r - B_S}{B_0} = \sigma_S - \sigma_r \tag{5.23}$$

Since σ_S and σ_r are extremely small, a different unit is usually selected in terms of field or frequency for expressing the chemical shift.

$$\delta = \frac{B_r\,(reference) - B_S\,(Sample)}{B_0} = x10^6\ ppm \tag{5.24}$$

$$\delta = \frac{\gamma_S\,(sample) - \gamma_r\,(reference)}{\gamma_0} = x10^6\ ppm \tag{5.25}$$

In general, the reference is selected in such a way that it gives the resonance at a very high field. This leads to a +ve δ in most of the cases. A different chemical shift τ which is the one commonly used by chemists, is some times employed.

$$\tau = 10.00 - \delta \tag{5.26}$$

The reference sample generally used is tetramethyl silane $(CH_3)_4$ Si, here after abbreviated as TMS. It is chemically inert and contains 12 photons of the same type. Hence only very little is required as reference sample and it gives a very intense sharp peak. From definition it is obvious that the τ value for TMS is 10.

Electron Spin Resonance Spectroscopy (ESR)

5.8 Introduction

ESR is a spectroscopic technique confined to the study of those species heaving one or more unpaired electrons. Among the large number of paramagnetic systems, the most important ones are transition metal ions, free radicals, ions and molecules having an odd number of electrons etc. So this spectroscopy is also called *Electron paramagnetic resonance (EPR) spectroscopy.*

5.9 Principle of ESR

When an electron having magnetic moment μ is placed in a magnetic field *B*, the interaction energy,

$$E = -\mu.B = -\mu B\cos\theta \tag{5.27}$$

Where θ is the angle between μ and B. If the system has only spin magnetic moment μ, then it is given by

$$\mu = -g\mu_B S = g\mu_B m_S \tag{5.28}$$

$\therefore$ The Eq.(5.27) becomes,

$$E = -g\mu_B B m_s \tag{5.29}$$

For electron, $m_s = \pm ½$ and we get two levels with energies (Fig.5.5)

$$E_{-½} = -\frac{1}{2} g\mu_B B, \quad E_{½} = \frac{1}{2} g\mu_B B$$

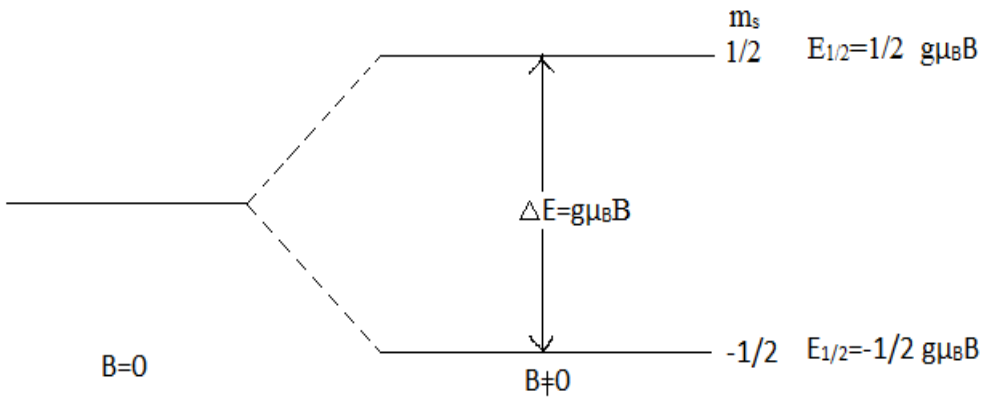

Fig. 5.5: Zeeman splitting of an impaired electron in a magnetic field B.

If electromagnetic radiation of frequency γ satisfying the relation.

$$h\gamma = E_{½} - E_{-½} = g\mu_B B, \tag{5.30}$$

is present, transition between these Zeeman levels occur which is studied by ESR. Eq.(5.30) gives the resonance condition for ESR observation. For free electron, g = 2.0023. In a field of 0.34T, from Eq. (5.30).

$$\gamma = \frac{2.0023(9.274 \times 10^{-24}\ J\,T^{-1})\,0.34T}{6.626 \times 10^{-34}\ J.Sec}$$

$$= 9528\,MH_Z$$

This frequency falls in the microwave region. Hence microwave source and techniques have to be applied for the observation of ESR.

5.10 ESR Spectrometer :

Successful observation of the ESR spectrum requires suitable values for the frequency γ and the magnetic field B to the satisfy the Eq (5.30), ie $h\gamma = g\mu_B B$, For magnetic field of

0.34T, γ comes out to be about $9.5 GH_z$. Spectrometers operating around this frequency are often referred to as *X-band spectrometers*. Spectrometers operating at higher magnetic fields $(B = 1.3T)$ with corresponding higher microwave frequency (~35GH$_z$) are also available. They are called *Q-band spectrometers*.

For continuous absorption one can either vary the frequency γ across resonance keeping the field *B* constant or the magnetic field is varied keeping the frequency constant. The latter method is usually preferred since it is easier to vary the magnetic field keeping the stability at very high levels.

(i) Basic requirements :

Some of the basic requirements of a X-band ESR spectrometer are :

(i) An electromagnet capable of supplying a homogeneous magnetic field which can be varied linearly on either side of the magnetic field.

(ii) Source of microwave radiation in the region of 9.5 GH$_z$.

(ii) Suitable sample cavity.

(iv) Arrangements for transmitting the radiation energy in to the sample cavity.

(v) Detection system to measure the variation in microwave power.

(vi) Suitable oscilloscope or recorder.

(ii) Description of the set-up :

A simple block diagram of balanced bridge ESR spectrometer is given in Fig.5.6.

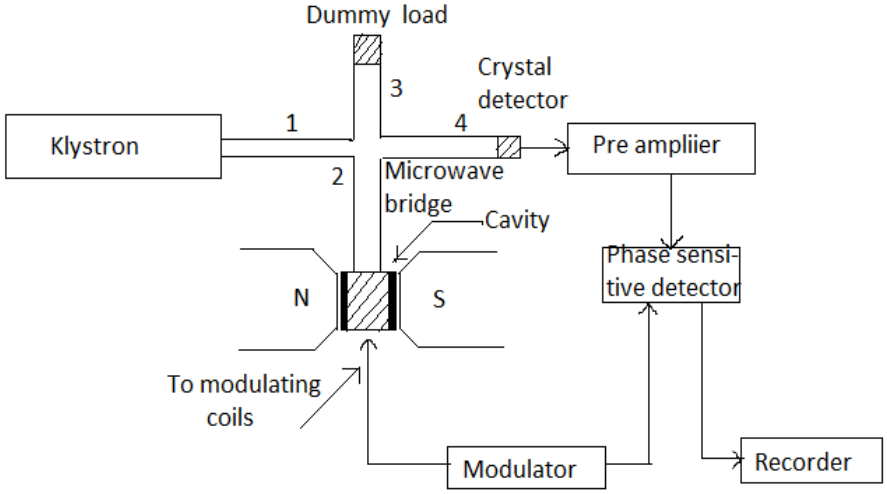

Fig.5.6 Block diagram of a simple balanced bridge ESR spectrometer.

The usual source of radiation is a klystron oscillator which produces monochromatic radiation of the required frequency. The radiation from the source is transmitted to the sample cavity through a microwave impedance bridge. The rectangular microwave cavity which

contains the sample is kept in between the pole pieces of the electromagnet. A dummy load is kept in the third arm and a semi–conductor crystal in the fourth arm of the microwave bridge. The radiations that arrive in the 4^{th} arm are detected by the crystal. It is then amplified and fed to a suitable recorder phase sensitive detectors are usually to detect ESR signals and represented as absorption or first derivative curves (Fig.5.7). The magnetic field is swept over a small range across the resonance condition by varying the current in a pair of sweep coils mounted on the cavity walls.

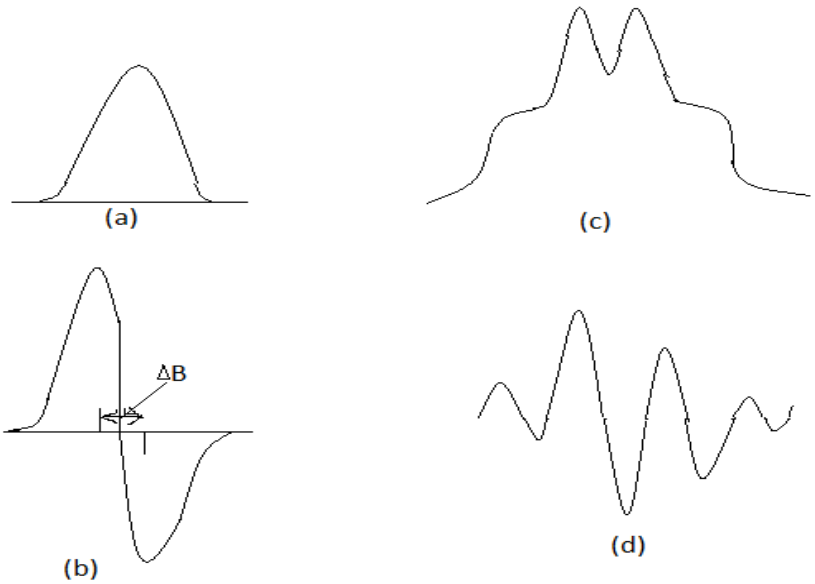

Fig.5.7 ESR signal (a) a single absorption line (b) its first derivative , (c) four equally spaced overlapping absorption lines, (d) first derivative of the spectrum in (c)

(iii) Working

When the bridge is in a balanced positive microwave power flows only in the two arms – the one cavity and the others to the dummy load. There will be any power in the fourth arm. Power in the fourth arm will be there only when the bridge is not balance. Thus, if balance exists, initially no signal appeal at the detector and when the sample absorbs, the balancing of the bridge is lost and power appears in the fourth arm. The width of ESR lines are fairly large and hence the spectrum is usually recorded in the first derivative mode which enable one to fix up the frequency position and estimation of intensity more precisely. Another advantage of derivative mode is that it gives a well – defined line width ΔB (Fig.5.7). Even if there are overlapping signals, it is still possible to do a good estimate of . ΔB .

5.11 Fine and Hyperfine structure :-

In E.S.R spectra, we may observed two kinds of multiplet structures, one is Fine structure and another one is Hyperfine structure.

Fine structure which occurs only in crystals containing more than one unpaired electron spin.

Hyperfine structure which arises when an unpaired electron can get close to a nucleus with non zero-spin.

(a) The Hyper fine structure of ESR absorption-(Electron-Nucleus coupling)

It is the interaction of the magnetic moment of the unpaired electron with those of any surrounding nucleus having non–zero spin which gives rise to hyperfine structure. For Simplicity, we shall limit our treatment here to nucleus of spin ½ which will split electron resonances into doublets. If more than are nucleus can interact with a given electron, the result can be predicted using the family free method.

The nuclear electron coupling is a direct dipole dipole interaction between the electron and nuclear magnetic moments. As this interaction depends upon the angle between the magnetic field and the line joining the two dipoles, it is directional and is referred to as the anisotropic interaction. Its magnitude is proportional to $1/r^3$ where r is the distance between the dipoles. For free radicals in solution, since the orientation of the radical with respect to the magnetic field changes rapidly, this interaction averages to zero and the hyperfine structure observed then is from the other mechanism.

Already we know that, the dipole – dipole interaction is given by

$$H_{dip} = g\, g_N\, \mu_B\, \mu_N \left[\frac{S.I}{r^3} - \frac{3(S.r)(I.r)}{r^s} \right] \qquad (5.31)$$

The second–nuclear interaction is the *Fermit contact interaction* which has no classical analogue. This represents the interaction between the nuclear moment and the magnetic field produced by the electron spin at the nucleus. This depends on the finite impaired electron density at the nucleus, which is possible when it occupies an S-orbital. This interaction is independent of orientation and is given by

$$H_F = \frac{8\pi}{3} g\, g_N\, \mu_B\, \mu_N |\psi(0)|^2\, S..I = a\, S..I \qquad (5.32)$$

Where $\psi(0)$ is the electron wave function at the centre of the nucleus, and ‘a’ is the hyperfine splitting constant.

$$a = \frac{8\pi}{3} g\, g_N\, \mu_B\, \mu_N |\psi(0)|^2 \qquad (5.33)$$

Since the Fermi contact term involves only ‘s’ electrons, the hyperline splitting constant is isotropic.

The single factor that makes ESR a very interesting one is the appearance of hyperfine structure. The hyperfine structure of ESR lines is due to the dipole – dipole interaction term,

Eq.(5.31) and the Fermi contact term Eq.(5.32). For free or valence electrons in liquids and gases, the dipole – dipole contribution averages out to zero. In such cases, V_{cryst} is also zero. Neglecting the field free electronic energy terms, the remaining term of the Hamiltonian are given by the spin Hamiltonian.

$$H = g\,\mu_B\, B.S - \sum_i g_N\,\mu_N\, B.\, I_i + \sum_i a_i\, I_i\, S. \qquad (5.34)$$

Where the summation is over the nuclei in the system. The second terms in Eq. (5.344) is approximately 2000 time smaller than the first term. Hence, as a first approximation we get,

$$H = g\,\mu_B\, B.S - \sum_i a_i\, I_i\, S. \qquad (5.35)$$

(b) ESR spectrum of Hydrogen atom :

For a hydrogen atom in its ground state, the total Hamiltonian has the simple form given in Eq.(5.35). Treating (a I.S) as a perturbation, the energy corrected to first order is given by

$$E_{m_S, m_I} = g\,\mu_B\, B\, m_s + a\, m_I\, m_S, \qquad m_S = \pm ½, m_I = \pm ½, \qquad (5.36)$$

$$E_{\frac{1}{2},\frac{1}{2}} = \frac{1}{2} g\,\mu_B\, B + \frac{a}{4},\; E_{-\frac{1}{2},\frac{1}{2}} = -\frac{1}{2} g\,\mu_B\, B - \frac{a}{4},$$

$$E_{\frac{1}{2},-\frac{1}{2}} = \frac{1}{2} g\,\mu_B\, B - \frac{a}{4},\; E_{-\frac{1}{2},-\frac{1}{2}} = -\frac{1}{2} g\,\mu_B\, B + \frac{a}{4}, \qquad (5.37)$$

The selection rules for ESR transitions are

$$\Delta m_S = \pm 1 \quad \text{and} \quad \Delta m_I = \pm 0 \qquad (5.38)$$

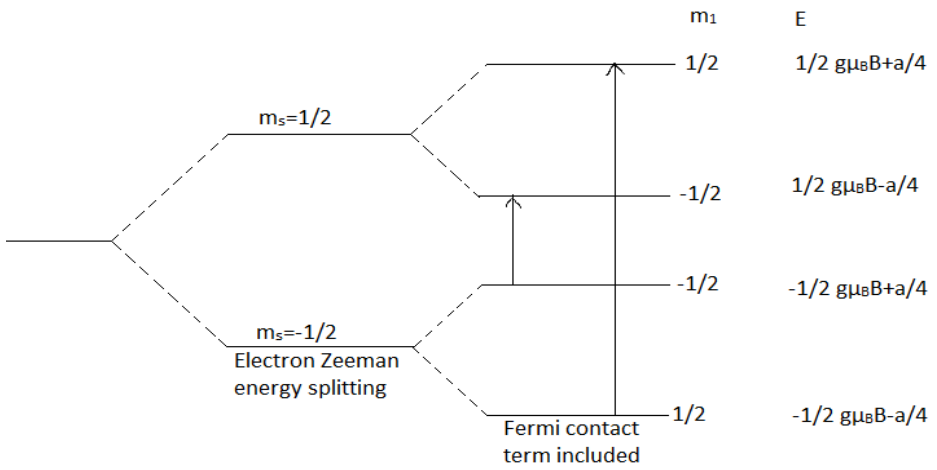

Fig.5.8 Energy levels and allowed transitions for hydrogen atom ($m_s = \pm 1/2$, $m_I = \pm 1/2$) neglecting the magnetic field nuclear spin interaction.

Two transitions are expected with spacing equal to the hyperfine splitting constant '*a*'. the frequencies of the two lines are given by

$$h\gamma_1 = g\mu_B B, +\frac{a}{2}, \quad h\gamma_2 = g\mu_B B, -\frac{a}{2}, \tag{5.39}$$

Figure 5.8 shows the energy levels and the allowed transitions for the hydrogen atom.

Fig.5.9 represents the energy levels and allowed transitions for an electron spin coupled to a nucleus spin I=1. The dipole – dipole contribution to hyperfine structure is assumed to be zero. Dropping the nuclear Zeeman energy term in Eq.(5.34)

$$E_{m_S,m_I} = g\,\mu_B\,B m_s + a\,m_S\,m_I, \quad m_S = \pm ½,\ m_I = 0_1 \pm 1.$$

Three transition of equal intensity, with separation equal to the hyperfine splitting constant are expected. Their energies are

$$h\gamma_1 = g\,\mu_B\,B - a$$
$$h\gamma_2 = g\,\mu_B\,B$$
$$h\gamma_3 = g\,\mu_B\,B + a \tag{5.40}$$

When an unpaired electron interacts with a nuclear spin I, the number of hyperfine components expected is 2I+1.

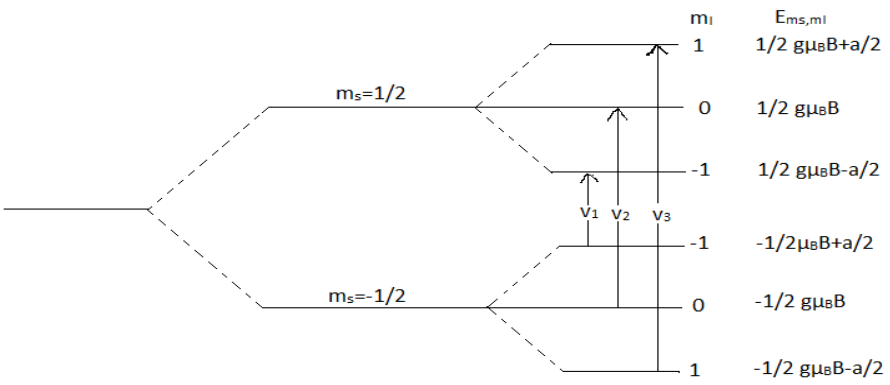

Fig. 5.9: Energy level diagram and allowed transition for an electron coupled to a nucleus of spin I=1. (I.B interaction reflected).

The situation is the same for a system having one unpaired electron interacting with two equivalent electrons. For each arrangement of the electron magnetic moment, there are four arrangements of the nuclear magnetic moments. Since $\Sigma\, m_I = 0$ state is doubly degenerate,

the transition between $\Sigma m_I = 0$ states will have double the intensity. Hence the intensity ratio of the observed lines will be similar to the one given in Fig.5.10

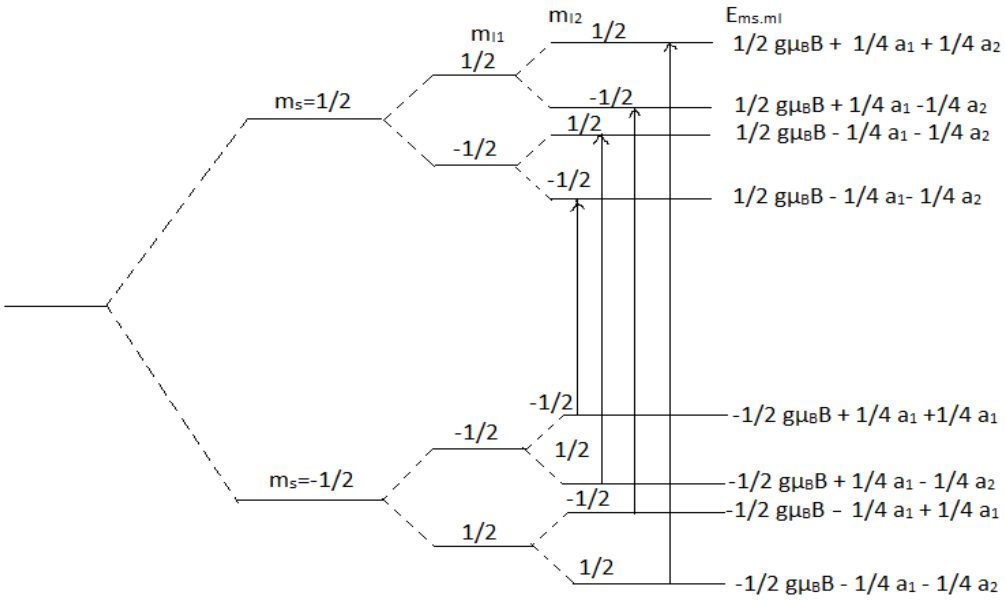

Fig.5.10 Energy level diagram and allowed transitions for an electron coupled for an electron coupled to a nucleus of spin I = 1.

Nuclear Quadrupole Resonance (NQR)

5.12 Introduction

Nuclear Quadrupole Resonance (NQR) is a branch of spectroscopy in the radio – frequency region of the e.m.spectrum like NMR. It also deals with the coupling between e.m. radiation and a set of energy levels, ie. Nuclear energy levels.

5.13 The Quadrupole nucleus :-

A nucleus with $I > \frac{1}{2}$ lack of the spherical symmetry along the spin axis. Such nucleus are shaped either elongated or compressed along the spin axis. The former one has a prolate spheroid shape (symmetrical egg) and the later an oblate spheroid shape (flattened disc). Even though the charge density inside a nucleus is uniform, the distorted shape gives rise to a charge distribution which is nonspherical. The electric quadrupole moment eQ is defined by

$$eQ = \int \rho(x, y, z)\, r^2\, (3\cos^2\theta - 1)\, d\tau \qquad (5.41)$$

Where +e is the charge on the proton, $\rho(x, y, z)$ is the charge density at (x, y, z), r is the distance of the volume clement $d\tau$ from the nucleus and θ is the angle which the radius

vector r makes in the nuclear spin axis. The nuclear quadrupole moment *eQ*, a measure of the departure from spherical symmetry of the nuclear charge, is greater than zero for prolate ones and less than zero for oblate one (Fig.5.11).

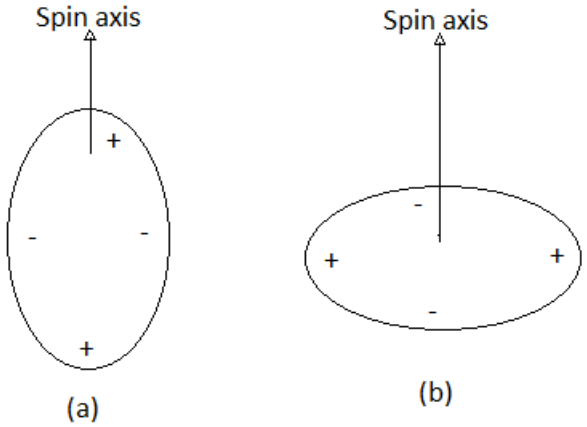

Fig.5.11 Representation of nuclei for quadrupole configurations : (a) I > 1: eQ > 0. (b) I > 1, eQ < 0.

The charges near a nucleus produces on electrostatic potential V at the nucleus. The electrostatic field gradient *eq* is defined as the second derivative of V and in general it is a tensor with nine components. The components are given by,

$$eq_{ij} = \frac{\partial^2 V}{\partial x_i \, \partial x_j} \qquad x_i, \quad x_j = x, y, z \tag{5.42}$$

If the coordinate axes are selected such that the tensor *eq* is diagonal, then terms such as $\frac{\partial^2 V}{\partial x \partial y}$, $\frac{\partial^2 V}{\partial x \partial z}$ vanish. In such a principal axes system, the *eq* term is traceless, so that,

$$q_{xx} + q_{yy} + q_{zz} = 0 \tag{5.43a}$$

$$\frac{\partial^2 V}{\partial x^2} + \frac{\partial^2 V}{\partial y^2} + \frac{\partial^2 V}{\partial z^2} = 0 \tag{5.43b}$$

Hence, out of q_{xx}, q_{yy} and q_{zz} only two are independent. The convention generally followed is that,

$$|q_{zz}| \geq |q_{yy}| \geq |q_{xx}| \tag{5.44}$$

If $q_{zz} = q_{yy} = q_{xx}$, the field gradient is spherical and the interaction of quadrupole moment with electronic charge varnishes, leading to degenerate quadrupole levels. If the field has an axial symmetry, q_{zz} lies along the symmetry axis Z, $q_{zz} \neq q_{yy} \neq q_{xx}$. When $q_{zz} \neq q_{yy} \neq q_{xx}$.to

measure the departure of the field gradient from axial symmetry, an asymmetry parameter η is introduced which is defined by

$$\eta = \frac{q_{xx} - q_{yy}}{q_{zz}} \tag{5.45}$$

In general η varies from 0 to 1, η =0 components to axial symmetry where as η =1 to the condition $\frac{\partial^2 V}{\partial x^2}$ =0, $\frac{\partial^2 V}{\partial y^2} = -\frac{\partial^2 V}{\partial y^2}$

5.14 NQR Principle

A quadrupolar nucleus will have different nuclear orientations caused by the interaction between the nuclear quadrupole moment of a nucleus and the electric field gradient giving rise to a set of quantized energy levels.

Nuclear quadrupole resonance spectroscopy deals with transitions between these quantized energy levels when e.m. radiation of porper frequency is allowed to interact with the system"

NQR is observed for solid samples because molecular motion averages the electric field gradient to zero in liquids and gases. Of the number of nuclear studied, ^{35}Cl and ^{14}N are the most common ones.

5.15 Differences between NMR and NQR

NMR		NQR	
1.	The set of nuclear levels are magnetic in origin	1.	The set of nuclear levels are electrical in origin.
2.	Splitting between energy levels are proportional to the applied magnetic field and transitions are usually studied by using a fixed frequency oscillator while varying the magnetic field	2.	In this, NQR as the electric field gradient is a fixed property of the solid, a variable frequency detection system must be used.

Similarity

Both NQR and NMR involve the coupling of r-f field with a set of nuclear energy levels.

5.16 Transitions for axially symmetric systems

(i) Frequency of transitions :-

For systems having axial symmetry, the Hamiltonian representing the interaction between the nuclear quadrupole moment of the nucleus and the electric field gradient leads to the energy Eigen values.

$$E_m = \frac{e^2 qQ\left[3m_I{}^2 - I(I+1)\right]}{4I(2I-1)} \qquad (5.46)$$

Where I is the nuclear spin quantum number, $eq = \frac{\partial^2 V}{\partial x^2}$ is the magnitude of the electric field gradient on the direction of the axis of symmetry, eQ is the nuclear quadrupole moment and m_I is the magnetic quantum number which takes the $(2I+1)$ values

$$m_I = I,\ I-1,\ \ldots\ldots\ldots -I$$

The states $+m_I$ and $-m_I$ are degenerate as m_I appears as $m_I{}^2$ in the expression. The selection rule for magnetic dipole moment is

$$\Delta m_I = \pm 1 \qquad (5.47)$$

The frequency of the $m_I - 1 \rightarrow m_I$ transition is given by

$$\gamma = \frac{3e^2 qQ}{4I(2I-1)h}\ \ (2|m_I| - 1) \qquad (5.48)$$

There will be $I - \frac{1}{2}$ transition frequencies for half intergral spins and I for intergral spins. The NQR frequencies of nucleus usually lie in the range $100\,KH_Z - 1000\,MH_Z$. The expression $e^2 qQ/h$ is called the *nuclear quadrupole coupling constant* and has unit of frequency.

(ii) Half – integral spins

For nuclei having spin $I = \frac{3}{2}$ $(^{35}Cl,\ ^{79}Br)$ Eq. (5.48) allows only a single transition of frequency.

$$\gamma = \frac{e^2 qQ}{2h} \qquad (5.49)$$

For nuclei with spin $I = \frac{5}{2}$ $(^{127}I,\ ^{121}Sb)$, there will be three levels and two transitions. They are,

$$\gamma_1 = \frac{3}{20h} e^2 qQ, \quad \gamma_2 = \frac{6}{20h} e^2 qQ, \tag{5.50}$$

The energy levels and transitions are illustrated in Fig.5.12. The order of the levels may change depending the sign of q or eQ.

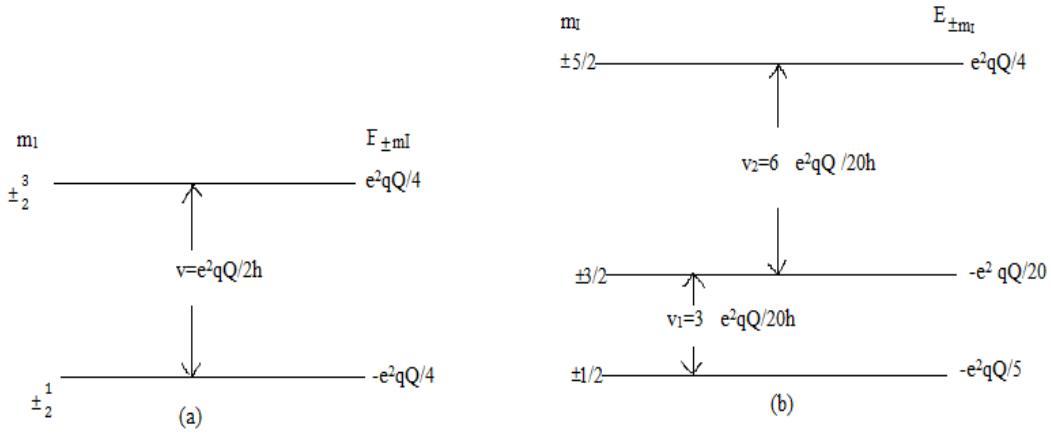

Fig.5.12 Energy levels and transitions for (a) I = 3/2 (b) I = 5/2.

(iii) Integral spins:-

For integral spins, the energy expression Eq.(5.46) leads to (I+1) doubly degenerate and one non – degenerate levels. A single resonance line results for nuclei having I=1, $(^{14}N,\ ^{6}Li)$ the frequency of which is given by

$$\gamma = \frac{3e^2 qQ}{4h} \tag{5.51}$$

For simple considerations, it can be shown that intensity of NQR line becomes a maximum when the r-f field is perpendicular to the symmetry axis and vanishes when it is parallel.

5.17 Transitions for Nonaxillay symmetric systems

When the field gradient is not axial $(\eta \neq 0)$, the energy levels and transition frequencies are more complex. In large number of systems, the nucleus under investigation is situated in axially symmetric systems in free molecules. The axial symmetry is destroyed within the crystal lattice due to intermolecular interaction.

(i) Half – integral spins :-

Formulation of exact solutions beyond $I=\frac{3}{2}$ will be difficult and will involve complicated expressions. Such systems are handled by using series approximations when η is small or by using numerical methods. For $I=\frac{3}{2}$, some of the diagonal matrix elements of the Hamiltonian are not zero and evaluation of the eigenvalues gives the secular equation,

$$E^2-3\left(\frac{e^2qQ}{12}\right)^2\eta^2-9\left(\frac{e^2qQ}{12}\right)^2=0 \qquad (5.52)$$

The two roots of this equation are,

$$E_{\pm\frac{1}{2}}=\frac{3e^2qQ}{12}\left(1+\frac{\eta^2}{3}\right)^{1/2} \qquad (5.53)$$

$$E_{\pm\frac{1}{2}}=\frac{-3e^2qQ}{12}\left(1+\frac{\eta^2}{3}\right)^{1/2} \qquad (5.54)$$

The selection rule $\Delta m_I=\pm1$ leads to a single transition having frequency γ given by

$$\gamma=\frac{e^2qQ}{2h}\left(1+\frac{\eta^2}{3}\right)^{1/2} \qquad (5.55)$$

The transition is represented in Fig.(5.13). As there is only one frequency, it is not possible to determine both the nuclear quadrupole conpling constant $\frac{e^2qQ}{h}$ and the asymmetry parameter η simultaneously. This difficulty which is unique for $I=\frac{3}{2}$ systems can be solved by investigating the spectrum in the presence of a weak magnetic field.

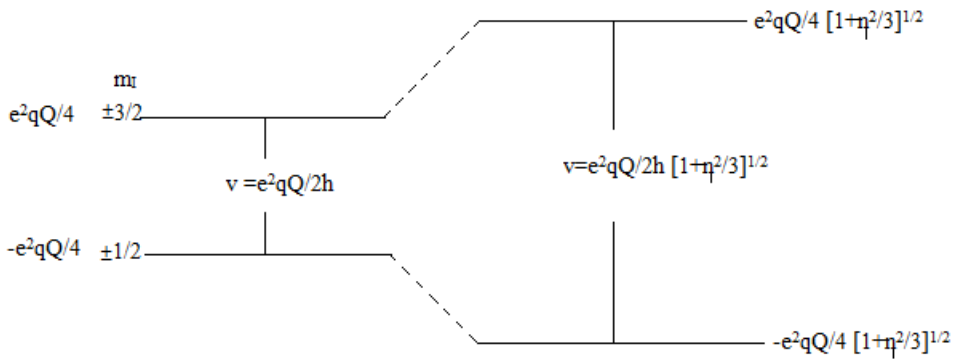

Fig.5.13 Energy levels and transition for I = 3/2 , $\eta \neq 0$. The one for η = 0 is given for comparison.

(ii) Integral spins :-

The introduction of asymmetry removes the degeneracy in m_I for integer spin systems. For nuclei of spin I=1, the secular equation for energy reduces to

$$\begin{vmatrix} A_1 - E & 0 & A_1\eta \\ 0 & -2\,A_1 - E & 0 \\ A_1\eta & 0 & A_1 - E \end{vmatrix} = 0 \qquad (5.56)$$

Where $$A_1 = \frac{e^2qQ}{4} \qquad (5.57)$$

The energy levels are then given by

$$E_0 = -2A_1$$

$$E_{\pm 1} = A_1(1 \pm \eta) \qquad (5.58)$$

The energy levels and allowed transitions are shown the Fig.5.14.

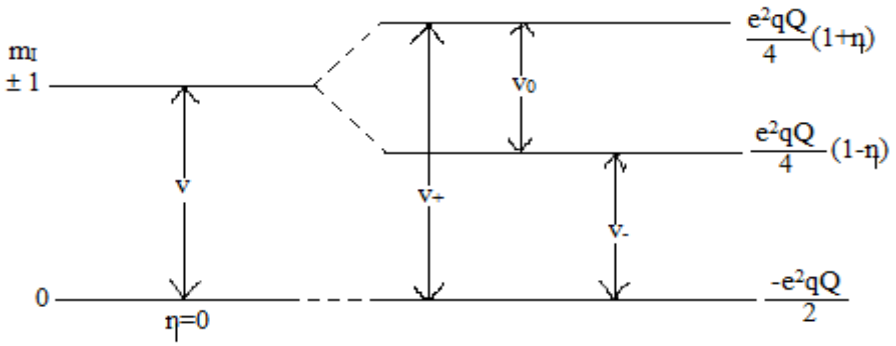

Fig.5.14 Energy levels and transition for an I = 1 system.

For comparison I=1, $\eta = 0$ case is also included. The frequencies of the three transitions are given by

$$\gamma_0 = \frac{1}{2}\frac{e^2qQ}{h}\,\eta \qquad (5.59)$$

$$\gamma_{\pm} = \frac{3}{4}\frac{e^2qQ}{h}\,(1 \pm \frac{\eta}{3}) \qquad (5.60)$$

When $\eta = 0$ these frequencies reduce to a single frequency given by

$$\gamma = \frac{3e^2qQ}{4h}$$

The familiar example for I=1 system is that of ^{14}N . Since the quadrupole coupling constant for nitrogen is of the order of $4MHz$, the γ_0 transition can only be observed when η is large.

5.18 NQR Instrumentation

The quadrupole frequencies to be detected range from as low as a few to as high as $1000MHz$. Three different methods are generally used for the detection of NQR frequencies,

(i) Super - regenerative oscillators,

(ii) Regenerative continuous wave oscillators and

(iii) Pulsed r-f or spin echo method.

In the first two, an r-f oscillator is used to act both as exciter of the nuclei and detector. In the third method, separate transmitter and receiver carry out these functions.

(i) Regenerative Continuous wave Oscillator method :

Regnerative continuous wave oscillator is some what simpler than super – regenerative oscillator method. A method of this type was first developed by Pound and Knight. A block diagram of this arrangement is illustrated in Fig.5.15

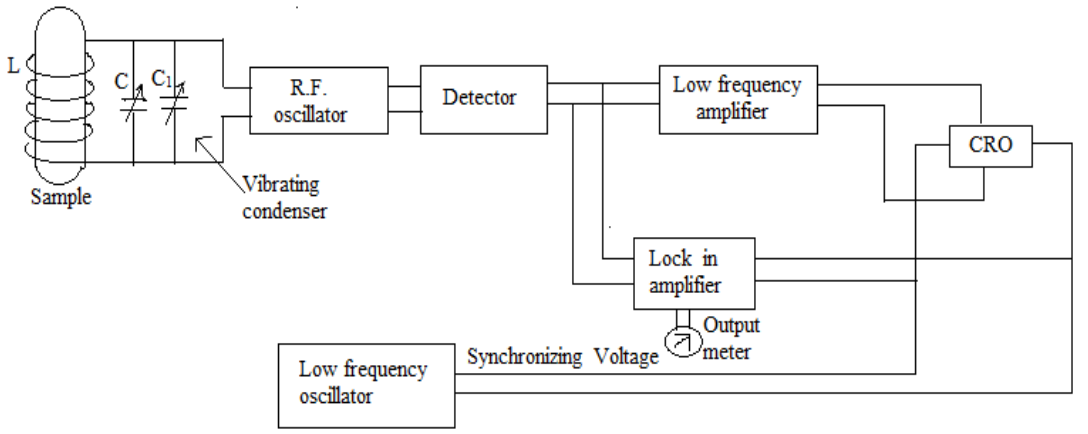

Fig. 5.15 : Block diagram of a regenerative continuous wave oscillator – detector arrangement to observe NQR

The sample is placed in the inductance L which is tuned to the transition frequency using the large capacitor C changes in frequency over a limited range is effected by changing it capacitance C. Using the LC circuit as the oscillating element with electronic feedback, the voltage level of oscillation becomes a function of nuclear absorption. This applied frequency is modulated about the resonant frequency by varying it small capacitor C_1 sinusoidally. The signal may be presented in an oscilloscope on the derivative of the signal can be recorded by the help of a narrow band lock in the system followed by a record.

Mossbauer Spectroscopy

5.19 Introduction :

Mossbauer spectroscopy, named after its discoverer who received a Nobel prize in 1961 his work, is concerned with transitions between energy levels within the nuclei of atoms.

The heavier elements formed by the radioactive decay of an isotope of the same or a different element are initially produced in an excited nuclear state, after a very short delay, the excited nucleus reverts to the ground state and emits energy of a very high frequency, usually in the γ-ray region of the spectrum. So Mossbauer or γ-ray spectroscopy is the study of $\gamma-$ray emission or reabsorption

Like NMR, NQR and ESR, the resonant absorption of $\gamma-$rays was suggested by Kuhn in 1929. It was observed only in 1959 by Mossbauer because of the high recoil energy of the nucleus which emitted to high energy $\gamma-$rays.

(i) Recoilless emission and absorption :-

Nuclear resonance absorption is in principle expected to occur when gamma radiation emitted in a transition from $E_i \, to \, E_f$ is reabsorbed by another nucleus of the same kind according to the scheme depicted in Fig.5.16

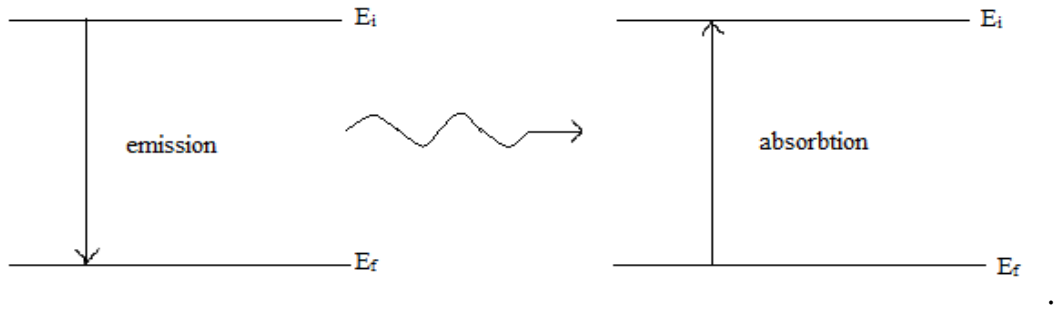

Fig.5.16 Nuclear resonance absorption.

Consider an isolated atom of mass M having a nuclear excited state E_i above the ground state E_f. Let E_o be the energy difference $E_i - E_f$ and E_{re} be the kinetic energy of the recoil nucleus. If P iS the recoil momentum

$$E_{re} = \frac{P^2}{2M} \qquad (5.61)$$

As this energy has to come from E_o, the emitted gamma ray will have an energy,

$$E_\gamma = E_0 - E_{re}$$

By the law of conversation of momentum,

Recoil momentum of the atom = momentum of the emitted $\gamma-$ray

$$P = \frac{E_\gamma}{C} \tag{5.62}$$

Where C is the velocity of light , Hence,

$$E_{re} = \frac{P^2}{2M} = \frac{E_r^{\,2}}{2MC^2} = \frac{(E_0 - E_{re})^2}{2MC^2} = \frac{E_0^{\,2}}{2MC^2} \tag{5.63}$$

Since $E_r^{\,2}$ iS small compared to E_0.

In absorption process, to excite the nucleus upto the same energy, the $\gamma-$ray must have the energy $E_r^{\,1}$ given by

$$E_r^{\,1} = E_0 - E_{re} \tag{5.64}$$

The effect of recoil is thus to introduce a difference of $(E_r^{\,1} - E_r)$ between the energies of the emitted and absorped gamma rays in a resonant process.

$$E_r^{\,1} - E_r = 2E_{re} = \frac{E_0^{\,2}}{MC^2} \tag{5.65}$$

If $2E_{re} << \Gamma$, the two curves would overlap and one would observe resonant absorption. Since E_{re} iS proportional to $E_0^{\,2}$, it increases appreciably as we go from the optical region (~2ev) to the gamma ray region (~10 Kev) of the e.m. spectrum.

(ii) Experimental techniques :-

To design an experiment to investigate Mossbauer effect, a solid matrix containing the excited nuclei of a given isotope called the source is placed next to a second matrix containing the same isotope in the ground state called the absorber. The amount of the energy profiles for the source and absorber decides the strength of resonant absorption. A movement of the source and absorber relative to each with velocity 'V' produces a Doppler shift in frequency equal to $\left(\frac{V}{C}\right)\gamma$, where C is the velocity of light and γ is the frequency of the $\gamma-$ray. If the effective resonance energies for source and absorber exactly match at a particular velocity 'V', the resonance absorption will be at a maximum.

Thus, the principle obtaining Mossbauer spectrum is the record the transmission of $\gamma-$rays from a source through an obsorber as a function of the Doppler velocity V between the source and absorber.

The absorbers are normally stable isotope of elements with which the Massbauer effect can be observed. As emitter (source), one selects the excited state of the very same isotope.

As the natural width of the resonance line depends on the lift time of excited state, nuclei with excited state lifetime in the range $10^{-6} < \tau < 10^{-10}$ sec are usually selected as the source, *Short lifetime* : ($<10^{-10}$ Sec) would make the line width too broad to be useful for hyperfine studies. *Longer life time* : ($>10^{-6}$ Sec) leads to too narrow resonance line which makes overlapping less portable.

The following examples some the Mossbauer transition.

1. Consider the source ^{57}CO which decays to $^{57}Fe*$ through electron capture. This excited nucleus comes to the stable ^{57}Fe through emission of $\gamma-$rays. The complete energy diagram is shown in Fig.5.17(a).
2. Another commonly used source is the 23.9 Kev Mossbauer transition in ^{119}Sn which is made in the form of $Pd_3\,Sn$ *or* $Ba\,S_n\,O_3$. The decay scheme of $119m_{Sn}$ is also given in Fig.5.17(b).

A good absorber should contain sufficient Mossbauer nuclei in the ground state. Thick absorbers are not recommended because the loss in intensity of transmitted gamma rays. In the above experimental arrangements, ^{57}Fe stable isotope which absorbs the 14.4 Kev gamma radiation source as the absorber. Alternately, ^{119}Sn which absorbs the 23.9 kev gamma radiation, if ^{119}Sn is the source can be used.

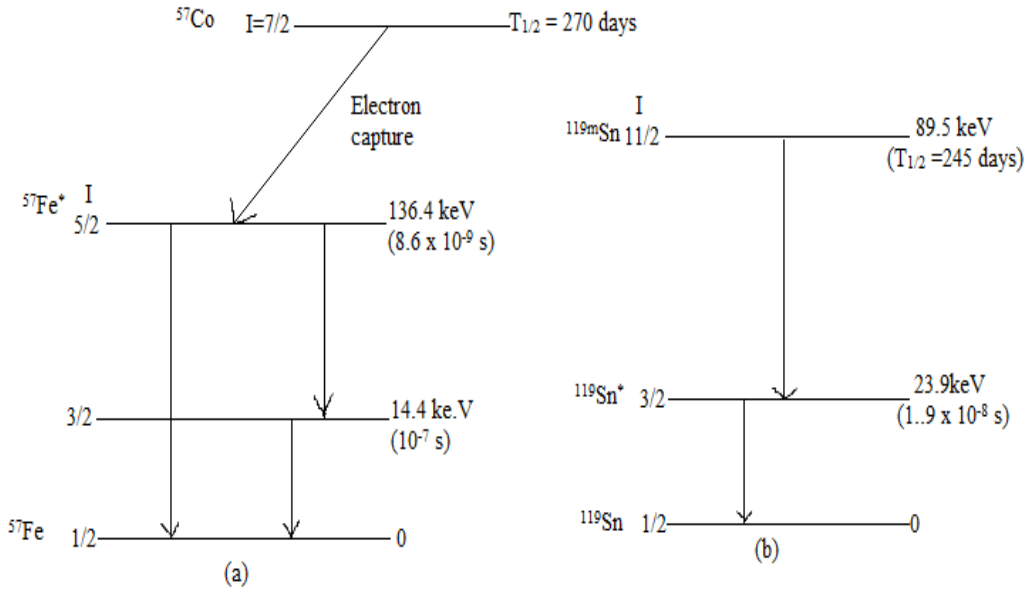

Fig.5.17: Decay scheme of (a) 57_{Co} **showing the energy levels in** 57_{Fe} **9b)** $119m_{Sn}$ **showing the energy levels in** 119_{Sn}

(iii) Mossbauer Spectrometer :-

Experimentally, two methods are possible for measuring the gamma – ray transmission as a function of Doppler velocity.

In one method, the source is mounted on a mechanical constant velocity device and the total number of counts is registered in a fixed time. The same is repeated at different velocities until the desired velocity is covered. A single channel analyser is used to limit the detection to only those pulses that have the required energy.

In the second method, the source is mounted on an oscillating drive which gives it a varying velocity relative to the sample. The detector output is fed to a multi-channel analyser which collected and sums the results.

The general experimental arrangement of a Mossbauer spectrometer is given in Fig.5.18.

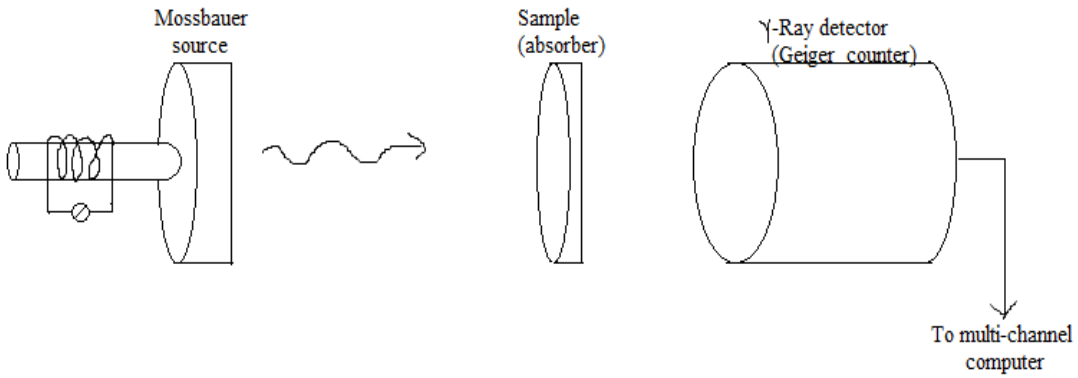

Fig.5.18 Experimental arrangement for Mossbauer spectroscopy.

The schematic arrangements of a modern Mossbauer spectrometer is shown in Fig.5.19.

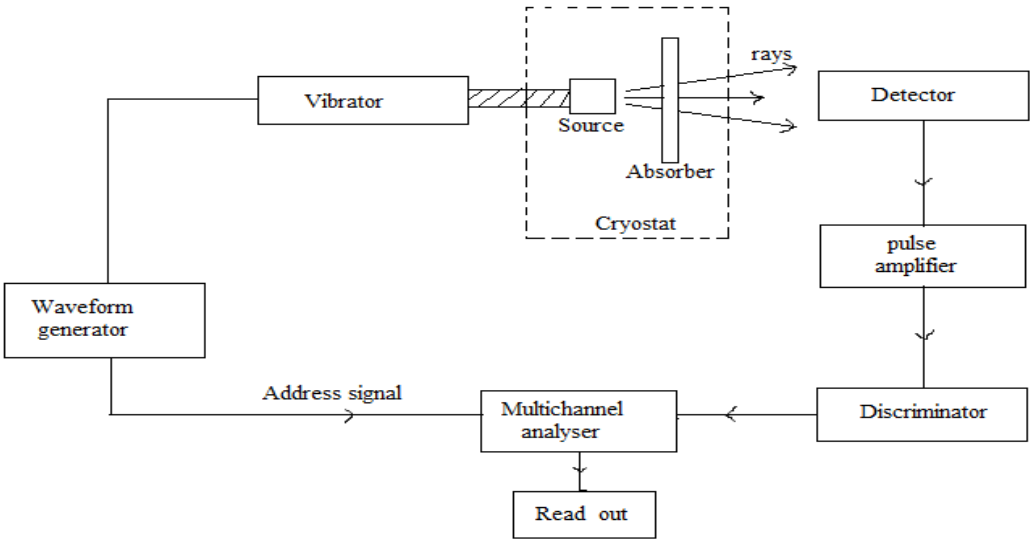

Fig.5.19 Schematic arrangements of a modern Mossbauer spectrometer.

The source ^{57}CO is mounted on a loud speaker coil whose motion is controlled by a wavefrom generator. A saw tooth variation of velocity with time is generally used. This arrangement makes the sample to move back and forth at regular integrals. This oscillatory motion gives the source a varying velocity relative to the sample. The velocity will be zero at the turning points and maximum at the centre.

The absorber which is also in the form of a foil covers the window of the detector. A scintillation counter or a gas – filled proportional counter are semi-conductor detector is used according to the situation. The signal from the detector as a function of the loud speaker velocity is fed to a multichannel analyser which collects the results and sums it over each cycle. The discreminator rejects most of the nonresonant background radiation. The final Mossbauer spectrum is displayed as counts per second as a function of relative velocity between the source and absorber.

The Mossbauer effect shown up strongly in the following way.

1. A relative velocity of 0.1mm/sec is sufficient to produce a marked reduction in the absorbtion of the 14.4Kev ^{57}Fe transition.
2. In certain cases, resonances are possible in room temperature, but in many cases, one has no cool the absorber and the source to liquid helium temperature. Due to this Doppler effect is reduced to a minimum.

The absorption of the gamma – ray by the sample is shown up by a fall in counts per second is shown in Fig. 5.20.

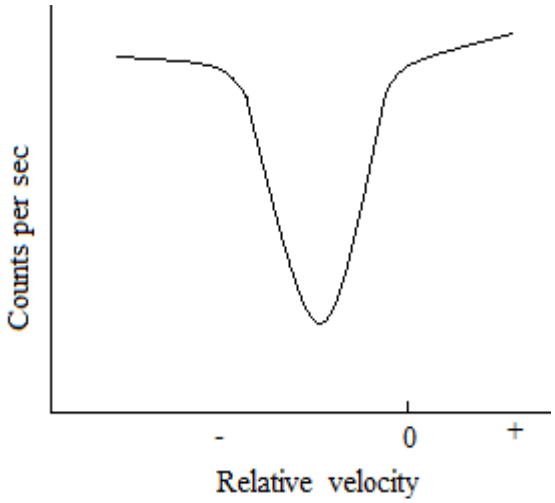

Fig.5.20 Typical Mossbauer spectrum

(iv) Isomer shift :-

In a Mossbauer experiment, if the environments of the emitting and absorbing nuclei are different, the energy of the nuclear transition E_0 may differ by a small amount. This energy difference in known as the *isomer shift* (δ) or *chemical shift*.

The effect of isomer shift on the Mossbauer spectrum is the shift the resonance line from the zero position. The value of δ can be +ve or –ve depending on the sample. (Fig.5.21). Isomer shift is the term more widely used since this effect depends on the energy difference in the ground and excitred (isomeric) states.

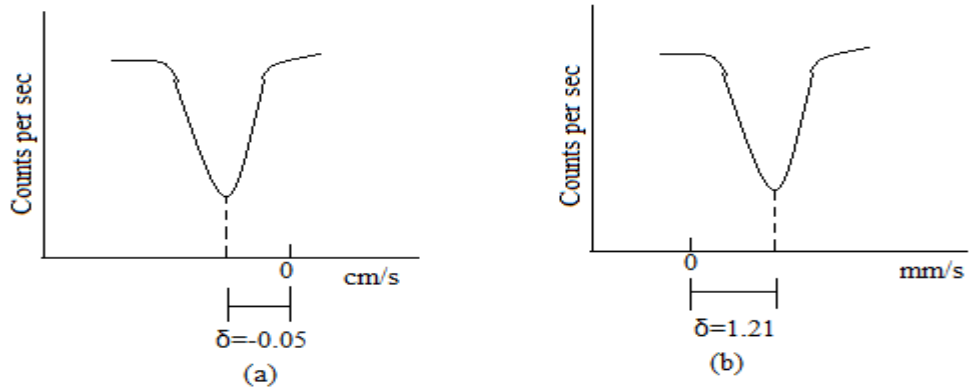

Fig. 5.21: Isomer shift in (a) $\left[Fe(CN)_6\right]^{-4}$ **(b)** $\left(C_6H_5\right)_4 S_n$

Isomer shift arises because the nucleus of an atom is not a point charge as assumed, but has a finite charge distribution. The electrostatic interaction between the nuclear charge distribution and the electron charge distribution brings about a change in the energy levels of the nucleus. The shift in the energy levels of the nucleus is given by

$$\Delta E = \frac{2\pi}{5} Ze^2 \, R^2 \, |\psi(0)|^2 \qquad (5.66)$$

Where $|\psi(0)|^2$ represents the total electron density at the site of the nucleus. The charge in energy $\delta\,(\Delta E)$ between the nuclear ground and first excited state . Hence.,

$$\delta(\Delta E) = (\Delta E)_{ex} - (\Delta E)_{ga} = \frac{2\pi}{5} Ze^2 \, |\psi(0)|^2 \, (R_{ex}{}^2 - R_{gr}{}^2) \qquad (5.67)$$

Writing R for radius of the equivalent sphere of uniform charge distribution and dR for $(R_{ex} - R_{gr})$

$$(R_{ex}{}^2 - R_{gr}{}^2) = 2R\,dR = 2R^2 \frac{dR}{R}$$

In the Mossbauer experiment, a source – absorber pair is involved and one measures only a difference in the nuclear electrostatic energy changes of the source and the absorber. Hence, the isomer shift δ is given by,

$$\delta = \delta\ (\Delta E)_a - \delta\ (\Delta E)_s$$

$$= \frac{4\pi}{5} Ze^2\ R^2\ \frac{dR}{R}\left[\ |\psi(0)|^2_a - |\psi(0)|^2_s\ \right] \qquad (5.68)$$

Where subscripts 'a' and 's' refer to the absorber and emitter (source) respectively.

The chemical term represents the difference in the total electron densities at the absorber and source nuclei and hence δ is sometimes referred to as chemical isomer shift. If $\frac{dR}{R}$ is +ve, a positive value of δ implies that $|\psi(0)|^2_a - |\psi(0)|^2_s$. Chemical isomer shift is the Mossbeuer parameter that gives the maximum amount of chemical information.

(v) Applications :-

1. It is used as a tool for studies in solid state and chemistry is mainly based on the observation of hyperfine structure.
2. The narrow line width of nuclear transitions is possible to investigate small interactions between nucleus and orbital electrons which cannot be studied by other methods.